

***PERFORMANCE COMPARISON OF SINGLE SLOPE  
SOLAR STILL LOADED WITH VARIOUS NANO-FLUIDS***

A THESIS SUBMITTED IN FULFILLMENT OF THE REQUIREMENT FOR THE  
AWARD OF THE DEGREE OF

**MASTER OF ENGINEERING  
IN THERMAL ENGINEERING**

SUBMITTED BY

**VIJAY KUMAR**

**REGISTRATION NO: 801783015**

UNDER THE SUPERVISION OF

**DR. MADHUP KUMAR MITTAL**

**ASSOCIATE PROFESSOR, MECHANICAL DEPARTMENT**



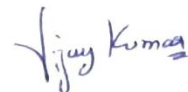
**THAPAR INSTITUTE  
OF ENGINEERING & TECHNOLOGY  
(Deemed to be University)**

**MECHANICAL ENGINEERING DEPARTMENT  
THAPAR INSTITUTE OF ENGINEERING AND TECHNOLOGY,  
(A DEEMED TO BE UNIVERSITY)  
PATIALA-147004, PUNJAB, INDIA**

## CERTIFICATE

---

I hereby declare that the dissertation entitled “Performance comparison of single slope solar still loaded with various Nano-Fluid” is an authentic record of my work carried out as requirements for the award of the degree of **Master of Engineering in Thermal Engineering** at **Thapar Institute of Engineering and Technology, (A Deemed to be University), Patiala** under the supervision of **Dr. Madhup Kumar Mittal (Associate Professor, Mechanical Engineering Department)**. No part of the matter embodied in this report has been submitted to any other university or institute for the award of any degree.



VIJAY KUMAR

(801783015)

Date : 22/8/2019

Place: PATIALA

It is certified that the above statement made by the student is correct to the best of my knowledge and belief.



Dr. Madhup Kumar Mittal

Associate Professor

Mechanical Engineering Department

Thapar Institute of Engineering and Technology,

(A Deemed to be University), Patiala-147004, Punjab.

## ACKNOWLEDGEMENTS

---

I would like to express my special thanks and a sense of gratefulness to my supervisor, **Dr. Madhup Kumar Mittal (Associate Professor)** Department of Mechanical Engineering, T.I.E.T Patiala for the guidance. I have been extremely lucky to have a supervisor who helped me in my work and I came to know about so many new things. He provided me the technical support, facilities, and skills that really helped me during the work. He cared so much about my work over the year. His patience, the adjustments he made, and trust and confidence he had in me really helped me to finish my work at the right time.

Furthermore, I would like to express my sincere gratitude to the Mechanical Engineering Department, **Thapar Institute of Engineering and Technology** for technical support and I am also very thankful to **Jagteshwer Singh**, Research scholar who devoted his valuable time for the completion of my dissertation.

Further, I would like to thank my friends **Gaganjot Singh Sidhu, Gurpreet Kaur Maan, Rohit Kumar, Kritika Sharma, Sarvesh Pratap Shahi, Virender Solanki, Divya Arora, Sheetal Vats, Saloni Goyal, Ravneet Kaur, Saarika Srivastava and Aastha** for their technical and moral support. Finally, Author would like to express his sense of sacrosanctity and gratitude for his beloved parents: **Jaswant Rai** and **Raj Kiran**. Author would like to dedicate this thesis to his highly respected parents whose inveterate optimism and faith in God provided unflinching support for the successful completion of this thesis work.

Date: 22/6/2019

Place: PATIALA



VIJAY KUMAR

(801783015)

Mechanical Engineering Department

Thapar Institute of Engineering and Technology

*Every challenging work needs self-efforts as well as guidance of elders*

*especially those who were very close to our heart.*

*My humble effort I dedicate it to my sweet and loving*

*Father & Mother,*

*Whose affection, love, encouragement and prayers of day and night make me*

*able to get such success and honour,*

*Along with all hard working and respected*

*Teachers*

## Abstract

---

In the present work, a thermal model of single slope basin type solar still (passive type) was developed (using Runge-kutta ODE) and validated with the experimental results carried out for the location Patiala, which is in a good agreement to each other, then the model was further modified by integrating different Nanofluids at different volume fractions 0.02, 0.05, 0.08, 0.12 and 0.2. The analysis for modified still has been carried out for optimised water depth of 0.02 m with different nanofluids. Yield obtained for nanofluid  $\text{Al}_2\text{O}_3$  was 14.22% higher than simple solar still without nanofluid, followed by CuO 10.82%, Ag 8.11%,  $\text{Fe}_2\text{O}_3$  7.63%, and SiC 7.61%. The effects of various parameters like water depth and volume fraction of the nanofluid were compared. It has been found that the optimum volume concentrations for maximum distillate output of different water based-nanofluid was 0.2 for  $\text{Al}_2\text{O}_3$ , 0.2 for CuO, 0.02 for Ag, 0.05 for  $\text{Fe}_2\text{O}_3$ , and 0.2 for SiC, and with the increase in water levels the performance of still decreases because of the sensible heat storage in the fluid, and by increasing the volume fraction of nanofluid, heat transfer coefficients increases but after certain values efficiency curve becomes linear with no change.

Keywords: Solar still, Single slope, Single glass solar still, Thermal model, Nanofluid, Solar desalination.

# TABLE OF CONTENTS

---

<b>CERTIFICATION</b>	<b>ii</b>
<b>ACKNOWLEDGEMENT</b>	<b>iii</b>
<b>DEDICATION</b>	<b>iv</b>
<b>ABSTRACT</b>	<b>v</b>
<b>TABLE OF CONTENTS</b>	<b>vi-viii</b>
<b>LIST OF FIGURES</b>	<b>ix-x</b>
<b>LIST OF TABLES</b>	<b>xi</b>
<b>NOMENCLATURE</b>	<b>xii</b>
<b>Chapter 1. Introduction</b>	<b>1-7</b>
1.1. Introduction	1
1.2. Working of solar still	1
1.3. Classification of solar still	2
1.3.1. Passive solar still	2
1.3.2. Active solar still	3
1.3.3. Classification of solar still based on modifications	4
1.3.3.1 Single slope single basin solar still	4
1.3.3.2. Double slope solar still	4
1.3.5. Multi effect solar still	4
1.3.6. Wick type solar still	5
1.4. Modified solar still by seeding Nanofluid	5
1.4.1. Effects of Nanofluid in solar stills	5

1.5. Motivation for present research work	6
1.6. Research objectives	6
1.7. Organisation of thesis	7
<b>Chapter 2. Literature Survey</b>	<b>8-19</b>
2.1. Literature review on solar still	8
2.2. Research gaps	19
2.3. Conclusions	19
<b>Chapter 3. Mathematical modelling and simulation</b>	<b>20-31</b>
3.1. Introduction	20
3.2. Mathematical model	20
3.2.1. Internal heat transfer	21
3.2.2. External heat transfer	21
3.3. Energy balance	23
3.3.1. Energy balance for basin liner	23
3.3.2. The transition energy balance for water mass	23
3.3.3. Energy balance for glass cover	24
3.4. Factors affecting the performance of solar still	26
3.5. Validating Theories	26
3.5.1. Temporal discretisation with a time step of 1 sec	26
3.5.2. Numerical Iterative method	27
3.6. Experimental setup and procedure	28
3.6.1. Design and Construction	28
3.6.2. Methodology	30

<b>Chapter 4. Results and Discussions</b>	<b>32-46</b>
4.1. Experimental results	32
4.2. Validation of Thermal model	34
4.3. Effect of water depth on the performance of the solar still	36
4.4. Variation in the performance of solar still with different Nano-fluids	38
4.4.1. Variations of performance in different volume fraction of Al <sub>2</sub> O <sub>3</sub> nanofluid	38
4.4.2. Variations of performance in different volume fraction of CuO nanofluid	40
4.4.3. Variations of performance in different volume fraction of Ag nanofluid	42
4.4.4. Variations of performance in different volume fraction of Fe <sub>2</sub> O <sub>3</sub> nanofluid	43
4.4.5. Variations of performance in different volume fraction of SiC nanofluid	44
4.4.6. Performance comparison of different nanofluid	45
<b>Chapter 5. Conclusions</b>	<b>47-48</b>
4.1. Conclusions	47
4.2. Future scope	47
<b>References</b>	<b>49-54</b>
<b>Appendix</b>	<b>55-79</b>
Appendix-A1	55
A1.1. Thermo physical properties of water vapour and water	55
A1.2. Thermo physical properties of Nano-fluid	56
A1.3. Properties of Nano-Particle	56
Appendix-A2	57
A2.1. MATLAB code for simple solar still	57
A2.2. MATLAB code for modified solar still having nanofluid	66

## LIST OF FIGURES

---

Figure 1.1. Basin type single solar still	2
Figure 1.2. Passive type of solar still	3
Figure 1.3. Active type of solar still	3
Figure 3.1. Basin type single slope solar still	21
Figure 3.2. Experimental setup of single slope solar still	29
Figure 3.3. Pyranometer to measure total solar incident radiation	29
Figure 3.4. Flowchart of thermal modelling	31
Figure 4.1. Variation of solar intensity on 14 <sup>th</sup> July	32
Figure 4.2. Variation of ambient temperature on 14 <sup>th</sup> July	32
Figure 4.3. Hourly variation of theoretical and experimental water temperature for 0.03m water depth	34
Figure 4.4. Hourly variation of theoretical and experimental glass temperature for 0.03m water depth	35
Figure 4.5. Hourly variation of theoretical and experimental distillate output for 0.03m water depth	35
Figure 4.6. Hourly variation of distillate output at different water depths in a solar still	36
Figure 4.7. Hourly variation in evaporative heat transfer coefficient of solar still at different water depths	37
Figure 4.8. Hourly variation in temperature of solar still at different water depth	37
Figure 4.9. Hourly variation of distillate produced by Al <sub>2</sub> O <sub>3</sub> at different volume fractions	39

Figure 4.10. Hourly variation of temperature difference $\Delta T$ between basefluid (water) and nanofluid ( $\text{Al}_2\text{O}_3$ ) at different volume fractions	39
Figure 4.11. Hourly variation of temperature difference $\Delta T$ between basefluid (water) and nanofluid ( $\text{CuO}$ ) at different volume fractions	40
Figure 4.12. Hourly variation of glass temperature of the solar still having simple water and nanofluid	41
Figure 4.13. Hourly variation of distillate produced by $\text{CuO}$ at different volume fractions in comparison with simple water	41
Figure 4.14. Hourly variation of temperature difference $\Delta T$ between basefluid (water) and nanofluid ( $\text{Ag}$ ) at different volume fractions	42
Figure 4.15. Hourly variation of temperature difference $\Delta T$ between basefluid (water) and nanofluid ( $\text{Fe}_2\text{O}_3$ ) at different volume fractions	43
Figure 4.16. Hourly variation of temperature difference $\Delta T$ between basefluid (water) and nanofluid ( $\text{SiC}$ ) at different volume fractions	44
Figure 4.17. Hourly variation of temperature difference $\Delta T$ between basefluid (water) and different nanofluids at different volume fractions	45
Figure 4.18. Hourly variation of distillate output for different nanofluids	46

## LIST OF TABLE

---

Table 4.1. Experimental data for single slope solar still	33
Table 4.2. Various design parameters of solar still	34
Table .A.1.1. Thermo Physical properties of water vapour	55
Table .A.1.2. Thermo Physical properties of Nanofluid	56
Table .A.1.3. Properties of nanoparticles	56

## NOMENCLATURE

---

$A_s$	-	Area of still ( $m^2$ ).
$A_w$	-	Area of water ( $m^2$ ).
$A_g$	-	Area of glass ( $m^2$ ).
$A_b$	-	Area of basin ( $m^2$ ).
$A_c$	-	Area of collector ( $m^2$ ).
$T_b$	-	Temperature of basin ( $^{\circ}C$ ).
$T_a$	-	Ambient temperature ( $^{\circ}C$ ).
$T_w$	-	Temperature of water ( $^{\circ}C$ ).
$T_{gi}$	-	Temperature of glass cover ( $^{\circ}C$ ).
$I(t)$	-	Solar incident radiation on solar still ( $W/m^2$ ).
$I(t')$	-	Solar incident radiation on Collector surface ( $W/m^2$ ).
$Q_{cw}, Q_{c,w-g}$	-	Convective heat transfer from water to glass (W).
$Q_{ew}, Q_{e,w-g}$	-	Evaporative heat transfer from water to glass (W).
$Q_{rw}, Q_{r,w-g}$	-	Radiative heat transfer from water to glass (W).
$Q_{c,b-w}$	-	Convective heat transfer from basin liner to water (W).
$Q_w, Q_{loss}$	-	Bottom and side heat transfer losses in the still (W).
$Q_{rg}, Q_{r,g-s}$	-	Radiative heat transfer between glass cover to sky (W).
$Q_{c,go}, Q_{c,g-a}$	-	Convective heat transfer between glass cover to ambient (W).
$Q_u$	-	Heat transfer from solar collector to the solar still (W).
$h_{cw}$	-	Convective heat transfer coefficient of water ( $W/m^2^{\circ}C$ ).
$h_{ew}$	-	Evaporative heat transfer coefficient of water ( $W/m^2^{\circ}C$ ).

$h_{rw}$	-	Radiative heat transfer coefficient between water and glass ( $W/m^2\text{°C}$ ).
$h_{cg}$	-	Convective heat coefficient between glass and ambient ( $W/m^2\text{°C}$ ).
$h_{rg}$	-	Radiative heat transfer coefficient between glass and sky ( $W/m^2\text{°C}$ ).
$h_w$	-	Heat transfer coefficient from basin to water ( $W/m^2\text{°C}$ ).
LH	-	Latent heat of vaporisation (J/kg).
$P_g$	-	Partial vapour pressure on glass temperature (Pa).
$P_w$	-	Partial vapour pressure on water temperature (Pa).
$F_R$	-	Heat removal factor.
$U_L$	-	Overall heat transfer coefficient ( $W/m^2\text{°C}$ ).
$\phi$	-	Volume fraction.
$d_p$	-	Nanoparticle size (nm).
$m_w$	-	Mass of water (kg).
$m_g$	-	Mass of glass cover (kg).
$m_b$	-	Mass of basin liner (kg).
$m_{ew}$	-	Mass of evaporated water (kg).
$m_d$	-	Hourly mass of distillate produced ( $kg/m^2\text{hr}$ ).
$K_w$	-	Thermal conductivity of water (W/mK).
$K_i$	-	Thermal conductivity of insulation (W/mK).
$K_{nf}$	-	Thermal conductivity of Nanofluid (W/mK).
$K_{np}$	-	Thermal conductivity of Nanoparticle (W/mK).
$K_v$	-	Thermal conductivity of water vapour inside still (W/mK).
$L_i$	-	Thickness of insulation (m).
$Cp_g$	-	Specific heat of glass (J/kgK).

$C_{pw}$	-	Specific heat of water (J/kgK).
$C_{nf}$	-	Specific heat of Nanofluid (J/kgK).
$C_{pb}$	-	Specific heat of basin liner (J/kgK).
$C_{np}$	-	Specific heat of Nanoparticle (J/kgK).
$C_v$	-	Specific heat of water vapour (J/kgK).
$Re$	-	Reynolds number = $(\rho V D / \mu)$ .
$Pr$	-	Prandtle number = $(\mu_f C_f / K_f)$ .
$\Delta t$	-	Time step (sec).

Greek letters:

$\epsilon_{eff}$	-	Effective emissivity.
$\epsilon_g$	-	Emissivity of glass.
$\epsilon_w$	-	Emissivity of water.
$r_w$	-	Reflectivity of water.
$r_g$	-	Reflectivity of glass.
$\tau_w$	-	Transmittivity of water.
$\tau_g$	-	Transmittivity of glass cover.
$\rho_w$	-	Density of water (kg/m <sup>3</sup> ).
$\rho_v$	-	Density of humid air (kg/m <sup>3</sup> ).
$\rho_b$	-	Density of basin liner (kg/m <sup>3</sup> ).
$\rho_g$	-	Density of glass cover (kg/m <sup>3</sup> ).
$\rho_{nf}$	-	Density of Nanofluid (kg/m <sup>3</sup> ).
$\rho_{np}$	-	Density of Nanoparticle (kg/m <sup>3</sup> ).

$\mu_w$	-	Dynamic viscosity of water (Ns/m <sup>2</sup> ).
$\beta$	-	Inclination angle of glass cover (degree).
$\mu_{nf}$	-	Dynamic viscosity of Nanofluid (Ns/m <sup>2</sup> ).
$\mu_v$	-	Dynamic viscosity of water vapour (Ns/m <sup>2</sup> ).
$\alpha_w$	-	Fraction of solar energy absorbed by water.
$\alpha_b$	-	Fraction of solar energy absorbed by basin liner.
$\alpha_g$	-	Fraction of solar energy absorbed by glass cover.
$\sigma$	-	Stefan-Boltzman's constant = $5.6697 * 10^{-8}$ , (W/m <sup>2</sup> K <sup>4</sup> ).
$(\alpha\tau)_c$	-	Product of absorptivity and transmittivity of collector.
$\beta_{nf}$	-	Coefficient of volumetric thermal expansion of Nanofluid (K <sup>-1</sup> ).
$\beta_v$	-	Coefficient of volumetric thermal expansion of water vapour (K <sup>-1</sup> ).
$\beta_{np}$	-	Coefficient of volumetric thermal expansion of Nanoparticle (K <sup>-1</sup> ).

#### Subscripts and Superscripts:

a	-	Ambient.
b	-	Basin.
v	-	Vapour.
g	-	Glass.
c	-	Convective.
e	-	Evaporative.
r	-	Radiative.
nf	-	Nanofluid.
bf	-	Basefluid.

### 1.1. Introduction

Earth known as the mother of life, has nectar-like fluid water. Two-third of the earth's surface is covered with water, 97% of which is salty and the remaining is fit for drinking. The quality of drinkable water is deteriorating due to regress development and industrial setups, so to improve its quality and to make it drinkable, different water purification methods are investigated, like reverse osmosis, filtration, multiple effect distillation, vapour compression distillation, electro dialysis, boiling and desalination of brackish water with the help of solar still [1]. Among all, using solar still is the cleanest way to purify water, because of its simple nature and low maintenance. The solar still only uses solar energy for the purification process, whereas other methods are complex and need high maintenance and skilled workers.

### 1.2. Working of solar still

Solar still has the same principle as of natural hydrological cycle. The incident solar radiations warm the surface of earth which creates temperature gradient and forms hot and cold regions in between sky and the Earth. Because of this, water from the sea and oceans gets vaporized and form water vapours. So, this natural process is taken into account for the purification of water by natural incident solar radiation, which is a clean and green type of distillation process [1].

Solar still having a top transparent cover made of glass, which allows incident solar rays to transmit through it. All the five sides of the still are insulated except from its top, the interior of the still is blackened so to improve the solar absorption. As the beams of sun falls on the basin liner, it gets heated up and the water in contact gets energy through conduction. Due to this rise of energy, water evaporates with an increase in moisture percentage in the still. The evaporated water vapour then condenses on the inner surface of the glass cover. Condensed water is collected through the distillate channel in the container. Figure 1.1 shows all the energy transition and the structure of simple (Passive type) single slope solar still.

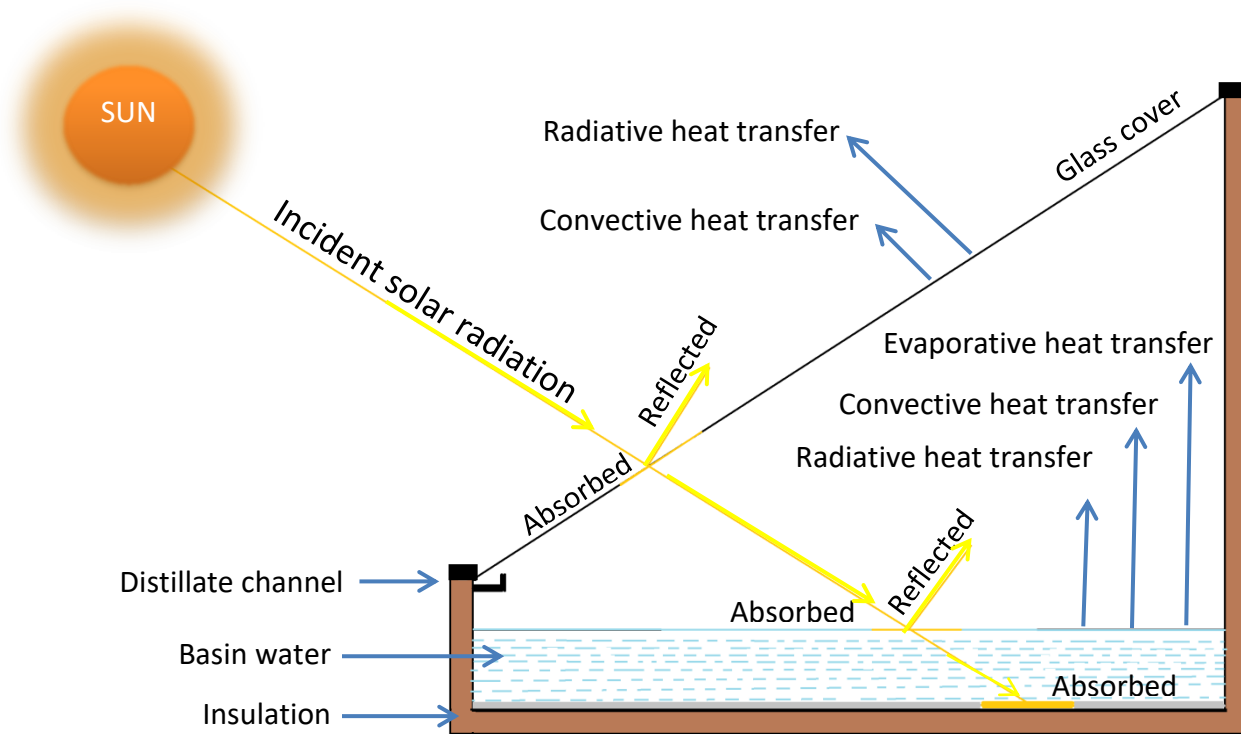


Figure 1.1. Basin type single slope solar still.

### 1.3. Classification of solar still

Solar stills can be categorised into two categories, passive solar still and active solar stills. Further they are classified into various modifications explained below. All of them work on the same principle of natural water cycle. The condensed water collected on the inner surface of the glass cover is collected through the distillate channel and then it is collected outside. Solar stills are classified as:

#### 1.3.1 Passive solar still

A conventional solar still, which uses only sun's energy for the conversion of brackish water into pure water. No external energy is used in passive type of solar stills [2].

Various modifications like change in construction, using wick systems, integrating double glass covers, installing reflective plates, etc. can be made to enhance the productivity of the still.

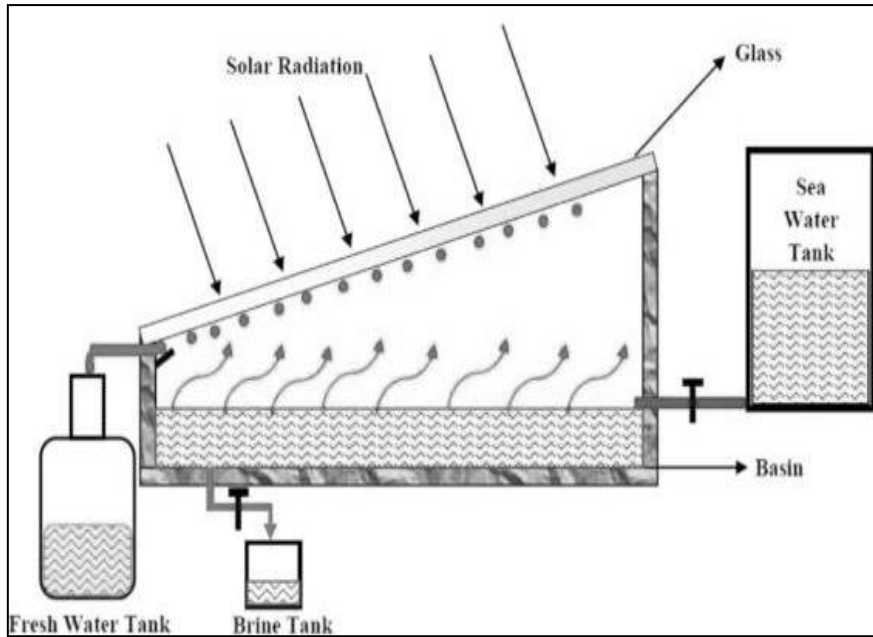


Figure 1.2. Passive type solar still [2].

### 1.3.2 Active solar still

Solar still using both natural and externally provided energy for the conversion of brackish water into pure water is termed as active solar still. For example, still attached with solar collector as shown in figure 1.3 is an active type of solar still [3].

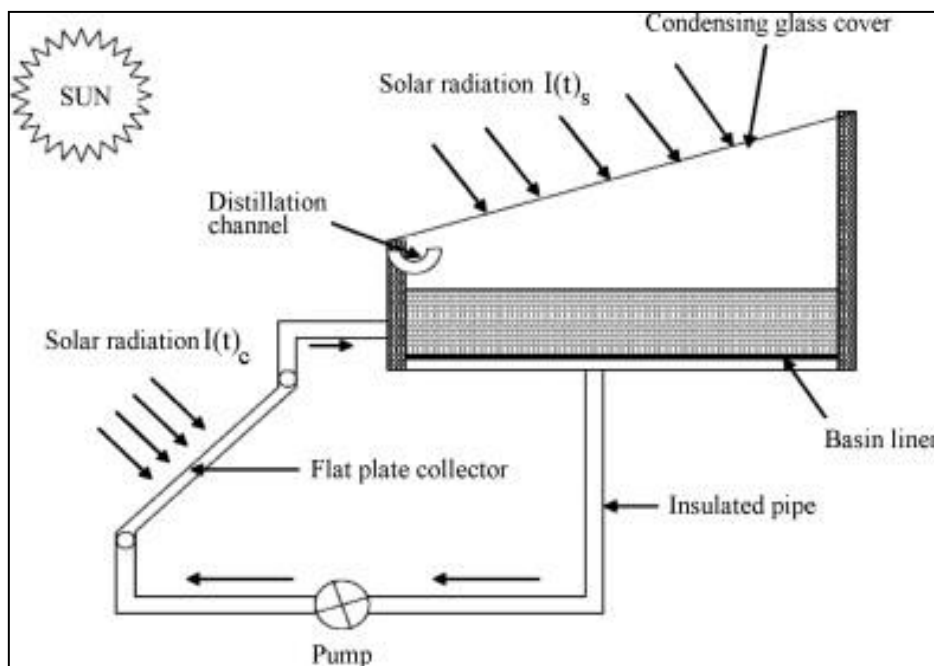


Figure 1.3. Active type solar still [3].

### **1.3.3. Classification of solar still based on modifications**

The solar still in the two main categories i.e. Active solar still and Passive solar still, as explained above, can be modified as follows.

#### **1.3.3.1. Single slope single basin solar still**

Still having one transparent glass cover as a condenser over which condensate is collected, and only one water basin is known as single slope single basin type solar still. The main components of single basin solar still are water basin, transparent cover, side insulations, collector tank, basin liner and supply of water. Transparent cover attached must have a high value of solar transmittance, for the radiations to pass through [3].

#### **1.3.4. Double slope solar still**

Still having two glass cover as a condenser over which condensate is collected, and only one water basin is known as double slope single basin solar still. Normally one side of the glass cover is placed in the Sun's trajectory and the other side is constructed in the opposite direction.

The efficiency of the still improves when two glass covers, as a condenser are used and the working of the still remains alike to that of single slope solar still [3]. Dwivedi et al. [4] investigates the working of double slope passive type solar still at three water levels. It was observed that, in the times of summers the performance of double slope solar still is more but the annual yield production of single slope solar still is greater than double slope solar still.

#### **1.3.5. Multi effect solar still**

The functionality of the still remains the same to that of simple single glass solar still. But instead of having one water basin this type of still have multiple basins. Earlier the latent heat of vaporisation released at the inner side of the glass cover directly dissipates to the ambient, but in these systems there exists multiple confinements. The latent heat of condensation released by the bottom confinement acts as a heat source for the upper basin and this creates multiple effect condensation. Basin liner of the upper confinement should be transparent so that solar radiations can reach to the bottom of the still [3].

### **1.3.6. Wick type solar still**

Solar still having wicks, suspended on the surface of the water are known as wick type solar stills. A portion of the sun's incident radiations gets absorbed by the exposed surface of the wick and the remaining energy is transmitted through the warm water, which is exposed to the direct solar incident radiation.

Water because of capillary action rises upward to the top surface of wick, due to which the evaporation area increases and hence distillate output [5]. Nafey et al. [6] used same kind of arrangement in his experiments, and found some major enhancements. Five floating wicks and a thin blackened sheet for absorber plate are used, and he observed 15% increase in yield produced with 3 cm of water depth and 40% increase in distillate output with 6 cm water depth.

## **1.4. Modified solar still by seeding Nanofluid**

Integrating nanoparticles with the solar still, is a hot topic for research because of its high heat transfer rates and transport properties.

Seeding Nano particles in base fluid enhances convective heat transfer coefficients, because of rise in the effective thermal conductivity of the Nano-fluid, resulting in higher performances. Performance of the still depends upon some parameters, like the volume fraction, particle size, and thermo-physical properties like specific heat capacity, viscosity of the fluid, and specific density. Nanoparticle generally is defined as the ratio, of its surface area to the volume, if it's significant then only it is known as Nano-scale material. As this ratio increases properties like thermal conductivity, thermal diffusivity, viscosity, electric conductance, optical sensitivity changes [7].

### **1.4.1 Effects of Nanofluid in solar stills**

Nanoparticles are the tiny particles of size in the range of 1 to 100 Nano-meters (nm). As the particle size decreases the transport and physical property of the particle changes, which affects the performance of the still. Every nanoparticle size has different wavelength at which it absorbs maximum solar energy, which is known as resonant wavelength. So size of the nanoparticle is an important parameter [7].

- Specific heat capacity of the fluid has a great effect on the efficiency of solar still. When solar incident radiations hit the surface, a portion of the sun's energy gets

absorbed in sensible heating and remaining goes into latent heat storage. Satisfying the equation  $Q = mC_p\Delta T$ , the less the specific heat the higher the temperature rises, which creates temperature gradient between glass cover and water [8].

- Thermal conductivity of the Nanoparticle increases when surface area to volume ratio increases, which means as size goes down, the performance of the solar still having nanofluid improves [9].
- Using metallic Nanoparticle of different sizes helps solar still to capture all the incident range because of different resonant wave length to each size [7].

## **1.5. Motivation for present research work**

Declining water quality and increased consumption rates creates a problematic situation to overcome the demand of potable water. Due to which large purification systems are needed to be installed all around the globe. Conventional energy source is not always possible in remote areas due to difficulties in the supply of fossil fuels and unavailability of electricity. In such cases using renewable energy sources, such as solar still working with solar energy for desalination is the best resort.

During the past few decades, researchers have focussed on investigating the possibility of improvement in solar stills. Various modifications had been done to improve its performance. This work is motivated by the need for potable water demand, featuring an energy efficient technology for solar energy in desalination field.

## **1.6. Research objectives**

The present work has been carried out to develop a thermal model for the performance analysis of a simple, single slope solar still (Passive type), first without Nanofluid and then with Nanofluid. This work investigates following objectives:

1. To study and investigate the performance of the solar still at different basin water depths and to optimise it for maximum performance.
2. To study and investigate the effects of different nanofluids and to optimise its volume concentration for maximum performance.
3. To study and investigate the performance of modified still having nanofluids with the conventional still.

## **1.7. Organisation of thesis**

The present study is divided into 5 chapters as given below:

### **Chapter 1**

This chapter presents the overview to the subject, advantages and incorporation of solar still to fulfil today's need. Also the basic working of the solar still is illustrated along with its modifications so as to enhance its performance. This chapter also have small discussion on the effects of nanofluid and its applications along with the motivation towards the work and research objectives.

### **Chapter 2**

This chapter is categorised into three sections. The first segment discusses the workings of various researchers on simple solar still and its types. The second section discusses about the modifications investigated by the researchers to enhance the productivity of the system and third section discusses the various developments in integration of nanofluids and its effects on performance.

### **Chapter 3**

This chapter discusses the novel system description and development of mathematical model for simple single slope solar still. The computational methodology of simulation model has also been presented.

### **Chapter 4**

This chapter deals with the experimental results. Validation of the developed mathematical model with experimental data presented. Selection of nanofluid and the optimum volume concentration for better performance is discussed here. Effects of different nanofluid with different concentrations are presented in graphical form.

### **Chapter 5**

The conclusion drawn from the results of simulation are presented in this chapter along with the scope of future work.

## Chapter 2

### Literature Survey

---

Numerous researchers have carried out a lot of investigations to study various parameters affecting the performance of solar still and this section reviews the literature presenting all the work and conclusions. It permits better understanding to the topic and also acts as the foundation to build it. Presented review deals with various modifications to improve the performance such as use of different types of wick materials, dyes, energy storage materials, nanoparticles and are arranged in chronological order for simplicity and easy comparison.

#### 2.1. Literature review on solar still

Karagiannis et al. [1] studied several types of solar desalination systems, renewable and non-renewable methods to purify water and its cost effectiveness. Also he discussed about the salinity of water and the effectiveness of the system to desalinate it.

Kalogirou et al. [2] reviewed many systems to clean brackish water with the help of renewable energy. The conventional system needs an external source of energy to separate impurities from water, so he conducted his investigations on various industrially tested desalination systems which includes study on solar collectors, photovoltaic, geothermal energy and solar ponds, which comprises of phase change processes like multistage flash, multiple effect boiling and vapour compression, and membrane processes like reverse osmosis and electro dialysis. To his conclusion solar still is the most clean and green type of desalination process.

Xiao et al. [3] reviews different type of solar stills and categorised them into six types based on its design. He then presented fundamental heat and mass transfer process analysis given by Dunkle, Adhikari, Kumar, Elsafty, Tanaka and Zheng. Conclusions as per his studies were installing solar reflectors and solar collectors are more effective where there are low solar radiations and relatively very less ambient temperature, and where there is abundant of solar radiation recovering latent heat, installing heat storage systems and enhancing condensation is more beneficial.

Dwivedi et al. [4] investigates the performance of double slope (passive type) solar still at three different water levels (0.01, 0.02 and 0.03). He then compared the theoretical accrued results with experimental data and found out that, the change in the convective heat transfer

coefficient for water level 0.01 to 0.03 was marginal. It was observed that the yearly yield production of single slope solar still (499.41 kg/m<sup>2</sup>/year) is more than double slope solar still (464.81 kg/m<sup>2</sup>year).

Tiwari et al. [5] analysed the effects of orientation of still and glass cover inclination for the maximum yield, and then compared various internal heat transfer parameters for different glass inclinations. He then concluded that by increasing the inclination angle, yield increases in winter times and vice-versa in summers, and there was a reduction in evaporative heat transfer coefficient with the rise in inclination angle both in summers and winters.

Singh et al. [10] investigated the effects of orientation on the still for a particular location, and efficiency of the still depends upon some parameters like glass cover material, environment condition, insolation per day, direct radiation, orientation of the still, wind speed, glass cover inclination and the specific heat capacity of the still. He observed maximum yield for the inclination angle of 55°, and stated that for east west orientation with inclination angle less than 55° produces maximum distillate, and the instantaneous thermal efficiency of the still decreases with a rise in water depth.

Aboul-Enein [11] investigates the heat transfer through the brackish water in the basin and the heat capacity and gave the optimum basin area and depth. As the depth rises the heat capacity increases and as a result in lower evaporation because of heat entrapment in the water itself resulting in lower yield. For the location (30°47' N) the daily efficiency of the still was found to be 27%. For the same experiment the optimum insulation was calculated to be 0.075 meters, and the optimum inclination angle of the glass cover was found to be 50° in winter and for summers it should be less than 50°.

Samee et al. [12] investigated various design parameters of single basin solar still and observed an optimum cover glass inclination and glass thickness of around 33.3° and 3mm both in summer and winters for the south west arid region. His average distillate output for the month of July, 2004 was 1.7 litres/day with the still basin water area of 0.54 m<sup>2</sup>. Efficiency of the still was found to be 30.66% with the maximum distillate output of 0.34 litre/hr.

Abu-Hijleh et al. [13] observed and performed some experiments which convey that the maximum the temperature difference between the transparent glass and the water basin the maximum is the heat transfer coefficients resulting in higher distillate output and to acquire

that he uses thin water film on the glass cover. The cooling water gains the latent heat while the water vapour is being condensed inside the still. He has also noticed that the efficiency of the water film cooling on the surface of glass cover of the still was not sensitive to the wind speed.

Khalifa et al. [14] observed that water basin depth has a substantial effect on the productivity like it is inversely proportional, and as the water level increases the volumetric heat capacity of the still reduces. He experimented on six different water levels (1, 4, 6, 8, 10 cm) and observed a variation of 48% distillate output.

Tiwari and Anil [15] analyzed seasonal variation of distillate output at different water depths and found that lower water levels absorbs less specific energy and hence produce larger amount of distillate output. He experimented on single slope solar still with an glass inclination angle of  $30^\circ$  and laboratory experiments were conducted throughout the year June-2004 to May-2005 for location New delhi of latitude ( $28^\circ 35'N$ ).

Dunkle et al. [16] gave the correlations for both convective heat transfer coefficient and evaporative heat transfer coefficient with an experimental validation. Multiple effect still was taken for determining the correlation and it was found to be in agreement with 2% variation.

Dwivedi et al. [17] investigates the performance of double slope (passive type) solar still at three water levels (0.01m, 0.02m and 0.03m). He then compared the theoretical accrued results with experimental results and found out that, the change in the convective heat transfer coefficient for water level 0.01 to 0.03 was marginal. He then observed that the annual yield production of single slope solar still ( $499.41 \text{ kg/m}^2/\text{year}$ ) is more than double slope solar still ( $464.81 \text{ kg/m}^2/\text{year}$ ).

Kumar et al. [18] presents the yearly performance of an active solar still for the location New Delhi, he observed that, an annual distillate is maximum for the solar collector with an angle of  $20^\circ$  and solar still with an angle of  $15^\circ$ .

Singh et al. [19] purposed an experimental and theoretical model on double slope solar still with an glass cover inclination of  $55^\circ$ . For thermal modelling of the still all the climatic parameters were simulated and observed a maximum distillate output for east west orientation with an angle of  $55^\circ$ . He observed that the instantaneous thermal efficiency rises with an increase of inclination angle of the still.

Sakthovel et al. [20] observed and purposed a thermal model to improve and understand the energy transfer by using jute cloth in the water medium, which maximises the surface area of water and helps in getting more evaporation rates. He kept jute type of cloth in a vertical position in the middle area of the still. Water in contact with cloth, rises upward because of capillary action some of the solar energy incident on the jute cloth results in rise of its temperature which then helps in evaporation of water being in contact with cloth.

Srivastava et al. [21] purposed an experimental setup with multiple porous floating absorbers and did its thermal modelling, by incorporating absorbers he observed some enhancements in the evaporation rates, because of its large surface area it requires very less time for evaporation. In these systems there is the problem of clogging salts in the porous material. As water evaporates, it leaves some salts behind which then accumulates in the spaces of the material, which after some time gives a performance decline. Due to this salt accumulation more heat is needed for the water to get evaporated, because of salts and impurities. So a regular cleaning of the setup is needed for the better results.

Aboul et al. [22] investigates the effects of deep basin solar still, and witnessed that daylight productivity of the still is less. The water inside still stores the energy during day, and during the nights that same energy is utilised to heat up the remaining water. But after some certain water depth the productivity decreases and there is more chances of heat to be lost in ambient because of increase in surface contact. The optimum glass cover angle was found to be  $50^\circ$  and  $10^\circ$  during winters and summers, and daily efficiency of the still was about 27%.

El-Bahi et al. [23] experimented with double glass on solar still which was really helpful as it helps minimising the solar irradiation leaks, he integrates a separate condenser inside still in vertical position and added a reflective surface, so as to get max solar intensity on the evaporator. After all the efforts he had observed an increase in efficiency of about 48% when only condenser is used and 70% when condenser is cooled by flowing water.

Abu-Arabi et al. [24] investigates on double glass (passive type) solar still with added film cooling effect on the glasses, this helps condensed water to release energy in more rapid manner. There was witnessed an increase in the overall efficiency of the system, and observed an increase in productivity of around 34% when the flowing brine water is at  $25^\circ\text{C}$ . This experiment shows a slight increase in productivity, and it was inferred that the performance of the still depends upon the lever of insulation used. Efficiency for the still

having perfect air tight insulation is more as compared to the double glass, but after certain level of heat loss double glass is efficient.

Aggarwal et al. [25] offered a thermal model on double condensing surface still with double glazing, one of the condensing chamber is fitted behind the back wall of the solar still, which has a steel based condensing plate. He observed and formulated a conclusion, that having second condenser helps to generate more condensate, as it is on the darker side of the still hence is cooler than the other condenser, so water vapour gets condensed on the surface of the condenser and an increase in 46% of productivity is observed. In the same work he calculated the C and n values for the equation  $Nu = C (Gr \cdot Pr)^n$ .

Integrating floating wick, coloured dyes, suspended absorbers, jute cloth, and fins increases the overall efficiency of a still and the distillate output. Many researchers have worked on these systems, some developed thermal model and some of them performed experiments. Each of the system works on different phenomenon, jute cloth and wick works on capillary action and increases the evaporation area of the basin, coloured dyes enhances the solar absorptivity of the water, whereas fins covered with cloth again increases the evaporation area of the still.

Nafey et al. [26] established a thermal model to estimate distillate output of the still having five floating balls and a thin sheet of black colour, which gets heated rapidly as solar irradiation falls on it. He observed a reduction in the heat loss, as the inner side of the plate is cooler and there is very high temperature on the outer side. He simulated this on two water depths, and get 15% increase in distillate output when water depth is 3 cm and 40% when still has 6 cm of water in it.

El-Sebaili [27] worked on the still having suspended absorber this divides the water in two halves, the water in the lower half raises through the vents in the absorber to the upper side, where all the evaporation is carried out. There is this increase in daily productivity of 18.5-20% and his thermal model variation was 8%. The best position for baffle type absorber was found to be in the middle of the solar still.

Velmurugan et al. [28] utilized five fin in his experiment, the performance of the still is then compared to the arrangement where sponges are used, he had also developed the theoretical

model on the same, and observed an increase of 15.3% efficiency when sponges were used, 29.6% when wicks were used and 45.5% when fins were used, with a total deviation of 6.2%, 10.8%, and 9.2% with his experimental data to that of theoretical model. Wick type of system works on capillary action and increases the evaporation area of the basin.

Srivastava et al. [29] conducted some experiments on still having extended porous fins and compared those results for winter and summer season. Finding out a considerable difference in distillate produced, 48% in the month of Feb and 56% in the month of May.  $7.5 \text{ kg/m}^2/\text{day}$  was the maximum distillate output achieved in the month of May and in the case of modified solar still, where he used polystyrene foam with excellent insulating properties. Also the distillate production increased with the decrease in water levels.

Al-Hussaini et al. [30] created vacuum inside the controlled volume of the solar still and he then observed some changes in the productivity. Earlier heat transfer in the still was through evaporation of water, convection and radiation but by creating vacuum the heat transfer happened only through evaporation and radiation. This system totally eliminates the convective heat transfer, because of which evaporative and radiative heat transfer values increases. He observed an increase of more than 100% when vacuum was created.

Abu-Qudais et al. [31] offered a thermal model for the still where external condensing surface was used, and predicts its overall efficiency and the mass of distillate obtained. He then used a low powered, speed variable fan in the still and had created a separate confinement for the condensation process. The fan installed pushes water vapours from the still to the external condenser with the help of which he found 47% higher yield.

Haddad et al. [32] suggested a thermal model of still having heat storage tank, which was used as an external condensing surface. He also integrates a low power, varying speed fan in the still and created a separate confinement for the condensation process, the fan pushes water vapours from still to external condenser where he found 47% higher yield. This condenser is then cooled while there was no sunshine using radiative cooling panels, with the help of cooled circulating water into the packed bed. At end of the cooling processes the temperature attained by the bed is close to the effective sky temperature. The water in the still may evaporate at low temperatures, provided that the basin water temperature is higher than the saturation temperature corresponding to the vapour partial pressure. He had made some conclusions such as productivity of the still increases with the rise in the solar intensity, but efficiency of still decreases, because of enhanced thermal losses to ambient.

Mousa et al. [33] experimented on the still having film cooling, as the external source cools the glass surface and the external condensing surface is cooled during the night time using radiative cooling panels with the help of circulating water. He observed some decrease in instantaneous efficiencies of the still when solar intensity is at peak. He then concluded that the still efficiency may increase by 20% provided proper use of film cooling, because flowing water cancels the effect of wind on the still.

El-Sebaili et al. [34] investigates on an active solar still, he provided heat in the still during the night time, when there is no solar irradiation present. The heat exchanged during the night time with the help of solar collector elevates the temperature of water which further increases the temperature gradient, hence increasing evaporation rates and results in higher yields. On a summer day he collected a distillate output of  $4\text{kg}/\text{m}^2/\text{day}$  with a day efficiency of 37.8%. the yearly productivity of the still was increased by 23.8% when storage medium is used.

Tanaka et al. [35] worked on simple solar still with both external and internal solar reflectors. Both the reflectors direct all the solar incident radiation into the still, because of which he observed an increase in efficiency of 48% when both the reflectors were used and 22% when only one of them was used.

Shukla et al. [36] experimented on double slope solar still, and determined, internal heat transfer coefficients for the experimental setup by calculating C and n values for the equation  $Nu = C(Gr * Pr)^n$  by mathematical regression model. He concluded from his research that for the estimation of convective and evaporative heat transfer coefficients inner glass temperature is more suited because of the poor thermal conductivity of the cover glass.

Tiwari et al. [37] experimented with simple solar still installed with dyes of different kinds, and by adding it the still shows improvement in the energy storage capacity and hence in productivity of the still. He observed a dominance of evaporative heat transfer fraction for the temperature range of 32-37 °C.

Kumar et al. [38] added charcoal pieces in the basin and using wick material to maximize evaporation rate he was working with active type of still which has charcoal pieces in it. Adding charcoal or some kind of wick system surely improves the performance and gives a significant yield enhancement.

Okeke et al. [39] used Black naphthylamine dyes at 172.5 ppm in the water basin for heat absorption, with this modification he got an increase of 29% in production rate compared to working on simple solar still seeded with coal powder.

Rajvanshi et al. [40] concluded from his research, that heat capacity of the still increases by adding the naphthylamine dye and productivity of the still also increases. The experiment and simulated data shows an increase of productivity by adding dye up to a concentration level of 500 ppm, after which it becomes independent of concentrations.

Murugavel et al. [41] increased the productivity by 15.3% with the help of sponges. The maximum deviance between the experimental and theoretical results was 10.2%. Putting sponges inside the still, increases the surface area for evaporation process, because of which evaporation rate enhances. But after some time the pores in the sponges gets filled by the impurities which reduces the performance.

Sodha et al. [42] used multiwick system and observed that average days yield of the still, with mica as the absorber increases by 42% (because of increased evaporative surface area) in comparison with conventional solar still having only water. Output of the modified still (having mica) was less reliant on the thickness of the plate but mostly it depends on the exposed surface area to the radiation.

Sometimes seeding Nano particles in base fluid enhances heat transfer coefficients and results in higher performances. Performance of the still depends upon some properties like the volume fraction, particle size, thermo physical properties like specific heat capacity, viscosity, and density of the Nano fluid. As nanoparticles has a property of coagulation, after some time stability and the flow behaviour changes which affect all the heat transfer properties therefore it is said that, sometimes seeding Nano-particles enhances the performance and vies-versa so as to overcome this problem some surfactant are used which stabilises nanofluid. Some of the researchers really worked hard for the performance analysis and some of the observations are being made. Nanoparticle is generally defined as the ratio of its surface to the volume, if its significant then only we can call it as Nano-scale material as this ratio increases properties like thermal conductivity, thermal diffusivity, viscosity, electric conductance, optical sensitivity changes.

Sahota et al. [43] uses three different nanoparticles ( $\text{Al}_2\text{O}_3$ ,  $\text{TiO}_2$ ,  $\text{CuO}$ ) with various volume fractions (0.01, 0.093, 0.131) and observed a rise in convective heat transfer coefficient by 67.03%, 63.56%, and 71.23%. and he also observed an increase in Nusselt number by 119.72%, 98.64%, and 151.62%.

Elango et al. [44] used various nanofluids and observed significant performance increase because of enhancement of surface to the volume ratio of the nanoparticle, which elevates the heat transfer properties and he observed a performance increase of 29.95%, 12.67% and 18.63% while using  $\text{Al}_2\text{O}_3$ ,  $\text{ZnO}$ ,  $\text{SnO}_2$ .

Sahota et al. [45] observed an decrease in entropy generation when  $\text{CuO}$  nanoparticle is used and he observed an performance trend of  $\text{CuO} > \text{TiO}_2 > \text{Al}_2\text{O}_3 > \text{SiO}_2$ . Heat transfer coefficients increases with the rise in volume fraction and concentration of the Nanoparticles. He also observed a problem of sedimentation, dispersion, and clustering of Nanoparticles which needs more complex design for maintainance.

Elango et al. [46] uses single slope solar still and found out that oxides are better photocatalysts then sulfides and dyes. Tray coated with metal sulfides like lead sulfides,  $\text{CuS}$ ,  $\text{Bi}_2\text{S}_3$  and  $\text{Sb}_2\text{S}_3$  shows great enhancement of performance. And  $\text{Al}_2\text{O}_3$ ,  $\text{ZnO}$ ,  $\text{SnO}_2$  shows 29.5%, 12% and 18% performance increase.

Omid et al. [47] reviews different nanofluids in the field of solar still. Nanoparticles has a peak absorption characteristics on a particular wavelength, with the change in diametrical size resonance nature changes. He observed that using nanofluid with optimum volume fraction transport and thermal properties enhances.

Omara et al. [48] uses solar still integrated with nanofluid and corrugated wick. He provides vacuum inside the controlled volume of the still which minimises convective heat transfer coefficients and as a result evaporative heat transfer coefficients increases. Wick system maximise the surface area and hence increases its productivity. Problem of clogging and clustering of nanoparticle with wick is seen.

Kabeel et al. [49] modifies solar still with external condenser. External condenser improves the performance with a very little input power, while nanofluid enhanced its thermal and transport properties. Integrating only external condenser enhances daily yield by 53.2% and integrating both was providing 116% enhancement.

Sharshir et al. [50] works with simple solar still with nanoparticles and glass cover film cooling effect. He used graphite and copper oxide flakes at various concentrations (0.125, 0.2) and different water cooling rates (1-12 kg/hr) and experienced a productivity increase of 44.91% and 53.95%. And if only nanoparticles are used there is an increase of productivity of 38% and 40%.

Elango et al. [51] observed, that aluminium oxide has produced more distillate output with an efficiency of 29.95% as compared to the other two nanoparticles Zinc oxide, and Tin oxide. They enhance the performance by 12.67 and 18.63% in case of single basin single condenser solar still with and without water based Nano-fluid.

Sahota et al. [52] studied different volume concentrations (0.04, 0.08, and 0.12%) and at various masses of water (35 kg, 80 kg), and they were taken for the experimental studies. He observed best results for the volume concentration of 0.08% with an efficiency of 12.2 and 8.4%. While taking 80kg during experiment he observed less efficiency as compared to 35 kg, because maximum of heat was trapped in the form of latent heat inside water he used passive double slope solar still with Al<sub>2</sub>O<sub>3</sub> Nanoparticle.

Rashidi et al. [53] used stepped solar still integrated with nanofluids, and he performed a CFD analysis on stepped type of solar still and analysed all the energy equations and got a result of 22% productivity increase for an hour variation. When nanoparticle concentration is increased from 0-5%. There is only 2.1 % variation between his experimental and simulated work.

Chen et al. [54] reviews optical and thermal properties of nanofluid. He observed that SiC nanoparticle has a good effect for enhancing both thermal (6% increase with 0.4% volume fraction) and transport properties. With the increase of salinity of the water, stability and thermal conductivity decreases. Optimum concentration of SiC nanoparticle with natural sea water is found to be 0.4%.

Kabeel et al. [55] worked with absorber plate coated with black nanoparticle. He observed that Nanoparticle has a great thermal property and conductance so, absorber plate coated with black nanoparticles enhances the absorptivity and increases the temperature without utilizing it in increasing its latent energy. Increases the still efficiency by 16% to 25% when 10% and 40% weight percentage nanoparticle is used.

Liu et al. [56] has solar collector integrated with nanoparticle. Observed a constant 10 °C rise in temperature of nanofluid with distilled water, which indicates that nanofluids can hold more heat energy. ZnO with the concentration ratio 0.2% by volume was found to be optimum for solar collectors.

Rufuss et al. [57] enhanced the performance with nanoparticle enhanced phase change material in solar still. So Nanoparticle seeded with the motive to add some heat energy in the form of latent heat as a storage medium. 35% of improvement was seen when CuO type nanoparticle is used as storage medium. 1.96 kg/0.5m<sup>2</sup>/day distillate was received and after seeding CuO nanoparticle it was about 2.64 kg/0.5m<sup>2</sup>/day with a significant increase.

Abujazar et al. [58] worked on inclined stepped solar still with copper trays. Performance of around 4.383 kg/m<sup>2</sup>/day was seen. Higher performance was seen because of higher conductivity of copper and, because it was a stepped still the recovered latent heat and the extended surface of step water has a key role for higher production.

Elashmawy et al. [59] used parabolic solar concentrator tracking system integrated with simple solar still (passive type). Parabolic solar trough collector enhances the performance of the solar still by 676% and for the made geometary 4.21, 3.6, and 3.53 kg/m<sup>2</sup>/day of distillate water was recovered. The daily efficiency was found to be 36.65%, 30.22%, and 28.54%.

Haddad et al. [60] experimented on basin type solar still with vertical rotating wick. Rotating wick device was made so as to change the system if required without stopping the operation and if it fails to operate it can still work as passive solar still.

Mahian et al. [61] Simple solar still coupled with solar collector with heat transfer nanofluid. He observed that using heat exchanger with less than 500 °C inlet temperature is found to be not advantageous, on the other hand 700 °C provides more yield. At high temperatures SiC-Water provides more evaporation rates than Cu-Water based nanofluid.

Sahota et al. [62] experimented on (double slope passive type) solar still with water based nanofluid and observed significant improvement in annual yield production of the system and found out an increase in 19.1%, 10.38%, 5.25% increase in productivity while using Al<sub>2</sub>O<sub>3</sub>, TiO<sub>2</sub> and CuO.

From the review, it is vibrant that the still distillate productivity rises with the rise in ambient temperatures and the total solar incident radiations, but with very high incident

radiation still efficiency decreases. For example, increasing the solar incident radiation from 200 to 1000 W/m<sup>2</sup>, which is 5 times the actual value leads to increase in the distillate output of only 3 times. This is due to the rise in the maximum temperature of the basin fluid which leads to higher thermal losses. Secondly, there is some delay in the response of solar still, this is because of the thermal heat storage capacity that absorbs a part of the incident radiation at early times. This heat storage enhances the productivity of still during the second half of the day.

## **2.2. Research gaps**

1. Limited research has been carried out on developing, a mathematical model of single slope solar still having nanofluids.
2. Very few studies have compared the effect of different nanofluid at different volume fractions.

## **2.3. Conclusions**

The above literature presents the work investigating the impact of various parameters like, water depth in the still, orientation and various modifications like, usage of different dyes in water, wick material, sponges and type of nanoparticle used. Following are the specific conclusions:

1. Integrating floating wick, suspended absorbers, jute cloth, and fins increases the overall efficiency of a still and the yield output because of the increased effective evaporative surface area and solar absorbance of the water increases by coloured dyes of black colour.
2. Performance of the still depends upon some properties like the volume fraction, particle size, thermo physical properties like specific heat capacity of the fluid, viscosity of Nano-fluid, and density of the Nano fluid.

### 3.1. Introduction

The effectiveness of the solar still generally depends upon various parameters like, water depth, glass inclination angle, salinity of water, and orientation of the still.

In this chapter, mathematical model has been developed for the following cases:

1. Effect due to water depth on the performance of the solar still.
2. Effect due to Nanofluids and its change in properties on the performance of solar still.

### 3.2. Mathematical model

The performance of the still can be evaluated for any time instance using the energy balances relations. This model attempts to describe the energy transition at every step of the still. Figure 3.1 shows the energy transfer involved in the still.

Assumptions taken during the simulation:

- 1) No vapour leakage from the still.
- 2) The heat capacity of the still has been neglected.
- 3) Reflectivity of the transparent cover and water was assumed to be negligible.
- 4) The absorptivity of the basin water and glass cover was assumed to be negligible.
- 5) There was no temperature gradients along the thickness of glass cover.
- 6) Each component of the system is perfectly insulated including pipes.
- 7) Controlled volume is vapour-leakage proof and is in Quasi-steady state.
- 8) The heat capacity of the transparent glass, insulating materials used in the solar still and the collectors was also assumed to be negligible.

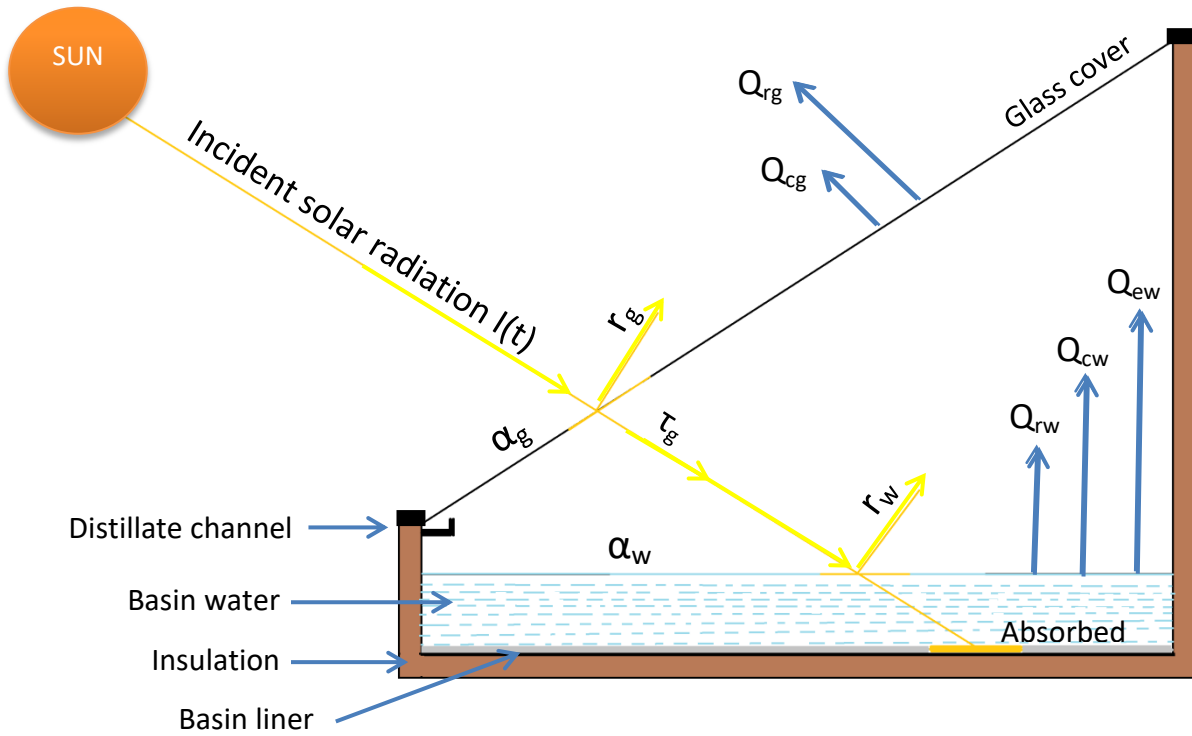


Figure 3.1. Basin type single slope solar still.

### 3.2.1. Internal Heat Transfer

The energy transfer among water and glass in the still is considered as internal energy transfer, and this energy transfer in the form of heat is in three modes.

- 1) Convection heat transfer
- 2) Radiation heat transfer
- 3) Evaporation heat transfer

**Convection heat transfer** involves the fluid in motion.

$$Q_{cw} = h_{cw} \times (T_w - T_{gi}) \quad (3.1)$$

Where,  $h_{cw}$  is the convective heat transfer concerning water and the glass surface.

**Radiation heat transfer** involves the emission of electromagnetic waves.

$$Q_{rw} = h_{rw} \times (T_w - T_{gi}) \quad (3.2)$$

Where,  $h_{rw}$  is the radiative heat transfer coefficient concerning water and inner glass surface.

**Evaporative Heat transfer** happens at the liquid vapour interface, as the vapour pressure is less than the saturation pressure of the liquid at that given temperature.

$$Q_{ew} = h_{ew} \times (T_w - T_{gi}) \quad (3.3)$$

Where,  $h_{ew}$  is the evaporative heat transfer coefficient concerning water and inner glass surface,  $T_w$  and  $T_{gi}$  are the temperatures for water and glass cover.

### 3.2.2. External heat transfer

Heat transfer with the help of convection and radiation process. It is reflected as the loss of energy from the solar still to the atmosphere.

- 1) Top loss heat transfer
- 2) Bottom and side heat transfer

**Top loss heat transfer** the energy transfer from the outer surface of the top cover, and lost to the atmosphere by the means of convection and radiation heat transfer process.

$$Q_{cg} = h_{cg} \times (T_g - T_a) \quad (3.4)$$

$$Q_{rg} = h_{rg} \times (T_g - T_{sky}) \quad (3.5)$$

Where,  $h_{cg}$  is the convective heat transfer concerning outer surface of the transparent cover to the ambient and  $h_{rg}$  is the radiative heat transfer coefficient concerning outer surface of the glass cover and the sky.

**Bottom and side heat transfer** the transfer of energy from water to the ambient through bottom of the still and insulation by the means of conduction, convection and radiation processes.

$$Q_w = h_b \times (T_b - T_a) \quad (3.6)$$

Where,  $h_b$  is the heat transfer from side and bottom insulation to ambient.

Heat transfer is largely categorised as either steady or transient. In steady state heat transfer, the heat flux rests fixed with time but in transient case this is time dependent. Most energy transfer processes come across in practice is transient in nature.

Mass of distillate can also be calculated by only knowing the heat transfer by evaporation and the latent heat of it.

$$m_{ew} = (q_{ew} \times 3600) / LH \quad (3.7)$$

$$\text{Where, } Q_{ew} = h_{ew} \times (T_w - T_{gi}) \quad (3.8)$$

Now, the efficiency for the still is defined as the ratio of the useful energy output to the total energy incident on the surface. The useful energy is defined as the product of distillate output to the latent heat absorbed by it.

$$\eta_{still} = \frac{m_{ew} \times LH}{A_s \times I(t)} \times 100 \quad (3.9)$$

Where,  $I(t)$  is the solar incident radiation for 't' time.

### 3.3. Energy balance

This section elaborates the equations that describe energy transition inside the still to the ambient, and this model further assist us to find the daily distillate productivity and efficiency of the system. Illustrating figure 3.1, the heat balance equations for the still can be written as

#### 3.3.1. Energy balance for basin liner

$$\alpha_b \tau_g \tau_w I(t) A_b = m_b c p_b \frac{dT_b}{dt} + Q_{cb} + Q_w \quad (3.10)$$

Where,  $Q_{cb}$  is the convective heat transfer from basin liner to water, which is calculated as

$$Q_{cb} = h_w A_b (T_b - T_w) \quad (3.11)$$

And  $Q_w$  is the heat lost to the ambient and can be calculated as

$$Q_w = h_b A_b (T_b - T_a) \quad (3.12)$$

$T_b$ ,  $T_a$ ,  $T_w$  are the basin temperature, ambient temperature and water temperature respectively.

#### 3.3.2. The transition energy balance for water mass

$$Q_u + \alpha_w \tau_g I(t) A_w + Q_{cb} = m_w c p_w \frac{dT_w}{dt} + Q_{cw} + Q_{rw} + Q_{ew} \quad (3.13)$$

$Q_u$  is the heat supplied by the solar pond for (active type) solar still.  $Q_u$  for passive type still is zero.  $\tau_g$  is the transmittivity of glass,  $\alpha_w$  is the absorptivity of water and  $I(t)$  is the solar incident for the time interval  $t$  second.

$Q_{cw}$  is the convective heat transfer from water to inner surface of glass which is dependent on vapour pressure on water and glass [16].

$$Q_{cw} = 0.884(T_w - T_g + \frac{(P_w - P_g)(T_w + 273.15)}{(268900 - P_w)}) A_w (T_w - T_g) \quad (3.14)$$

Where,  $P_w$  and  $P_g$  are partial vapour pressure at water surface and the glass cover surface and can be determined as [10].

$$P_w = \exp(25.317 - \frac{5144}{T_w + 273.15}) \quad (3.15)$$

$$P_g = \exp(25.317 - \frac{5144}{T_g + 273.15}) \quad (3.16)$$

$Q_{rw}$  is radiative heat transfer concerning water and inner surface of the glass,  $\varepsilon_{eff}$  is the effective emittance, and  $\sigma$  is the Stefan-Boltzman's constant, and can be calculated as [16]

$$Q_{rw} = \sigma \varepsilon_{eff} A_w ((T_w + 273.15)^4 - (T_g + 273.15)^4) \quad (3.17)$$

$Q_{ew}$  is evaporative heat transfer concerning water and inner glass and can be calculated as [16]

$$Q_{ew} = \frac{0.016237(h_{c,w-g}(P_w - P_g))}{(T_w - T_g)} A_w (T_w - T_g) \quad (3.18)$$

If it's passive solar still,  $Q_u = 0$  which signifies the heat transfer by solar collector or solar pond and it can be calculated as [17]

$$Q_u = A_c F_R (\alpha \tau)_c I(t)' - U_L (T_w - T_a) \quad (3.19)$$

Where,  $I(t)'$  is incident radiation on solar collector surface.

### 3.3.3. Energy balance for glass cover

$$\alpha_g I(t) A_g + Q_{cw} + Q_{rw} + Q_{ew} = m_g c_p g \frac{dT_g}{dt} + Q_{rg} + Q_{cg} \quad (3.20)$$

$Q_{cg}$  is convective heat transfer concerning outer surface of the glass to the ambient, and ‘V’ is the wind velocity [17]

$$Q_{cg} = (2.8 + 3V) A_g (T_g - T_a) \quad (3.21)$$

$Q_{rg}$  is the radiative heat transfer concerning outer surface of the glass cover to the sky [17].

$$Q_{rg} = \sigma \varepsilon_g A_g \left( \frac{(T_g + 273.15)^4 - (T_{sky} + 273.15)^4}{(T_g - T_a)} \right) (T_g - T_a) \quad (3.22)$$

To find the hourly distillate of the still

$$m_d = \frac{h_{ew}(T_w - T_g)}{LH} \times 3600 \quad (3.23)$$

Where, LH is latent heat of vaporisation and can be determined as [17]

$$LH = 2.4935 \times 10^6 (1 - 9.4779 \times 10^{-4} T_w + 1.3132 \times 10^{-7} T_w^2 - 4.7974 \times 10^{-9} T_w^3) \quad (3.24)$$

( If  $T_w < 70^\circ \text{C}$  )

$$LH = 3.1615 \times 10^6 (1 - 7.616 \times 10^{-4} T_w) \quad (3.25)$$

( If  $T_w > 70^\circ \text{C}$  )

A generalised first ODE is developed with the help of energy balance equations (3.10), (3.13) and (3.20) to find temperatures ( $T_w$ ,  $T_g$ ,  $T_b$ ) after time interval  $\Delta t$  [15].

$$\frac{dT_w}{dt} + aT_w = f(t) \quad (3.26)$$

$$a = \frac{A_c F_R + U_{lb} A_b + U_{lg} A_b}{m_w c_w} \quad (3.27)$$

$$f(t) = \frac{A_c F_R (\alpha \tau)_c I'(t)}{m_w c_w} + \frac{(A_c F_R U_l + U_{lb} A_b + U_{lg} A_b) T_a}{m_w c_w} + \frac{(\alpha_g h' + \alpha_w \tau_g + \alpha_b \tau_g \tau_w h A_s I(t))}{m_w c_w} \quad (3.28)$$

Where, equation (3.26) can be written as

$$T_{w(i+1)} = \frac{f(t)}{a} [1 - \exp(-at)] + T_{w(i)} \exp(-at) \quad (3.29)$$

$T_{w(i+1)}$  is the water temperature after  $\Delta t$  time interval.

There are some assumptions made by Tiwari [15]

- Temperature  $T_a$  and intensity  $I(t)$  is assumed to be same for the time period  $\Delta t$  and  $\Delta t$  is taken to be very small.
- $f(t)$  is assumed to be same for the time interval  $\Delta t$ .
- Temperature along the water basin is assumed to be same at every point.
- Specific heat capacities of glass and basin liner was neglected.

### **3.4. Factors affecting the performance of solar still**

- Tilt angle of the glass cover. “It should always be in normal position to the solar incident so that no incident radiation gets reflected,”
- Depth of water. “An important parameter for design the higher the water depth more the energy it store in latent form and less the temperature rise of the water.”
- Cover plate temperature. “The cooler the cover plate will be the larger the temperature gradient will exist and because of which evaporation rate will increase.”
- Convective heat transfer from cover plate and side walls. “Losses to the ambient.”
- Solar tracking. ”maximum incident radiation will get entrapped in the still.”
- External enhancements like condenser, cooler, heat pipe or solar pond.
- Effect of still.” Multi-effect, double slope.”
- Design of structure and its shape.
- Feed water flow rate.
- Coating.

### **3.5. Validating Theories**

#### **3.5.1. Temporal discretisation with a time step of 1 sec**

A mathematical technique adopted for transient conditions that happen to be the field of applied physics and mathematics here transient equations are being solved both by discretizing space and time.

Backward differencing for first order equation is used which is stated as

$$\frac{dT_{w,g,b}}{dt} = \frac{T_{w,g,b(i+1)} - T_{w,g,b(i)}}{\Delta t} \quad (3.30)$$

Where,  $T_{w,g,b}$  is the temperature of water at that instance and  $T_{w,g,b(i+1)}$  is water temperature after  $\Delta t$  time.

Now for temporal discretisation equation (3.10), (3.13) and (3.20) are be written as for the time step of 1 second.

$$T_{w(i+1)} = (A_c F_R (\alpha \tau)_c I(t)' + A_c F_R U_L T_a + \alpha_w (1 - \alpha_g) A_w I(t) + h_{c,b-w} A_w T_b + h_{lw} A_w T_g - h_{c,b-w} A_w T_w - h_{lw} A_w T_w - A_c F_R U_L T_w + \frac{m_w c_w}{\Delta t} T_w) \frac{\Delta t}{m_w c_w} \quad (3.31)$$

$$T_{g(i+1)} = \alpha_g A_g I(t) + h_{lw} A_w T_w + h_{lg} A_g T_a - h_{lw} A_w T_g - h_{lg} A_g T_g + \frac{m_g c_g}{\Delta t} T_g) \frac{\Delta t}{m_g c_g} \quad (3.32)$$

$$T_{b(i+1)} = (\alpha_b (1 - \alpha_g) (1 - \alpha_w) A_b I(t) + h_{c,b-w} A_b T_w + h_b A_b T_a - h_{c,b-w} A_b T_b - h_b A_b T_b + \frac{m_b c_b}{\Delta t} T_b) \frac{\Delta t}{m_b c_b} \quad (3.33)$$

So by knowing the initial temperatures  $T_w$ ,  $T_g$ ,  $T_b$ , and  $T_a$ ,  $I(t)$  for every time interval  $\Delta t$  we can estimate  $T_{w(i+1)}$ ,  $T_{g(i+1)}$ ,  $T_{b(i+1)}$  and further mass of distillate.

### 3.5.2. Numerical Iterative method

This model is based on iterative solution by using the functions given by Kumar and Tiwari [13] which are then employed in this study. Runga kutta method for ODE is used for simulation with the time step of 1 second for accuracy, data of 24 hours is being simulated. Equation (3.10), (3.13) and (3.20) are used which are the  $f(T_g, T_w, T_a, T_b, I(t), t)$  and they then iterated for  $i = 24 * 3600$ .

$$T_w(i + 1) = T_w(i) + (1/6)(k1tw + (2 * k2tw) + (2 * k3tw) + k4tw) * t \quad (3.34)$$

$$T_g(i + 1) = T_g(i) + (1/6)(k1tg + (2 * k2tg) + (2 * k3tg) + k4tg) * t \quad (3.35)$$

$$T_b(i + 1) = T_b(i) + (1/6)(k1tb + (2 * k2tb) + (2 * k3tb) + k4tb) * t \quad (3.36)$$

Where,

$$k1tw = hf(T_w, T_g, T_b, T_a, I(t), t) \quad (3.37)$$

$$k1tg = hf(T_w, T_g, T_b, T_a, I(t), t) \quad (3.38)$$

$$k1tb = hf(T_w, T_g, T_b, T_a, I(t), t) \quad (3.39)$$

$$k2tw = hf\left(T_w + \frac{k1tw}{2}, T_g + \frac{k1tg}{2}, T_b + \frac{k1tb}{2}, T_a, I(t), t + \frac{h}{2}\right) \quad (3.40)$$

$$k2tg = hf\left(T_w + \frac{k1tw}{2}, T_g + \frac{k1tg}{2}, T_b + \frac{k1tb}{2}, T_a, I(t), t + \frac{h}{2}\right) \quad (3.41)$$

$$k2tb = hf\left(T_w + \frac{k1tw}{2}, T_g + \frac{k1tg}{2}, T_b + \frac{k1tb}{2}, T_a, I(t), t + \frac{h}{2}\right) \quad (3.42)$$

$$k3tw = hf\left(T_w + \frac{k2tw}{2}, T_g + \frac{k2tg}{2}, T_b + \frac{k2tb}{2}, T_a, I(t), t + \frac{h}{2}\right) \quad (3.43)$$

$$k3tg = hf\left(T_w + \frac{k2tw}{2}, T_g + \frac{k2tg}{2}, T_b + \frac{k2tb}{2}, T_a, I(t), t + \frac{h}{2}\right) \quad (3.44)$$

$$k3tb = hf\left(T_w + \frac{k2tw}{2}, T_g + \frac{k2tg}{2}, T_b + \frac{k2tb}{2}, T_a, I(t), t + \frac{h}{2}\right) \quad (3.45)$$

$$k4tw = hf(T_w + k3tw, T_g + k3tg, T_b + k3tb, T_a, I(t), t + h) \quad (3.46)$$

$$k4tg = hf(T_w + k3tw, T_g + k3tg, T_b + k3tb, T_a, I(t), t + h) \quad (3.47)$$

$$k4tb = hf(T_w + k3tw, T_g + k3tg, T_b + k3tb, T_a, I(t), t + h) \quad (3.48)$$

In order to validate and see the accuracy of the mathematical model, experiment was conducted on solar still on 14 July 2019, description of the experimental setup and experimental procedure is explained below. Distillate output was measured on hourly basis.

## 3.6. Experimental setup and procedure

### 3.6.1 Design and Construction

Simple single slope solar still have been constructed, basin is made of stainless steel - grade 304 in the shape of rectangular tray. The toughened glass cover was fitted on the top of the section. The sides and base of the tray was insulated with glass wool, rubber type material was used as basin liner of thickness 5 mm, so as to grip maximum solar energy and to transmit that energy to basin water. A constant water level was maintained by a constant head device arrangement. Gasket was installed between the glass cover and the tray, which helps

to ensure there are no gaps between the glass panels. The tray is insulated from the ambient conditions. Figure 3.2 shows the experimental arrangement.



Fig 3.2. Experimental setup of single slope solar still.

The system is oriented towards the south. A window glass was used as a vapour condensing surface, and as a transparent cover from where incident radiation enters into the still. To avoid distillate to fall back to the basin water, a plastic cross section channel is fixed to the bottom of the glass cover.



Fig 3.3. Pyranometer to measure total solar incident radiation.

In addition to this K type thermocouples were used to measure temperatures and a data logger is employed to log all the data, to measure solar intensity pyranometer is used

which logs all the direct radiation and diffused radiations incident on the surface. The whole still is kept insulated, except from its glass cover.

### **3.6.2. Methodology**

An experiment was carried out on simple single basin solar still on the day 14<sup>th</sup> June-2019 at the location Patiala, water level of the still is maintained at 3 cm. The developed thermal model was validated with the corresponding results obtained by the experiment. During the simulation, firstly temporal discretization is being carried out, which is a FEM (finite element method) technique, to get minimum deviation from results. Runge-kutta method is employed with the time step of 0.1 second, which generates lower scope of error because of the closeness in the ambient temperature and intensities for the time gap. The perimeters of both experimental model and thermal model are then compared for the hourly variation of distillate output and heat transfer coefficients.

After validation, the same thermal model is extended to determine the performance while using nanoparticles at different volume fractions. This model is carried out with a assumptions that the value of ambient temperature and solar intensity falling on surface is not changing for  $\Delta t$  time.

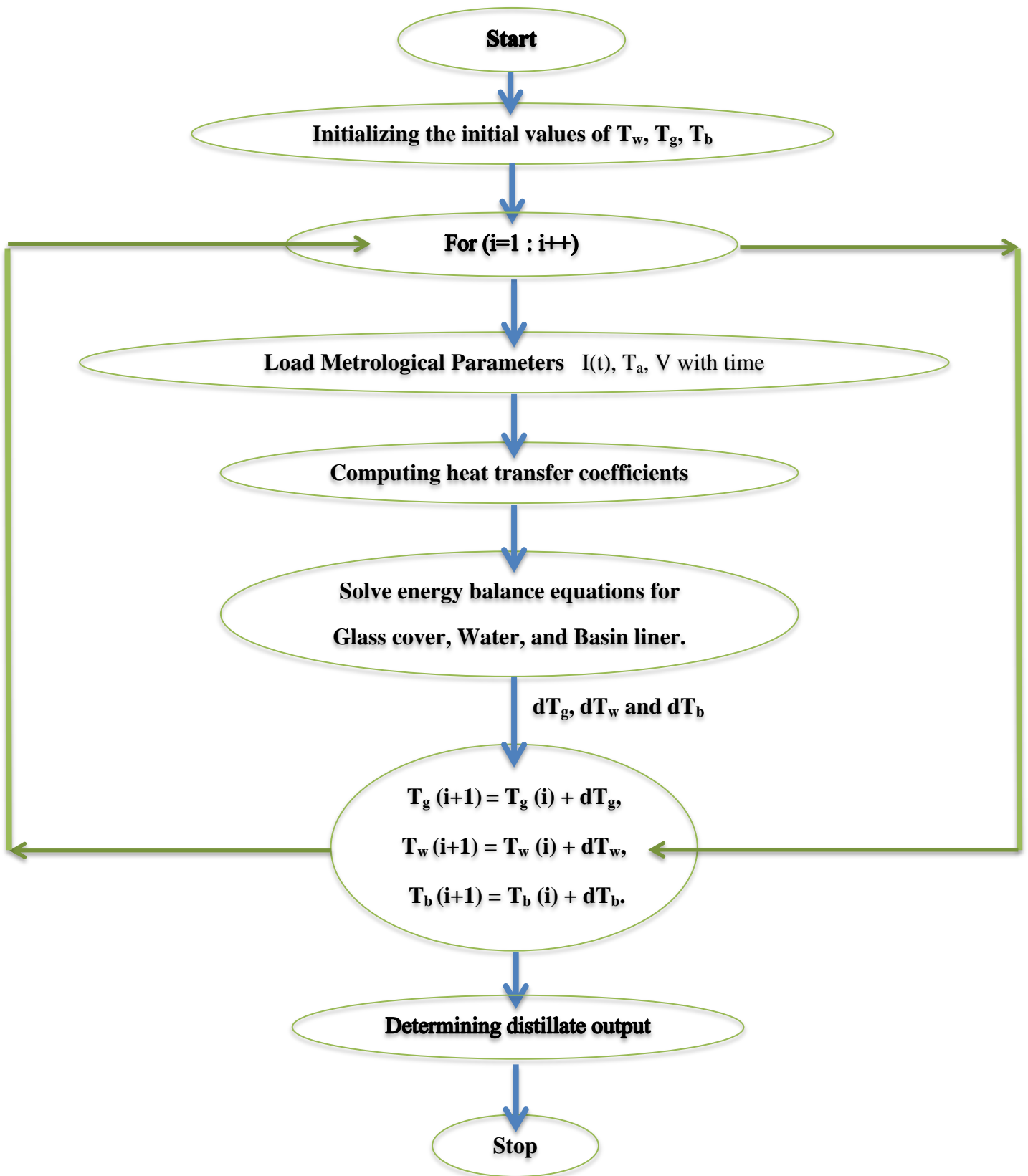


Figure 3.4. Flowchart of thermal modelling.

4.1. Experimental results

An experiment was performed on a single slope solar still (Passive type) with a water depth of 0.03m and glass tilt angle of 30° on 14<sup>th</sup> July, 2019 , total mass of distillate for a day obtained was 3.327 kg/m<sup>2</sup>/day. The hourly variation of solar intensity and ambient temperatures with respect to time are shown in the figures 4.1 and 4.2, it can be comprehended from the graphs that solar intensity and ambient temperature is maximum around 12:00 PM – 01:00 PM respectively. The extreme value of solar intensity was 830 W/m<sup>2</sup> and for ambient temperature it was 41°C.

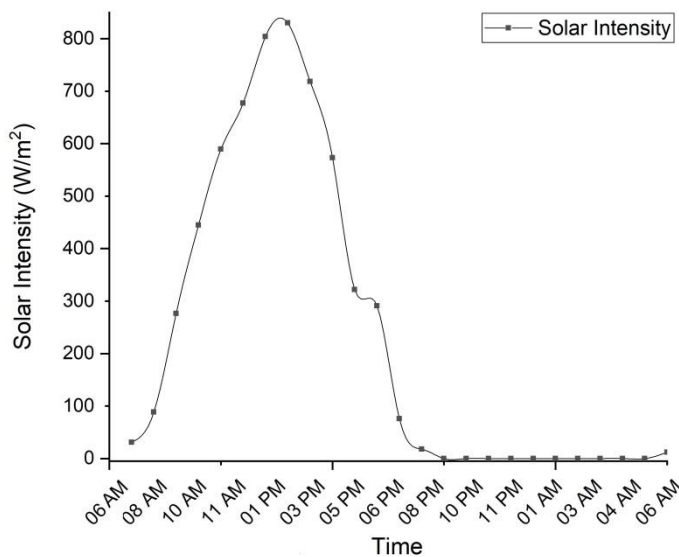


Figure 4.1.Variation of solar intensity on 14<sup>th</sup> July.

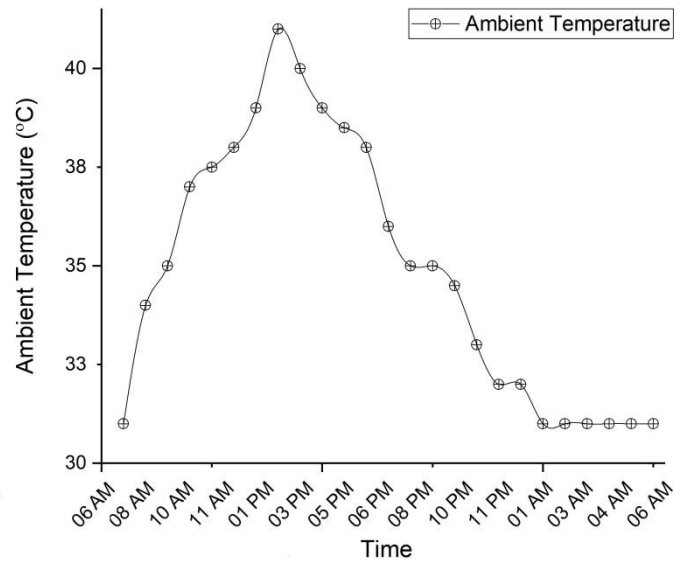


Figure 4.2.Variation of ambient temperature on 14<sup>th</sup> July.

Experimental data is provided in the table 4.1. However, in this study hourly experimental and theoretical observations are compared.

**Table.4.1. Experimental data for single slope solar still :**

<b>Time</b>	<b>T<sub>w</sub></b> <b>(°C)</b>	<b>T<sub>g</sub></b> <b>(°C)</b>	<b>T<sub>a</sub></b> <b>(°C)</b>	<b>I(t)</b> <b>( W/m<sup>2</sup>)</b>	<b>Wind velocity</b> <b>(m/s)</b>	<b>m<sub>d</sub></b> <b>(kg/m<sup>2</sup>/hr)</b>
<b>7am</b>	33	31	31	88.428	0.1	0.013
<b>8am</b>	36	36	34	276.488	0.7	0.0089
<b>9am</b>	43	43	35	444.613	0.9	0.0297
<b>10am</b>	53	51	38	589.351	0.9	0.0952
<b>11am</b>	69	64	38	677	2.5	0.175
<b>12pm</b>	66	59	38	804	0.9	0.258
<b>1pm</b>	71	64	39	830	1.2	0.3011
<b>2pm</b>	77	69	41	718	1.5	0.3324
<b>3pm</b>	76	68	40	573	1.2	0.3823
<b>4pm</b>	68	59	39	322	0.7	0.3812
<b>5pm</b>	62	55	39	291	1	0.3545
<b>6pm</b>	57	49	38	76	1.6	0.3056
<b>7pm</b>	52	45	36	18	0.6	0.201
<b>8pm</b>	47	43	35	0	0.2	0.1158
<b>9pm</b>	46	42	35	0	0.1	0.1012
<b>10pm</b>	42	39	35	0	0.2	0.0698
<b>11pm</b>	40	35	33	0	0.1	0.0512
<b>12am</b>	38	34	32	0	0.1	0.0389
<b>1am</b>	37	33	32	0	0.1	0.0264
<b>2am</b>	36	33	31	0	0.1	0.0185
<b>3am</b>	35	32	31	0	0.1	0.0142
<b>4am</b>	34	31	31	0	0.1	0.0092
<b>5am</b>	34	31	31	0	0.1	0.008
<b>6am</b>	33	31	31	12	0.1	0.0054
<b>7am</b>	33	31	31	31	0.1	0.013

**Table.4.2. Various design parameters of solar still:**

$A_b$	$1 \text{ m}^2$	$r_w$	0.05
$A_s$	$1 \text{ m}^2$	$r_g$	0.05
$A_g$	$A_b/\cos(\beta_s) \text{ m}^2$	$\tau_g$	0.9
<b>Water depth</b>	0.03 m	<b>ul</b>	8
<b>Glass angle</b>	$30^\circ$	$\xi_w$	0.95
$C_w$	4190 (J/kgK)	$\xi_g$	0.94
$C_g$	753 (J/kgK)	$V$	1 m/s
$C_b$	460 (J/kgK)	$\alpha_b$	0.95
$\rho_g$	$1500 \text{ (kg/m}^3\text{)}$	$\alpha_g$	0.05
$\alpha_w$	$1-\tau_w-r_w$		

## 4.2. Validation of Thermal model

As mentioned earlier an experiment was performed on single slope solar still (Passive type) with a water depth of 0.03m and glass tilt angle of  $30^\circ$ . Theoretical model has been developed and compared with the experimental obtained results.

Numerical Iterative model using Runge-kutta ODE integrated with analytical model by Tiwari [12] was studied, which forecasts the values of water temperature and glass temperature in an average deviation range of 8% and 6% presented in figure 4.3 and figure 4.4.

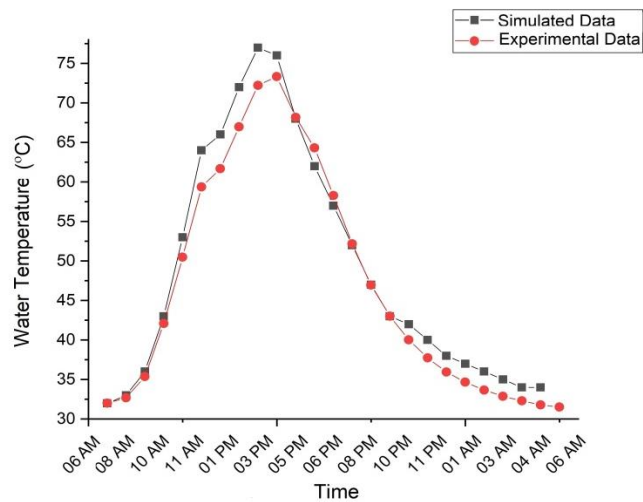


Figure 4.3. Hourly variation of theoretical and experimental water temperature for 0.03m water depth.

From figure 4.3 and figure 4.4 it can be perceived, that at higher temperature ranges the deviation from the experimental results are significant, and this is because of the fact that heat losses from the side insulations increases at higher temperatures.

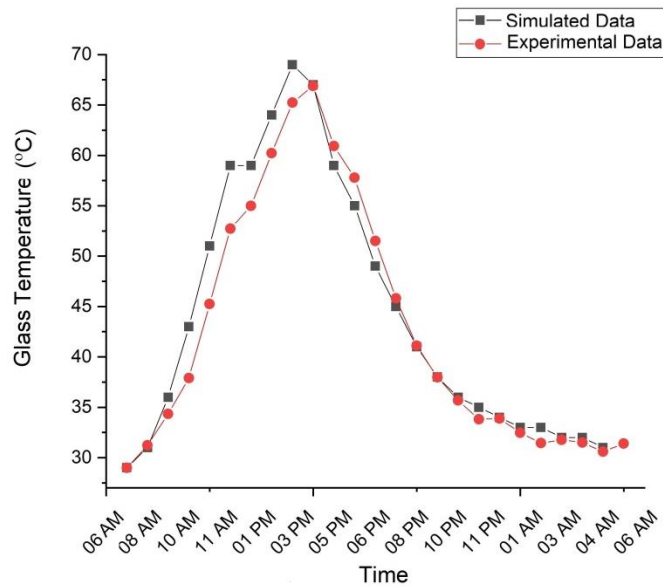


Figure 4.4. Hourly variation of theoretical and experimental glass temperature for 0.03m water depth.

Figure 4.5 displays the variation in theoretical and experimental distillate produced. The total deviation for a day between both the results is around 12.24%. And at higher temperatures the range of deviation is more.

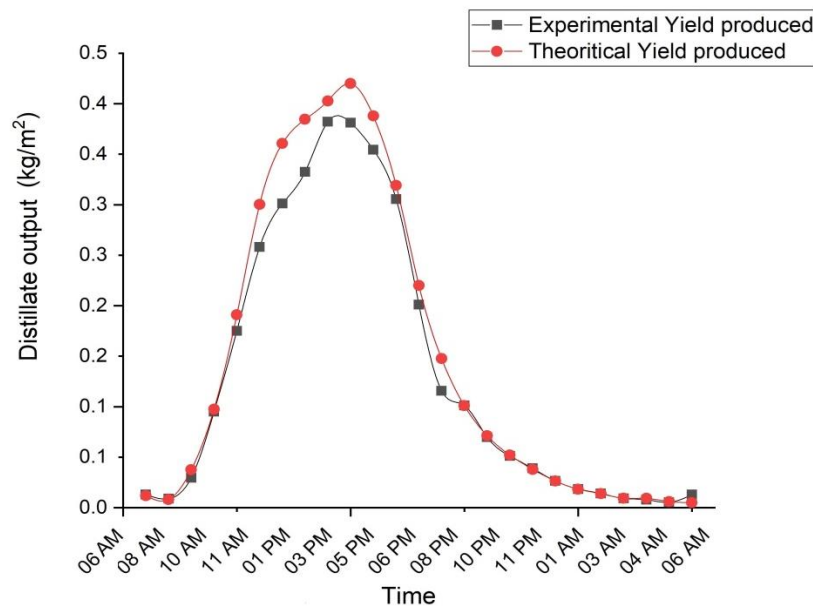


Figure 4.5. Hourly variation of theoretical and experimental distillate output for 0.03m water depth.

### 4.3. Effect of water depth on the performance of the solar still

Performance of the still considerably depends on the water depth, as the level of water in the basin rises the heat storage capacity increases. With the increase in heat storing capacity the maximum temperature obtained during peak intensity of solar radiation decreases, which affects our distillate output.

To obtain optimum water level, a mathematical simulation was carried at different water depths (0.01, 0.02, 0.03, 0.04, 0.05, 0.06, 0.07 and 0.08m). From the results, 0.02m of water level was found to give the maximum distillate output because of the low heat storing capacity. Figure 4.6 shows the difference in mass of distillate at different water depths, and figure 4.7 shows the evaporative heat transfer coefficients.

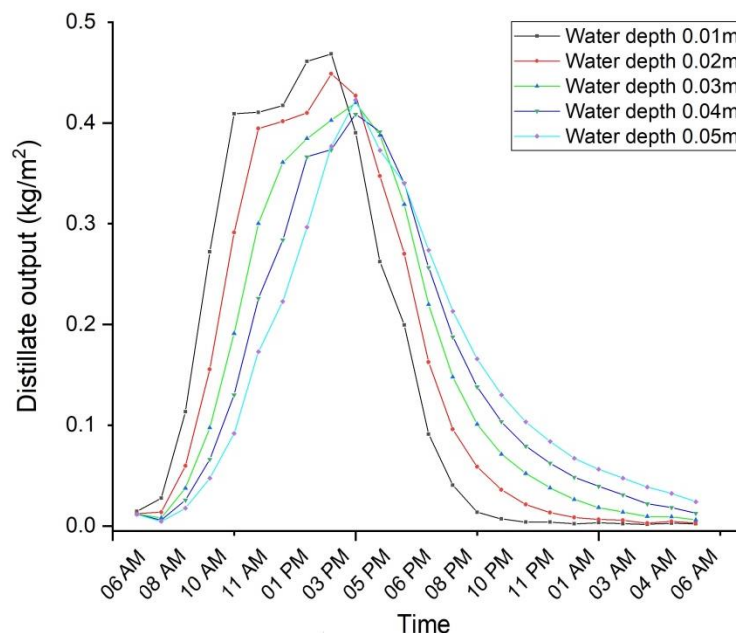


Figure 4.6. Hourly variation of distillate output at different water depths in a solar still.

With the maximum of  $3.65 \text{ kg/m}^2/\text{day}$ , 0.02m water depth is the optimum water level for a solar still, as because of its low specific heat capacity temperature gradient increases. As illustrated in figure 4.6 and at 0.01m water depth, there exists a maximum peak value for distillate produced during the time 12:00 PM - 2:00 PM. As water depth increases the graph shifts towards the right hand side, which is because of the heat storing capacity of water. The maximum distillate output was recorded for 0.02m with  $3.65 \text{ kg/m}^2/\text{day}$  and minimum for 0.08m with  $3.10 \text{ kg/m}^2/\text{day}$ .

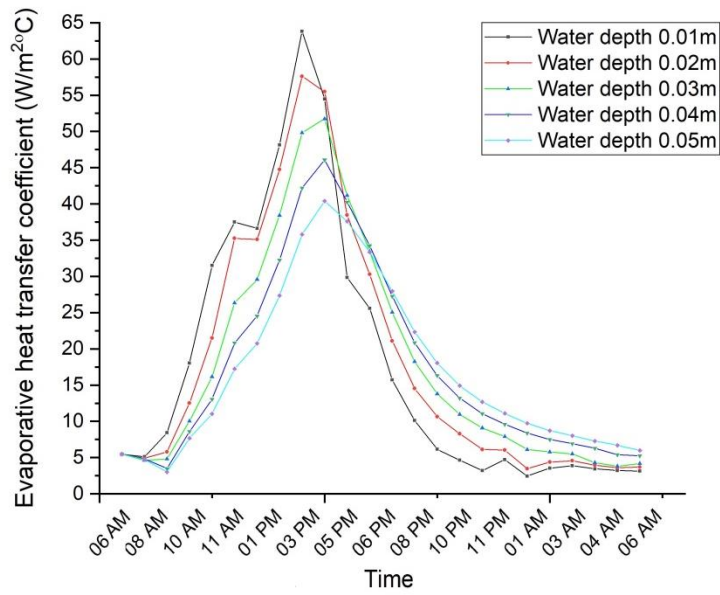


Fig 4.7. Hourly variation in evaporative heat transfer coefficient of solar still at different water depths.

Evaporative heat transfer coefficient, for different water levels is, maximum for the water level at 0.01m having a peak during 2:00PM, followed by 0.02m. Figure 4.7 displays the hourly variation of evaporative heat transfer coefficient.

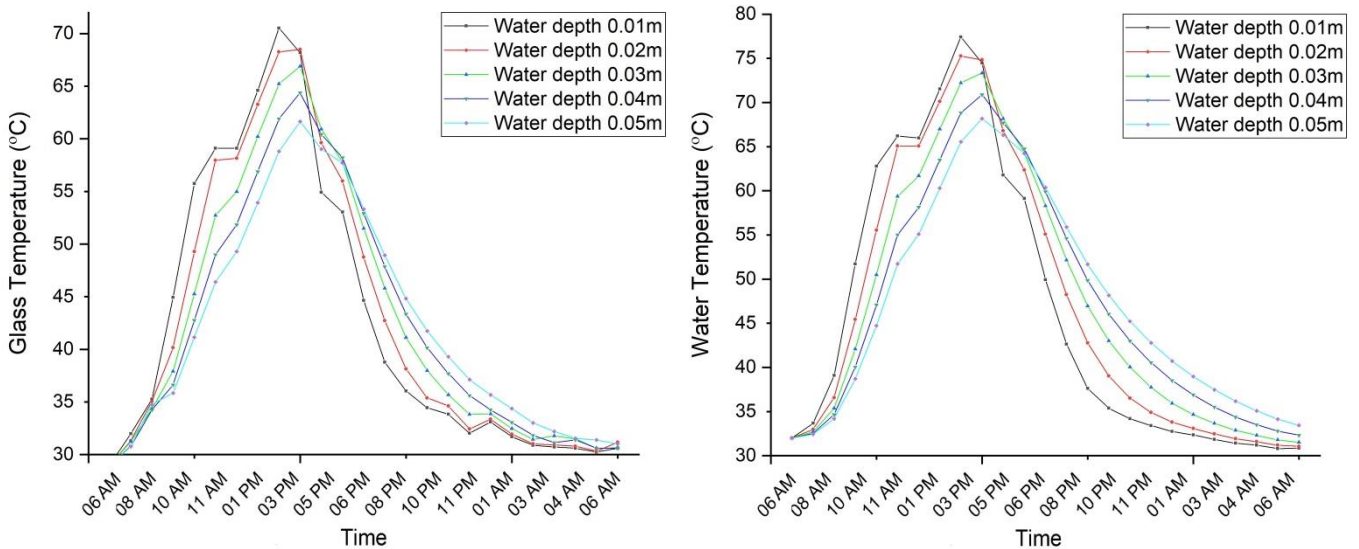


Fig 4.8. Hourly variation in water temperature of solar still at different water depths.

Figure 4.8 illustrates, the hourly variation in water and glass temperatures of the still having different water depths. Because of storage of the heat, the peak value of temperatures shifts downwards for each water level.

As water depth decreases internal heat transfer coefficients increases because of increased water temperatures. Decreased water levels have less heat storage capacity. With the maximum distillate output of 3.65 kg/m<sup>2</sup>/day, 0.02m is the optimum water level to continue mathematical simulation for modified solar still, which is seeded with Nanofluids.

#### **4.4. Variation in the performance of solar still with different Nano-fluids**

Seeding Nano particles in the base fluid enhances heat transfer coefficients and results in higher performances. Still's performance depends upon some parameters like the volume fraction, particle size, and thermo physical properties like heat capacity of fluid, viscosity of fluid, and density of the Nano fluid. Also, increasing the volume concentration of the Nanoparticle, the effective medium (surface area to volume ratio) increases, which contributes to higher efficiencies due to increase in surface area.

Exceeding some levels of concentrations there is a noticeable change in flow resisting properties (with increase in mass concentrations, the flow friction increases), and as a result viscosity increases. Increasing viscosity decreases the heat transfer efficiency and therefore an optimum value of volume fraction is employed [63].

##### **4.4.1. Variations in the performance of solar still with different volume fraction of Al<sub>2</sub>O<sub>3</sub> nanofluid**

Al<sub>2</sub>O<sub>3</sub> nanofluid at different volume fractions (0.02, 0.05, 0.08, 0.12 and 0.2) are simulated in the mathematical model.

In comparison with water, 14.22% increase in distillate was noticed when Al<sub>2</sub>O<sub>3</sub> nanofluid was used. Figure 4.9 displays the variation in yield produced, at different volume fraction of nanofluid. In the given figure the curve for nanofluid at volume fraction 0.2 has shown the maximum yield produced, followed by 0.12, 0.08, 0.05 and minimum for 0.02.

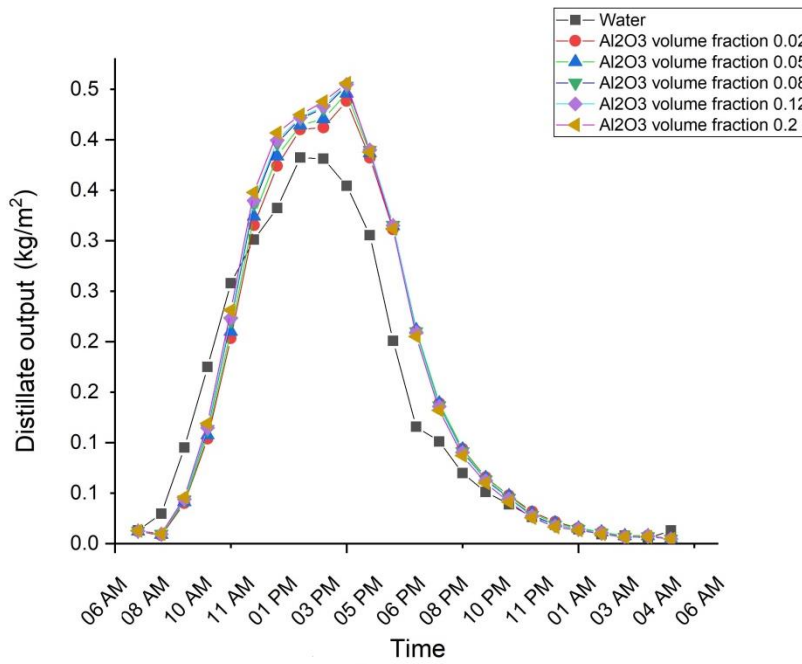


Figure 4.9. Hourly variation of distillate produced by  $\text{Al}_2\text{O}_3$  at different volume fractions.

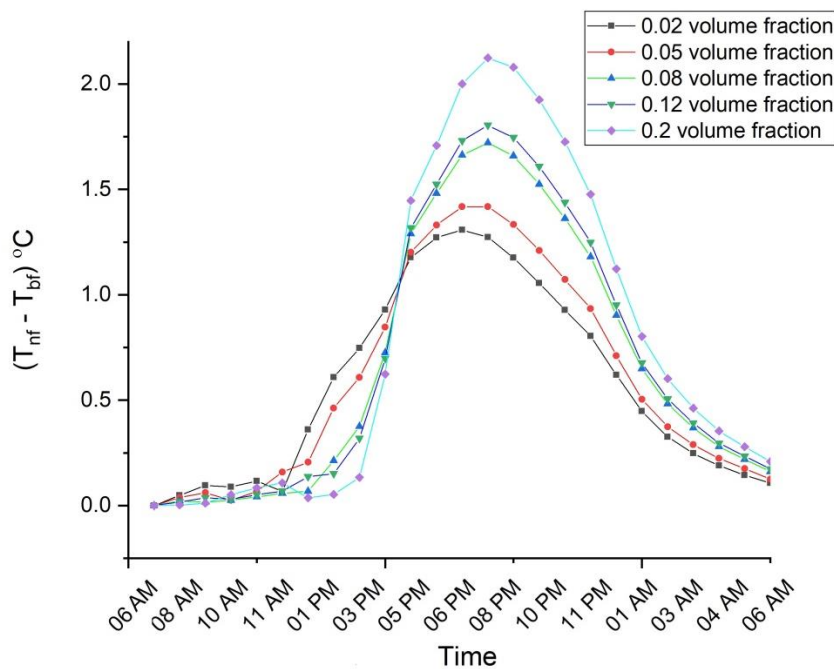


Figure 4.10. Hourly variation of temperature difference  $\Delta T$  between Base-fluid (water) and nanofluid ( $\text{Al}_2\text{O}_3$ ) at different volume fractions.

Figure 4.10 above shows comparison of temperature difference  $\Delta T$  between Base-fluid (water) and Nano-fluid ( $\text{Al}_2\text{O}_3$ ) at different volume concentrations, because of the enhanced thermo-physical properties of Nano-fluid, volume concentration 0.2 shows maximum temperature gradient during the sunshine hours.

#### 4.4.2. Variations in the performance of solar still with different volume fraction of CuO nanofluid

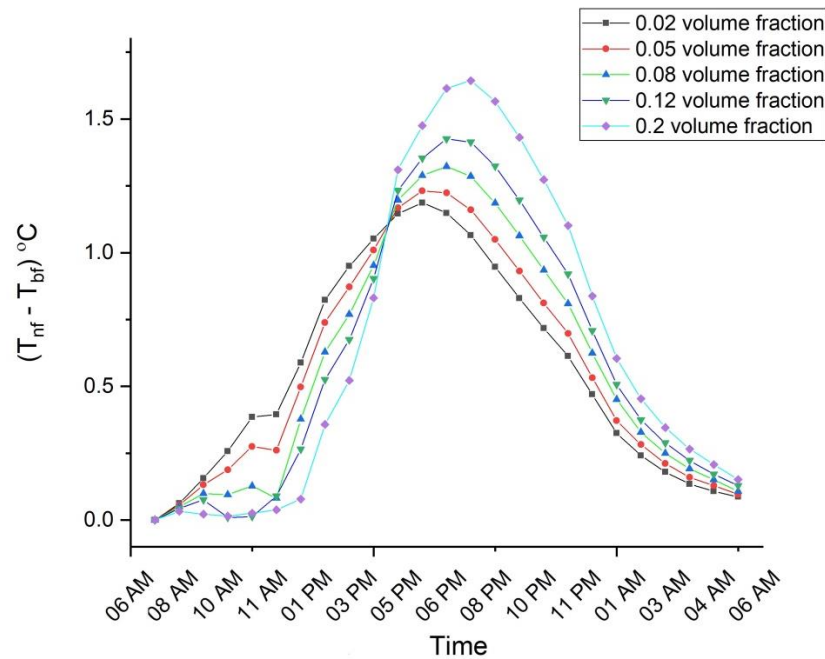


Figure 4.11 Hourly variation of temperature difference  $\Delta T$  between basefluid (water) and nanofluid (CuO) at different volume fractions.

Blending CuO nanoparticles, with base fluid water shows an enhancement in the performance of the solar still. Figure 4.11 shows the hourly deviation of temperature difference  $\Delta T$  between Base-fluid (water) and Nano-fluid (CuO) at different volume fractions. Comparing the curves, the still blended with nanoparticle having 0.2 volume concentration, reaches higher temperature because of its low specific heat capacity and enhanced thermo-physical properties.

Same for figure 4.12 hourly variation of glass temperature is shown, because of high heat transfer rates in comparison with simple water, the energy released at the glass cover is higher and maximum for nanofluid having volume fraction 0.2.

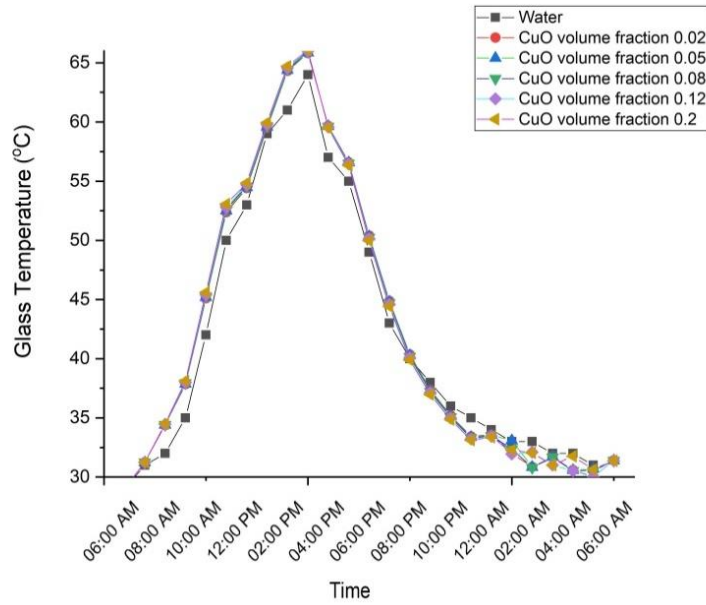


Figure 4.12. Hourly variation of glass temperature of the solar still having simple water and nanofluid.

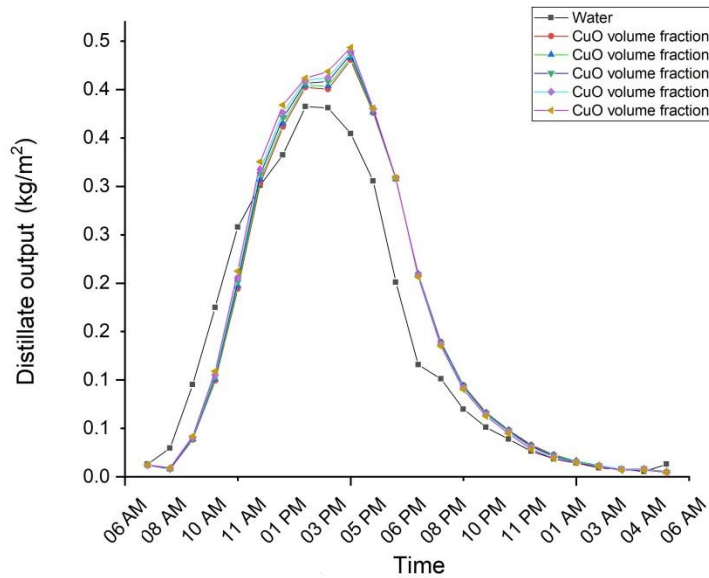


Figure 4.13. Hourly variation of distillate produced by CuO at different volume fractions in comparison with simple water.

The performance of the solar still increased by 10.82% in terms of yield produced when nanofluid was used. From figure 4.13 CuO having volume fraction 0.2 has maximum output, with 3.68 kg/m<sup>2</sup>/day, followed by 0.12, 0.08, 0.05 and 0.02 with 3.59 kg/m<sup>2</sup>/day.

#### 4.4.3. Variations in the performance of solar still with different volume fraction of Ag nanofluid

Ag nano-particle with different volume fraction (0.02, 0.05, 0.08, 0.12 and 0.2) is blended with the base fluid (water). Nanofluid with volume fraction 0.02, have the maximum yield produced with the performance enhancement of 8.11%. According to the results the utmost value of distillate produced is around 2:00 PM - 3:00 PM, because of maximum solar incident radiation.

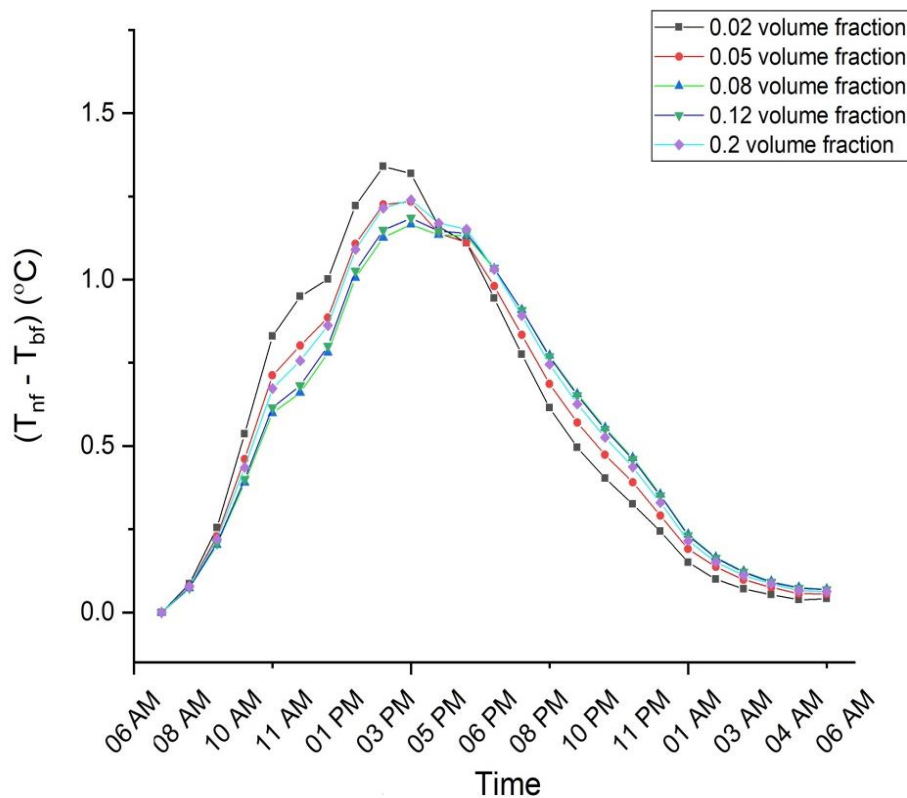


Figure 4.14. Hourly variation of temperature difference  $\Delta T$  between basefluid (water) and nanofluid (Ag) at different volume fractions.

From figure 4.14 it was witnessed that there is no significant difference between the temperatures of water, even in comparison with 0.05 and 0.2 volume fractions. Also evaporative heat transfer coefficient shows no significant variation.

Comparing the curves, the still blended with nanoparticle having 0.02 volume concentration, reaches higher temperature because of its low specific heat capacity of nanofluid and enhanced thermo-physical properties.

#### 4.4.4. Variations in the performance of solar still with different volume fraction of Fe<sub>2</sub>O<sub>3</sub> nanofluid

Fe<sub>2</sub>O<sub>3</sub> nano-particle, having high specific heat capacity of 670 J/°C has a performance enhancement of 7.63% in terms of distillate produced in comparison with still having simple water. Because of which, temperature rise in the still during peak timing was not high. Still having volume fraction 0.05 gives the best performance with the distillate output of 3.58 kg/m<sup>2</sup>/day.

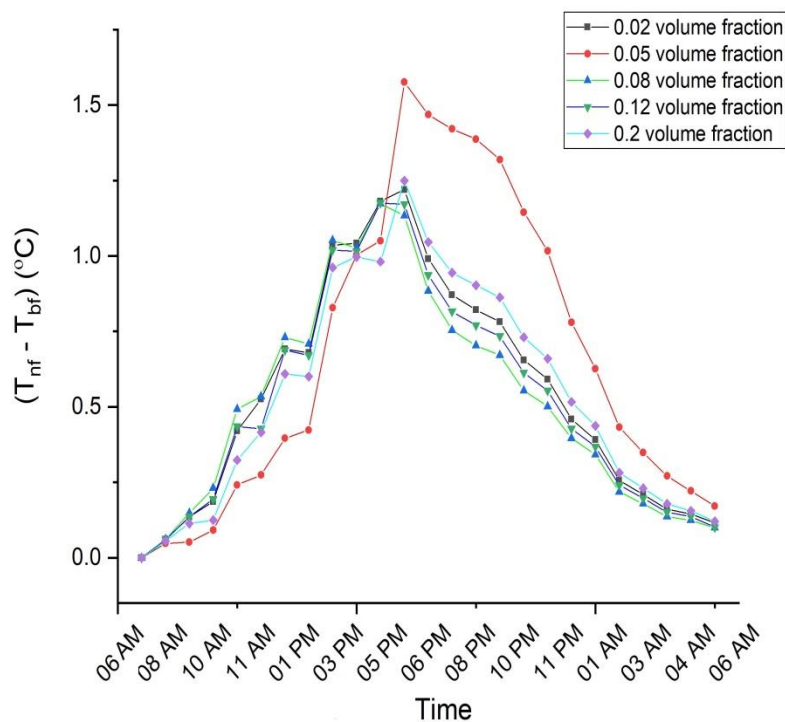


Figure 4.15. Hourly variation of temperature difference  $\Delta T$  between basefluid (water) and nanofluid (Fe<sub>2</sub>O<sub>3</sub>) at different volume fractions.

The hourly deviation of distillate output and the performance of the still was maximum for 0.05 volume concentration, and it decreases for volume fraction 0.12 and 0.2, with the yield of 3.57 kg/m<sup>2</sup>/day and 3.51 kg/m<sup>2</sup>/day.

From figure 4.15, temperature difference between basefluid and nanofluid is maximum for fluid having 0.05 volume concentration, and this is because of the change in thermo-physical properties of the nanofluid.

#### 4.4.5. Variations in the performance of solar still with different volume fraction of SiC nanofluid

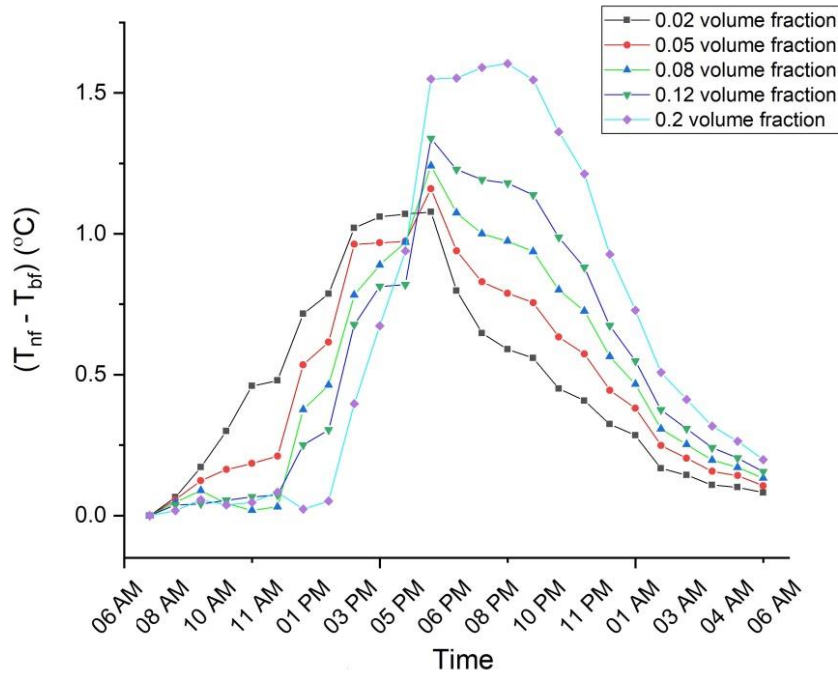


Fig 4.16. Hourly variation of temperature difference  $\Delta T$  between basefluid (water) and nanofluid (SiC) at different volume fractions.

From figure 4.16, graph illustrates comparison between temperature difference  $\Delta T$  between Base-fluid (water) and Nano-fluid (SiC). Nanofluid having volume fraction 0.2 shows a peak value of gradient at sunshine hours. From the graph also a sudden rise in  $\Delta T$  was seen for the same concentration of 0.2, because of change in heat capacity of fluid and its thermo-physical properties.

The distillate output for the volume fraction 0.2 is found to be maximum with 3.58 kg/m<sup>2</sup>/day, followed by 0.12, 0.05, 0.2 and 0.02.

#### 4.4.2. Performance comparison of different nanofluids

Thermo-physical behaviour of a nanofluid depends on the particle size, volume fraction used and the physical characteristics like density, thermal conductivity and specific heat capacity. Results for five different Nano-particles (CuO, Al<sub>2</sub>O<sub>3</sub>, SiC, Fe<sub>2</sub>O<sub>3</sub>, and Ag) were simulated in MATLAB using Runge kutta Numerical integration method.

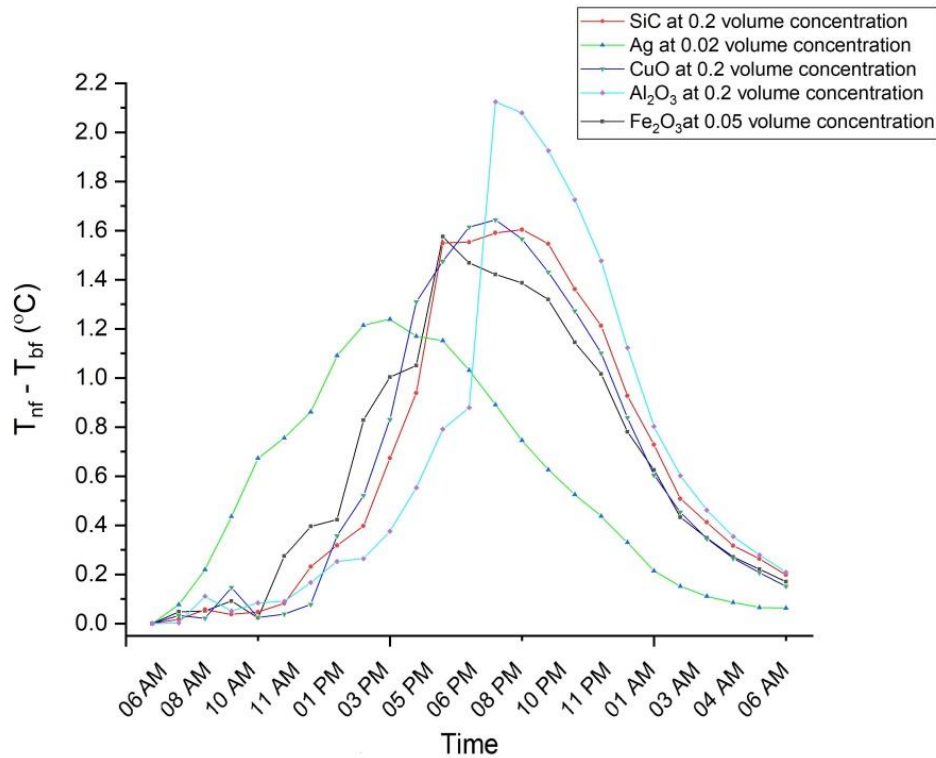


Figure 4.17. Hourly variation of temperature difference  $\Delta T$  between basefluid (water) and different nanofluids at different volume fractions.

The maximum temperature of Al<sub>2</sub>O<sub>3</sub> nanofluid is higher because of improved thermo-physical properties, as compared to the other simulated nanofluids. From figure 4.17, it has been noticed that the peak temperatures for all the nanofluid are during the sunshine hours, which sun's incident radiation was maximum. Solar absorption for the nanoparticle is maximum during sunshine hours because of the resonant nature in near IR and visible spectrum.

As temperature of the nanofluid increases, total heat transfer rate increases. During the sunshine hours because of greater temperatures the heat transfer curve elevates and during

night and early morning time it descends as seen from the results. Heat transfer coefficients are higher for  $\text{Al}_2\text{O}_3$  nanofluid followed by  $\text{CuO}$ ,  $\text{Ag}$ ,  $\text{Fe}_2\text{O}_3$  and  $\text{SiC}$ .

The simulation has been carried out for optimised water level of 0.02 m. From the figure 4.18 it is noticeable that higher yield was obtained for nanofluid  $\text{Al}_2\text{O}_3$  with 14.22% increase at volume fraction 0.2, in comparison to water, followed by  $\text{CuO}$  (10.82%) at 0.2,  $\text{Ag}$  (8.11%) at 0.02,  $\text{Fe}_2\text{O}_3$  (7.63%) at 0.05, and  $\text{SiC}$  (7.61%) at 0.2 volume fraction. Summing up the results, it was evident that, by increasing the volume fraction of nanofluid, heat transfer coefficients increases but after certain values efficiency curve becomes linear with no change.

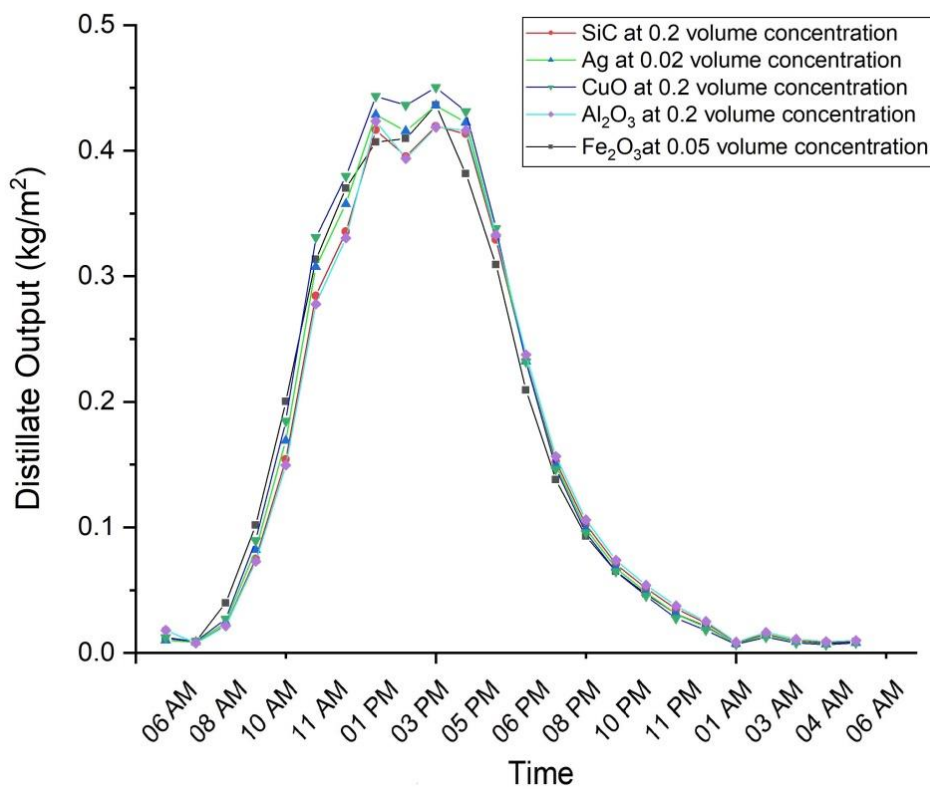


Figure 4.18. Hourly variation of distillate output for different nanofluids.

#### 5.1. Conclusions

In the present study, the performance of five different nanofluids and base-fluid has been analysed. On the basis of this learning, the following conclusions are drawn:

- The optimum water depth for single slope solar still, having water as a basin fluid is found to be 2cm.
- The peak temperature value during sunshine hours was found to be maximum for  $\text{Al}_2\text{O}_3$  at volume concentration 0.2, followed by CuO, Ag,  $\text{Fe}_2\text{O}_3$ , and SiC.
- The optimum volume concentrations for maximum distillate output for different water based-nanofluid was found to be (0.2) for  $\text{Al}_2\text{O}_3$ , (0.2) for CuO, (0.02) for Ag, (0.05) for  $\text{Fe}_2\text{O}_3$ , and (0.2) for SiC respectively.
- It can be seen that, at peak sunshine hours there is a small dip in distillate output curve which is due to small temperature gradients between glass cover and the basin water.
- Yield obtained for nanofluid  $\text{Al}_2\text{O}_3$  was found to be 14.22% higher than simple solar still without nanofluid, followed by CuO (10.82%), Ag (8.11%),  $\text{Fe}_2\text{O}_3$  (7.63%) and SiC (7.61%).

#### 5.2. Future scope

The main downside of a simple single slope solar still is its productivity. Many researchers have tried to improve its productivity by modifying its design, as discussed in the literature. The developed stills are not capable for the long run operations because of some major issues related to the performance which should be resolved.

- More research could be conducted to find the nanoparticle's optimum concentration and the effects of its size on the performance.
- Properties of composite Nanofluid are completely an untouched area so what kind of effects we will have on solar still can be simulated or experimented.
- Glass used is unable to communicate latent heat at its fullest, from the inner side to the ambient because of poor thermal conductivity.

- Research could be conducted to automatically clean the, scaling which deposits on the surface, which is responsible for hot spot and reduction in heat interaction.

## References

---

- 1) Karagiannis, Ioannis C., and Petros G. Soldatos. "Water desalination cost literature: review and assessment." *Desalination* 223, no. 1-3 (2008): 448-456.
- 2) Kalogirou, Soteris A. "Seawater desalination using renewable energy sources." *Progress in energy and combustion science* 31, no. 3 (2005): 242-281.
- 3) Xiao, Gang, Xihui Wang, Mingjiang Ni, Fei Wang, Weijun Zhu, Zhongyang Luo, and Kefa Cen. "A review on solar stills for brine desalination." *Applied Energy* 103 (2013): 642-652.
- 4) Dwivedi, V. K., and G. N. Tiwari. "Comparison of internal heat transfer coefficients in passive solar stills by different thermal models: an experimental validation." *Desalination* 246, no. 1-3 (2009): 304-318.
- 5) Tiwari, G. N., J. M. Thomas, and Emran Khan. "Optimisation of glass cover inclination for maximum yield in a solar still." *Heat Recovery Systems and CHP* 14, no. 4 (1994): 447-455.
- 6) Nafey, A. Safwat, M. Abdelkader, A. Abdelmotalip, and A. A. Mabrouk. "Enhancement of solar still productivity using floating perforated black plate." *Energy Conversion and Management* 43, no. 7 (2002): 937-946.
- 7) Mahian, Omid, Ali Kianifar, Soteris A. Kalogirou, Ioan Pop, and Somchai Wongwises. "A review of the applications of nanofluids in solar energy." *International Journal of Heat and Mass Transfer* 57, no. 2 (2013): 582-594.
- 8) Sharshir, S. W., Guilong Peng, Lirong Wu, Nuo Yang, F. A. Essa, A. H. Elsheikh, Showgi IT Mohamed, and A. E. Kabeel. "Enhancing the solar still performance using nanofluids and glass cover cooling: experimental study." *Applied Thermal Engineering* 113 (2017): 684-693.
- 9) Elango, T., A. Kannan, and K. Kalidasa Murugavel. "Performance study on single basin single slope solar still with different water nanofluids." *Desalination* 360 (2015): 45-51.
- 10) Singh, A. K., G. N. Tiwari, P. B. Sharma, and Emran Khan. "Optimization of orientation for higher yield of solar still for a given location." *Energy Conversion and Management* 36, no. 3 (1995): 175-181.
- 11) Aboul-Enein, S., A. A. El-Sebaei, and E. El-Bialy. "Investigation of a single-basin solar still with deep basins." *Renewable Energy* 14, no. 1-4 (1998): 299-305.

- 12) Samee, Muhammad Ali, Umar K. Mirza, Tariq Majeed, and Nasir Ahmad. "Design and performance of a simple single basin solar still." *Renewable and Sustainable Energy Reviews* 11, no. 3 (2007): 543-549.
- 13) Abu-Hijleh, Bassam AK. "Enhanced solar still performance using water film cooling of the glass cover." *Desalination* 107, no. 3 (1996): 235-244.
- 14) Khalifa, Abdul Jabbar N., and Ahmad M. Hamood. "On the verification of the effect of water depth on the performance of basin type solar stills." *Solar Energy* 83, no. 8 (2009): 1312-1321.
- 15) Tiwari, Anil Kr, and G. N. Tiwari. "Thermal modeling based on solar fraction and experimental study of the annual and seasonal performance of a single slope passive solar still: the effect of water depths." *Desalination* 207, no. 1-3 (2007): 184-204.
- 16) Dunkle, R. V. "Solar water distillation: the roof type still and a multiple effect diffusion still." In *Proc. International Heat Transfer Conference, University of Colorado, USA*, vol. 5, p. 895. 1961.
- 17) Dwivedi, V. K., and G. N. Tiwari. "Comparison of internal heat transfer coefficients in passive solar stills by different thermal models: an experimental validation." *Desalination* 246, no. 1-3 (2009): 304-318.
- 18) Kumar, Sanjeev, G. N. Tiwari, and H. N. Singh. "Annual performance of an active solar distillation system." *Desalination* 127, no. 1 (2000): 79-88.
- 19) Singh, A. K., G. N. Tiwari, P. B. Sharma, and Emran Khan. "Optimization of orientation for higher yield of solar still for a given location." *Energy Conversion and Management* 36, no. 3 (1995): 175-181.
- 20) Sakthivel, M., S. Shanmugasundaram, and T. Alwarsamy. "An experimental study on a regenerative solar still with energy storage medium—Jute cloth." *Desalination* 264, no. 1-2 (2010): 24-31
- 21) Srivastava, Pankaj K., and S. K. Agrawal. "Experimental and theoretical analysis of single sloped basin type solar still consisting of multiple low thermal inertia floating porous absorbers." *Desalination* 311 (2013): 198-205.
- 22) Aboul-Enein, S., A. A. El-Sebaei, and E. El-Bialy. "Investigation of a single-basin solar still with deep basins." *Renewable Energy* 14, no. 1-4 (1998): 299-305.
- 23) El-Bahi, A., and D. Inan. "Analysis of a parallel double glass solar still with separate condenser." *Renewable Energy* 17, no. 4 (1999): 509-521.

- 24) Abu-Arabi, Mousa, Yousef Zurigat, Hilal Al-Hinai, and Saif Al-Hiddabi. "Modeling and performance analysis of a solar desalination unit with double-glass cover cooling." *Desalination* 143, no. 2 (2002): 173-182.
- 25) Aggarwal, Shruti, and G. N. Tiwari. "Convective mass transfer in a double-condensing chamber and a conventional solar still." *Desalination* 115, no. 2 (1998): 181-188.
- 26) Nafey, A. Safwat, M. Abdelkader, A. Abdelmotalip, and A. A. Mabrouk. "Enhancement of solar still productivity using floating perforated black plate." *Energy Conversion and Management* 43, no. 7 (2002): 937-946.
- 27) El-Sebaili, A. A., S. Aboul-Enein, and E. El-Bialy. "Single basin solar still with baffle suspended absorber." *Energy conversion and management* 41, no. 7 (2000): 661-675.
- 28) Velmurugan, V., M. Gopalakrishnan, R. Raghu, and K. Srithar. "Single basin solar still with fin for enhancing productivity." *Energy Conversion and Management* 49, no. 10 (2008): 2602-2608.
- 29) Srivastava, Pankaj K., and S. K. Agrawal. "Winter and summer performance of single sloped basin type solar still integrated with extended porous fins." *Desalination* 319 (2013): 73-78.
- 30) Al-Hussaini, H., and I. K. Smith. "Enhancing of solar still productivity using vacuum technology." *Energy Conversion and Management* 36, no. 11 (1995): 1047-1051.
- 31) Abu-Qudais, Mohamad, and Othman N. Othman. "Experimental study and numerical simulation of a solar still using an external condenser." *Energy* 21, no. 10 (1996): 851-855.
- 32) Haddad, O. M., M. A. Al-Nimr, and A. Maqableh. "Enhanced solar still performance using a radiative cooling system." *Renewable Energy* 21, no. 3-4 (2000): 459-469.
- 33) Mousa, Hasan A. "Water film cooling over the glass cover of a solar still including evaporation effects." *Energy* 22, no. 1 (1997): 43-48.
- 34) El-Sebaili, A. A., S. J. Yagmour, F. S. Al-Hazmi, Adel S. Faidah, F. M. Al-Marzouki, and A. A. Al-Ghamdi. "Active single basin solar still with a sensible storage medium." *Desalination* 249, no. 2 (2009): 699-706.
- 35) Tanaka, Hiroshi, and Yasuhito Nakatake. "Theoretical analysis of a basin type solar still with internal and external reflectors." *Desalination* 197, no. 1-3 (2006): 205-216.
- 36) Shukla, Kumar Shailendra, and Ajeet Kumar Rai. "Analytical thermal modeling of double slope solar still by using inner glass cover temperature." *Thermal Science* 12, no. 3 (2008): 139-152.

- 37) Tiwari, Anil Kr, and G. N. Tiwari. "Thermal modeling based on solar fraction and experimental study of the annual and seasonal performance of a single slope passive solar still: the effect of water depths." *Desalination* 207, no. 1-3 (2007): 184-204.
- 38) Kumar, Sanjeev, G. N. Tiwari, and H. N. Singh. "Annual performance of an active solar distillation system." *Desalination* 127, no. 1 (2000): 79-88.
- 39) Okeke, C. E., S. U. Egarievwe, and A. O. E. Animalu. "Effects of coal and charcoal on solar-still performance." *Energy* 15, no. 11 (1990): 1071-1073.
- 40) Rajvanshi, Anil K. "Effect of various dyes on solar distillation." *Solar Energy* 27, no. 1 (1981): 51-65.
- 41) Murugavel, K. Kalidasa, and K. Srithar. "Performance study on basin type double slope solar still with different wick materials and minimum mass of water." *Renewable Energy* 36, no. 2 (2011): 612-620.
- 42) Sodha, M. S., Ashvini Kumar, G. N. Tiwari, and R. C. Tyagi. "Simple multiple wick solar still: analysis and performance." *Solar energy* 26, no. 2 (1981): 127-131.
- 43) Sahota, Lovedeep, V. S. Gupta, and G. N. Tiwari. "Analytical study of thermo-physical performance of nanofluid loaded hybrid double slope solar still." *Journal of Heat Transfer* 140, no. 11 (2018): 112404.
- 44) Elango, T., A. Kannan, and K. Kalidasa Murugavel. "Performance study on single basin single slope solar still with different water nanofluids." *Desalination* 360 (2015): 45-51.
- 45) Elango, T., A. Kannan, and K. Kalidasa Murugavel. "Performance study on single basin single slope solar still with different water nanofluids." *Desalination* 360 (2015): 45-51.
- 46) Elango, T., A. Kannan, and K. Kalidasa Murugavel. "Performance study on single basin single slope solar still with different water nanofluids." *Desalination* 360 (2015): 45-51.
- 47) Mahian, Omid, Ali Kianifar, Soteris A. Kalogirou, Ioan Pop, and Somchai Wongwises. "A review of the applications of nanofluids in solar energy." *International Journal of Heat and Mass Transfer* 57, no. 2 (2013): 582-594.
- 48) Omara, Z. M., A. E. Kabeel, and F. A. Essa. "Effect of using nanofluids and providing vacuum on the yield of corrugated wick solar still." *Energy conversion and management* 103 (2015): 965-972.

- 49) Kabeel, A. E., Z. M. Omara, and F. A. Essa. "Enhancement of modified solar still integrated with external condenser using nanofluids: An experimental approach." *Energy conversion and management* 78 (2014): 493-498.
- 50) Sharshir, S. W., Guilong Peng, Lirong Wu, Nuo Yang, F. A. Essa, A. H. Elsheikh, Showgi IT Mohamed, and A. E. Kabeel. "Enhancing the solar still performance using nanofluids and glass cover cooling: experimental study." *Applied Thermal Engineering* 113 (2017): 684-693.
- 51) Elango, T., A. Kannan, and K. Kalidasa Murugavel. "Performance study on single basin single slope solar still with different water nanofluids." *Desalination* 360 (2015): 45-51.
- 52) Sahota, Lovedeep, and G. N. Tiwari. "Effect of Al<sub>2</sub>O<sub>3</sub> nanoparticles on the performance of passive double slope solar still." *Solar Energy* 130 (2016): 260-272.
- 53) Rashidi, Saman, Masoud Bovand, Nader Rahbar, and Javad Abolfazli Esfahani. "Steps optimization and productivity enhancement in a nanofluid cascade solar still." *Renewable Energy* 118 (2018): 536-545.
- 54) Chen, Wenjing, Changjun Zou, Xiaoke Li, and Lu Li. "Experimental investigation of SiC nanofluids for solar distillation system: stability, optical properties and thermal conductivity with saline water-based fluid." *International Journal of Heat and Mass Transfer* 107 (2017): 264-270.
- 55) Kabeel, A. E., Zakaria Mohamed Omara, F. A. Essa, A. S. Abdullah, T. Arunkumar, and Ravishankar Sathyamurthy. "Augmentation of a solar still distillate yield via absorber plate coated with black nanoparticles." *Alexandria Engineering Journal* 56, no. 4 (2017): 433-438.
- 56) Liu, Xianglei, and Yimin Xuan. "Full-spectrum volumetric solar thermal conversion via photonic nanofluids." *Nanoscale* 9, no. 39 (2017): 14854-14860.
- 57) Rufuss, D. Dsilva Winfred, L. Suganthi, S. Iniyan, and P. A. Davies. "Effects of nanoparticle-enhanced phase change material (NPCM) on solar still productivity." *Journal of Cleaner Production* 192 (2018): 9-29.
- 58) Abujazar, Mohammed Shadi S., S. Fatihah, and A. E. Kabeel. "Seawater desalination using inclined stepped solar still with copper trays in a wet tropical climate." *Desalination* 423 (2017): 141-148.
- 59) Elashmawy, Mohamed. "An experimental investigation of a parabolic concentrator solar tracking system integrated with a tubular solar still." *Desalination* 411 (2017): 1-8.

- 60) Haddad, Zakaria, Abla Chaker, and Ahmed Rahmani. "Improving the basin type solar still performances using a vertical rotating wick." *Desalination* 418 (2017): 71-78.
- 61) Mahian, Omid, Ali Kianifar, Saeed Zeinali Heris, Dongsheng Wen, Ahmet Z. Sahin, and Somchai Wongwises. "Nanofluids effects on the evaporation rate in a solar still equipped with a heat exchanger." *Nano Energy* 36 (2017): 134-155.
- 62) Sahota, L., and G. N. Tiwari. "Effect of nanofluids on the performance of passive double slope solar still: a comparative study using characteristic curve." *Desalination* 388 (2016): 9-21.
- 63) Sahota, L., and G. N. Tiwari. "Effect of nanofluids on the performance of passive double slope solar still: a comparative study using characteristic curve." *Desalination* 388 (2016): 9-21.

**Appendix-A1**

**A1.1. Thermo physical properties of water vapour and water**

---



---

**Table.A.1.1. Thermo Physical properties of water vapour:**

---

<b>Density</b>	$\rho_v$	$353.44 / (T_v + 237.15)$
<b>Specific heat</b>	$C_v$	$999.2 + 0.1434 T_v + 1.101 T_v^2 - 6.7581 * 10^{-8} T_v^3$
<b>Viscosity</b>	$\mu_v$	$1.718 * 10^{-5} + 4.620 * 10^{-8} T_v$
<b>Thermal Conductivity</b>	$K_v$	$0.0244 + 0.7673 * 10^{-4} T_v$
<b>Thermal expansion coefficient</b>	$\beta_v$	$1 / (T_v + 273.15)$

---

**Properties of water:**

---

<b>Density</b>	$\rho_w$	$1000 [1 - (T_w - 4)^2 / (119000 + 1365 T_w - 4 T_w^2)]$
<b>Specific heat</b>	$C_w$	$4217.629 - 3.20888 T_w + 0.09503 T_w^2 - 0.00132 T_w^3$ $+ 9.415 * 10^{-6} T_w^4 - 2.5479 * 10^{-8} T_w^5$
<b>Viscosity</b>	$\mu_w$	$0.00169 - 4.25263 * 10^{-5} T_w + 4.9255 * 10^{-7} T_w^2$ $- 2.0993504 * 10^{-9} T_w^3$
<b>Thermal Conductivity</b>	$K_w$	$0.56112 + 0.00193 T_w - 2.60152749 * 10^{-6} T_w^2 - 6.08803$ $* 10^{-8} T_w^3$

---



---

## A1.2. Thermo physical properties of Nano-fluid

**Table.A1.2. Thermo Physical properties of Nanofluid:**

Density	$\rho_{nf}$	$\rho_{nf} = (1 - \phi_p)\rho_{bf} + \phi_p\rho_p$
Specific heat	$C_{nf}$	$C_{nf} = [(1 - \phi_p)\rho_{bf}C_{bf} + \phi_p\rho_pC_p]/\rho_{nf}$
Viscosity	$\mu_{nf}$	$[(1 + \phi_p)^{11.3}(1 + \frac{T_{nf}}{70})^{-0.038}(1 + \frac{d_p}{170})^{-0.061}] \mu_{bf}$
Thermal Conductivity	$K_{nf}$	$K_{eff} = [1 + 4.4(Re^{0.4}Pr^{0.66})$ $(T_{nf}/T_{fr})^{10}(K_p/K_{bf})^{0.03}\phi_p^{0.66}]K_{bf}$
Thermal expansion coefficient	$\beta_{nf}$	$\beta_{nf} = (1 - \phi_p)\beta_{bf} + \phi_p\beta_{np}$

## A1.3. Properties of Nano-Particle

**Table.A1.3. Properties of nanoparticles:**

Material	' $\rho$ ' (kg/m <sup>3</sup> )	'K' (W/mK)	'C <sub>p</sub> ' (J/K)
SiC	3160	490	675
Al <sub>2</sub> O <sub>3</sub>	3880	36	773
Cu	8954	383	386
Cuo	6350	69	535
Fe <sub>3</sub> O <sub>4</sub>	5180	6	670
SiO <sub>2</sub>	2220	1.4	745
TiO <sub>2</sub>	4175	8.4	692
ZnO	5600	29	514
ZrO <sub>2</sub>	5500	1.7	502
Ag	10490	0.235	429
Titania	4000	8.4	711

## Appendix-A2

### A2.1. MATLAB code for simple solar still

Main function

```
clc
clear all
load ta.dat;
load j.dat
%passive solar still with 0.1m water depth and of 1m2 area
tw(1)=input('Enter the value of basin water temperature in deg centigrade:');
tg(1)=input('Enter the value of inner glass cover temperature in deg centigrade:');
tb(1)=input('Enter the value of basin liner temperature in deg centigrade:');
for i=1:1440
    ta(i)=ta(i,1);
    j(i)=j(i,1);
    %ta1(i)=input('Enter the value of ambient temperature in deg centigrade:');
    %j(i)=input('Enter the value of incident radiation:');
    tsky(i)=ta(i)-6;
    idash=0;
    betas=pi/6;      % glass angle
    fr=0; as=1; ab=1; aw=1; ac=0; ag=ab/cos(betas); g=9.81;
    waterdepth=0.08;mw=ab.*waterdepth.*1000;
    t=60; cw=4190; rohg=1500; thickness=0.003;
    mg=rohg.*ag.*thickness;
    cg=753; mb=6; cb=460; li=0.009; ki=0.035; v=1;
    hb=((li./ki)+(1./(5.7+3.8.*v))).^(-1);          %losses through basin liner
    alphab=0.95; alphag=0.05; alphatc=0.7; rw=0.05; rg=0.05; taog=0.9;
    taow=(0.36-0.08.*log(waterdepth));
    alphaw=1-(taow+rw);
    alphaw=1-rw-taow;
    alphataoc=0.7; ul=8; hw(i)=100;    % test
    ephsilonw=0.95; ephsilong=0.94;
```

```

ephsiloneff=((1./ephsilong)+(1./ephsilow)-1).^(-1);

%runge kutta method
%for k1tw
pw(i)=exp(25.317-(5144./(tw(i)+273.15)));
pg(i)=exp(25.317-(5144./(tg(i)+273.15)));
if (tw(i)>tg(i))
    hcw(i)=0.884.*(tw(i)-tg(i)+(((pw(i)-pg(i)).*(tw(i)+273.15))./(268.9.*1000-
pw(i))))).^0.33333);
elseif (tw(i)<tg(i))
    hcw(i)=0.884.*(tg(i)-tw(i)+(((pw(i)-pg(i)).*(tw(i)+273.15))./(268.9.*1000-
pw(i))))).^0.33333);
elseif (tw(i)==tg(i))
    hcw(i)=0.884.*((tw(i)+0.0012)-tg(i)+(((pw(i)-pg(i)).*(tw(i)+273.15))./(268.9.*1000-
pw(i))))).^0.33333);
end;
%          hcw(i)=0.884.*(tw(i)-tg(i)+(((pw(i)-pg(i)).*(tw(i)+273.15))./(268.9.*1000-
pw(i))))).^0.33333);
if (tw(i)>tg(i))
    hrw(i)=0.884*ephsiloneff*(5.67)*10^(-8)*(((tw(i)+273.15)^4)-
(tg(i)+273.15)^4)/(tw(i)-tg(i));
elseif (tw(i)<tg(i))
    hrw(i)=0.884*ephsiloneff*(5.67)*10^(-8)*(((tg(i)+273.15)^4)-(tw(i)+273.15)^4)/(tg(i)-
tw(i));
elseif (tw(i)==tg(i))
    hrw(i)=0.884*ephsiloneff*(5.67)*10^(-8)*(((tw(i)+273.15235)^4)-
(tg(i)+273.15)^4)/((tw(i)+0.00025)-tg(i));
end;
% hrw(i)=0.884*ephsiloneff*(5.67)*10^(-8)*(((tw(i)+273.15)^4)-(tg(i)+273.15)^4)/(tw(i)-
tg(i));
if (tw(i)>tg(i))
    hew(i)=16.273*10^(-3)*hcw(i)*((pw(i)-pg(i))/(tw(i)-tg(i)));
elseif (tw(i)<tg(i))
    hew(i)=16.273*10^(-3)*hcw(i)*((pw(i)-pg(i))/(tg(i)-tw(i)));

```

```

elseif (tw(i)==tg(i))
    hew(i)=16.273*10^(-3)*hcw(i)*((pw(i)-pg(i))/((tw(i)+0.0025)-tg(i)));
end;
% hew(i)=16.273*10^(-3)*hcw(i)*((pw-pg)/(tw(i)-tg(i)));
hlw(i)=hcw(i)+hrw(i)+hew(i);
hcg(i)=2.8+3.*v;
if (tg(i)>ta(i))
    hrg(i)=ephsilong*5.67*10^(-8)*(((tg(i)+273.15)^4)-(tsky(i)+273.15)^4)/(tg(i)-ta(i));
elseif (tg(i)<ta(i))
    hrg(i)=ephsilong*5.67*10^(-8)*(((tg(i)+273.15)^4)-(tsky(i)+273.15)^4)/(ta(i)-tg(i));
elseif (tg(i)==ta(i))
    hrg(i)=ephsilong*5.67*10^(-8)*(((tg(i)+273.15)^4)-
(tsky(i)+273.15)^4)/((tg(i)+0.0025)-ta(i));
end;
% hrg(i)=ephsilong*5.67*10^(-8)*(((tg(i)+273.15)^4)-(tsky+273.15)^4)/(tg(i)-ta);
hlg(i)=hcg(i)+hrg(i);
h(i)=(hw(i)./(hw(i)+hb));
hdash(i)=(hlw(i)./(hlg(i)+hlw(i).*cos(betas)));
ulb(i)=(hb.*h(i));
ulg(i)=(hlg(i).*hdash(i));
udashl(i)=((ac.*fr.*ul)+(ulb(i).*ab)+(ulg(i).*ab));
a(i)=(udashl(i)./(mw.*cw));
f(i)=((ac.*fr.*alphatc.*idash)./(mw.*cw))+(((ac.*fr.*ul+ulb(i).*ab+ulg(i).*ab).*ta(i))./(mw.*
cw))+(((alphag.*hdash(i)+alphaw.*taog+alphab.*taog.*taow.*h(i)).*as.*j(i))./(mw.*cw));
k1tw(i)=f(i)-a(i).*tw(i);
k1tg(i)=(alphag.*ag.*j(i)+hlw(i).*aw.*(tw(i)-tg(i))+hlg(i).*ag.*(ta(i)-tg(i)))./(mg.*cg);
k1tb(i)=(alphab.*(1-alphag).(1-alphaw).*ab.*j(i)-hw(i).*ab.*(tb(i)-tw(i))+hb.*ab.*(tb(i)-
ta(i)))./(mb.*cb);
% k2tw
pw(i)=exp(25.317-(5144./(tw(i)+(k1tw(i)./2)+273.15)));
pg(i)=exp(25.317-(5144./(tg(i)+(k1tg(i)./2)+273.15)));
if (tw(i)>tg(i))
    hcw(i)=0.884.*((tw(i)+(k1tw(i)./2))-(tg(i)+(k1tg(i)./2))+(((pw(i)-
pg(i)).*(tw(i)+(k1tw(i)./2)+273.15))./(268.9.*1000-pw(i))).^(0.33333));

```

```

elseif (tw(i)<tg(i))
    hcw(i)=0.884.*((tg(i)+(k1tw(i)./2))-(tw(i)+(k1tw(i)./2))+((pw(i)-
pg(i)).*(tw(i)+(k1tw(i)./2)+273.15))./(268.9.*1000-pw(i))))).^0.33333);
    elseif (tw(i)== tg(i))
    hcw(i)=0.884.*((tw(i)+(k1tw(i)./2)+0.0012)-(tg(i)+(k1tw(i)./2))+((pw(i)-
pg(i)).*(tw(i)+(k1tw(i)./2)+273.15))./(268.9.*1000-pw(i))))).^0.33333);
    end;
%           hcw(i)=0.884.*(tw(i)-tg(i)+((pw(i)-pg(i)).*(tw(i)+273.15))./(268.9.*1000-
pw(i))))).^0.33333);
if (tw(i)>tg(i))
    hrw(i)=0.884*ephiloneff*(5.67)*10^(-8)*(((tw(i)+(k1tw(i)./2)+273.15)^4)-
(tg(i)+(k1tw(i)./2)+273.15)^4)/((tw(i)+(k1tw(i)./2))-(tg(i)+(k1tw(i)./2))));
    elseif (tw(i)<tg(i))
    hrw(i)=0.884*ephiloneff*(5.67)*10^(-8)*(((tg(i)+(k1tw(i)./2)+273.15)^4)-
(tw(i)+(k1tw(i)./2)+273.15)^4)/((tg(i)+(k1tw(i)./2))-(tw(i)+(k1tw(i)./2))));
    elseif (tw(i)==tg(i))
    hrw(i)=0.884*ephiloneff*(5.67)*10^(-8)*(((tw(i)+(k1tw(i)./2)+273.15235)^4)-
(tg(i)+(k1tw(i)./2)+273.15)^4)/((tw(i)+(k1tw(i)./2)+0.00025)-(tg(i)+(k1tw(i)./2))));
    end;
% hrw(i)=0.884*ephiloneff*(5.67)*10^(-8)*(((tw(i)+273.15)^4)-(tg(i)+273.15)^4)/(tw(i)-
tg(i));
if (tw(i)>tg(i))
    hew(i)=16.273*10^(-3)*hcw(i)*((pw(i)-pg(i))/((tw(i)+(k1tw(i)./2))-(tg(i)+(k1tw(i)./2))));
elseif (tw(i)<tg(i))
    hew(i)=16.273*10^(-3)*hcw(i)*((pw(i)-pg(i))/((tg(i)+(k1tw(i)./2))-(tw(i)+(k1tw(i)./2))));
elseif (tw(i)==tg(i))
    hew(i)=16.273*10^(-3)*hcw(i)*((pw(i)-pg(i))/((tw(i)+(k1tw(i)./2)+0.0025)-
(tg(i)+(k1tw(i)./2))));
    end;
% hew(i)=16.273*10^(-3)*hcw(i)*((pw-pg)/(tw(i)-tg(i)));
hlw(i)=hcw(i)+hrw(i)+hew(i);
hcg(i)=2.8+3.*v;
if (tg(i)>ta(i))

```

```

    hrg(i)=ephsilong*5.67*10^(-8)*(((tg(i)+(k1tg(i)./2)+273.15)^4)-
(tsky(i)+273.15)^4)/((tg(i)+(k1tg(i)./2))-ta(i));
    elseif (tg(i)<ta(i))
        hrg(i)=ephsilong*5.67*10^(-8)*(((tg(i)+(k1tg(i)./2)+273.15)^4)-
(tsky(i)+273.15)^4)/((ta(i)+(k1tg(i)./2))-tg(i));
    elseif (tg(i)==ta(i))
        hrg(i)=ephsilong*5.67*10^(-8)*(((tg(i)+(k1tg(i)./2)+273.15)^4)-
(tsky(i)+273.15)^4)/((tg(i)+(k1tg(i)./2)+0.0025)-ta(i));
    end;
% hrg(i)=ephsilong*5.67*10^(-8)*(((tg(i)+273.15)^4)-(tsky+273.15)^4)/(tg(i)-ta);
hlg(i)=hcg(i)+hr(i);
h(i)=(hw(i)./(hw(i)+hb));
hdash(i)=(hlw(i)./(hlg(i)+hlw(i).*cos(betas)));
ulb(i)=(hb.*h(i));
ulg(i)=(hlg(i).*hdash(i));
udashl(i)=(ac.*fr.*ul)+(ulb(i).*ab)+(ulg(i).*ab);
a1(i)=(udashl(i)./(mw.*cw));
f1(i)=(ac.*fr.*alphatc.*idash)./(mw.*cw)+(((ac.*fr.*ul+ulb(i).*ab+ulg(i).*ab).*ta(i))./(mw.*cw))+(((alphag.*hdash(i)+alphaw.*taog+alphab.*taog.*taow.*h(i)).*as.*j(i))./(mw.*cw));
k2tw(i)=f1(i)-a1(i).*(tw(i)+(k1tw(i)./2));
k2tg(i)=(alphag.*ag.*j(i)+hlw(i).*aw.*((tw(i)+(k1tw(i)./2))-
(tg(i)+(k1tg(i)./2)))+hlg(i).*ag.*(ta(i)-(tg(i)+(k1tg(i)./2))))./(mg.*cg);
k2tb(i)=(alphab.*(1-alphag).*(1-alphaw).*ab.*j(i)-hw(i).*ab.*((tb(i)+(k1tb(i)./2))-
(tw(i)+(k1tw(i)./2)))+hb.*ab.*((tb(i)+(k1tb(i)./2))-ta(i)))./(mb.*cb);
% k3tw
pw(i)=exp(25.317-(5144./(tw(i)+(k2tw(i)./2)+273.15)));
pg(i)=exp(25.317-(5144./(tg(i)+(k2tg(i)./2)+273.15)));
if (tw(i)>tg(i))
    hcw(i)=0.884.*((tw(i)+(k2tw(i)./2))-tg(i)+(k2tg(i)./2))+(((pw(i)-
pg(i)).*(tw(i)+(k2tw(i)./2)+273.15))./(268.9.*1000-pw(i))).^(0.33333);
    elseif (tw(i)<tg(i))
        hcw(i)=0.884.*((tg(i)+(k2tw(i)./2))-tw(i)+(k2tw(i)./2))+(((pw(i)-
pg(i)).*(tw(i)+(k2tw(i)./2)+273.15))./(268.9.*1000-pw(i))).^(0.33333);
    elseif (tw(i)==tg(i))

```

```

    hcw(i)=0.884.*((tw(i)+(k2tw(i)./2)+0.0012)-(tg(i)+(k2tg(i)./2))+((pw(i)-
pg(i)).*(tw(i)+(k2tw(i)./2)+273.15))./(268.9.*1000-pw(i))))).^0.33333);
    end;
%           hcw(i)=0.884.*(tw(i)-tg(i)+((pw(i)-pg(i)).*(tw(i)+273.15))./(268.9.*1000-
pw(i))))).^0.33333);
if (tw(i)>tg(i))
    hrw(i)=0.884*ephsiloneff*(5.67)*10^(-8)*(((tw(i)+(k2tw(i)./2)+273.15)^4)-
(tg(i)+(k2tg(i)./2)+273.15)^4)/((tw(i)+(k2tw(i)./2))-(tg(i)+(k2tg(i)./2))));
    elseif (tw(i)<tg(i))
        hrw(i)=0.884*ephsiloneff*(5.67)*10^(-8)*(((tg(i)+(k2tg(i)./2)+273.15)^4)-
(tw(i)+(k2tw(i)./2)+273.15)^4)/((tg(i)+(k2tg(i)./2))-(tw(i)+(k2tw(i)./2))));
    elseif (tw(i)==tg(i))
        hrw(i)=0.884*ephsiloneff*(5.67)*10^(-8)*(((tw(i)+(k2tw(i)./2)+273.15235)^4)-
(tg(i)+(k2tg(i)./2)+273.15)^4)/((tw(i)+(k2tw(i)./2)+0.00025)-(tg(i)+(k2tg(i)./2))));
    end;
% hrw(i)=0.884*ephsiloneff*(5.67)*10^(-8)*(((tw(i)+273.15)^4)-(tg(i)+273.15)^4)/(tw(i)-
tg(i));
if (tw(i)>tg(i))
    hew(i)=16.273*10^(-3)*hcw(i)*((pw(i)-pg(i))/((tw(i)+(k2tw(i)./2))-(tg(i)+(k2tg(i)./2))));
    elseif (tw(i)<tg(i))
        hew(i)=16.273*10^(-3)*hcw(i)*((pw(i)-pg(i))/((tg(i)+(k2tg(i)./2))-(tw(i)+(k2tw(i)./2))));
    elseif (tw(i)==tg(i))
        hew(i)=16.273*10^(-3)*hcw(i)*((pw(i)-pg(i))/((tw(i)+(k2tw(i)./2)+0.0025)-
(tg(i)+(k2tg(i)./2))));
    end;
% hew(i)=16.273*10^(-3)*hcw(i)*((pw-pg)/(tw(i)-tg(i)));
hlw(i)=hcw(i)+hrw(i)+hew(i);
hcg(i)=2.8+3.*v;
if (tg(i)>ta(i))
    hrg(i)=ephsilong*5.67*10^(-8)*(((tg(i)+(k2tg(i)./2)+273.15)^4)-
(tsky(i)+273.15)^4)/((tg(i)+(k2tg(i)./2))-ta(i));
    elseif (tg(i)<ta(i))
        hrg(i)=ephsilong*5.67*10^(-8)*(((tg(i)+(k2tg(i)./2)+273.15)^4)-
(tsky(i)+273.15)^4)/(ta(i)-(tg(i)+(k2tg(i)./2))));

```

```

elseif (tg(i)==ta(i))
    hrg(i)=ephsilong*5.67*10^(-8)*(((tg(i)+(k2tg(i)/2)+273.15)^4)-
(tsky(i)+273.15)^4)/((tg(i)+(k2tg(i)/2)+0.0025)-ta(i));
    end;
% hrg(i)=ephsilong*5.67*10^(-8)*(((tg(i)+273.15)^4)-(tsky+273.15)^4)/(tg(i)-ta);
hlg(i)=hcg(i)+hr(i);
h(i)=(hw(i)/(hw(i)+hb));
hdash(i)=(hlw(i)/(hlg(i)+hlw(i).*cos(betas)));
ulb(i)=(hb.*h(i));
ulg(i)=(hlg(i).*hdash(i));
udashl(i)=((ac.*fr.*ul)+(ulb(i).*ab)+(ulg(i).*ab));
a2(i)=(udashl(i)/(mw.*cw));
f2(i)=((ac.*fr.*alphatc.*idash)/(mw.*cw))+(((ac.*fr.*ul+ulb(i).*ab+ulg(i).*ab).*ta(i))/(mw.*cw))+(((alphag.*hdash(i)+alphaw.*taog+alphab.*taog.*h(i)).*as.*j(i))/(mw.*cw));
k3tw(i)=f2(i)-a2(i).*(tw(i)+(k2tw(i)/2));
k3tg(i)=(alphag.*ag.*j(i)+hlw(i).*aw.*((tw(i)+(k2tw(i)/2))-
(tg(i)+(k2tw(i)/2)))+hlg(i).*ag.*(ta(i)-(tg(i)+(k2tw(i)/2))))/(mg.*cg);
k3tb(i)=(alphab.*(1-alphag).*(1-alphaw).*ab.*j(i)-hw(i).*ab.*((tb(i)+(k2tb(i)/2))-
(tw(i)+(k2tw(i)/2)))+hb.*ab.*((tb(i)+(k2tb(i)/2))-ta(i)))/(mb.*cb);
% k4tw
pw(i)=exp(25.317-(5144/(tw(i)+(k3tw(i))+273.15)));
pg(i)=exp(25.317-(5144/(tg(i)+(k3tg(i))+273.15)));
if (tw(i)>tg(i))
    hcw(i)=0.884.*((tw(i)+(k3tw(i)))-(tg(i)+(k3tg(i)))+(((pw(i)-
pg(i)).*(tw(i)+(k3tw(i))+273.15))/(268.9.*1000-pw(i))))^(0.33333);
    elseif (tw(i)<tg(i))
        hcw(i)=0.884.*((tg(i)+(k3tg(i)))-(tw(i)+(k3tw(i)))+(((pw(i)-
pg(i)).*(tw(i)+(k3tw(i))+273.15))/(268.9.*1000-pw(i))))^(0.33333);
    elseif (tw(i)== tg(i))
        hcw(i)=0.884.*((tw(i)+(k3tw(i))+0.0012)-(tg(i)+(k3tg(i)))+(((pw(i)-
pg(i)).*(tw(i)+(k3tw(i))+273.15))/(268.9.*1000-pw(i))))^(0.33333);
    end;
% hcw(i)=0.884.*(tw(i)-tg(i)+(((pw(i)-pg(i)).*(tw(i)+273.15))/(268.9.*1000-
pw(i))))^(0.33333);

```

```

if (tw(i)>tg(i))
    hrw(i)=0.884*ephiloneff*(5.67)*10^(-8)*(((tw(i)+(k3tw(i))+273.15)^4)-
(tg(i)+(k3tg(i))+273.15)^4)/((tw(i)+(k3tw(i)))-(tg(i)+(k3tg(i))));
    elseif (tw(i)<tg(i))
        hrw(i)=0.884*ephiloneff*(5.67)*10^(-8)*(((tg(i)+(k3tg(i))+273.15)^4)-
(tw(i)+(k3tw(i))+273.15)^4)/((tg(i)+(k3tg(i)))-(tw(i)+(k3tw(i))));
    elseif (tw(i)==tg(i))
        hrw(i)=0.884*ephiloneff*(5.67)*10^(-8)*(((tw(i)+(k3tw(i))+273.15235)^4)-
(tg(i)+(k3tg(i))+273.15)^4)/((tw(i)+(k3tw(i))+0.00025)-(tg(i)+(k3tg(i))));
    end;
% hrw(i)=0.884*ephiloneff*(5.67)*10^(-8)*(((tw(i)+273.15)^4)-(tg(i)+273.15)^4)/(tw(i)-
tg(i));
if (tw(i)>tg(i))
    hew(i)=16.273*10^(-3)*hcw(i)*((pw(i)-pg(i))/((tw(i)+(k3tw(i)))-(tg(i)+(k3tg(i))));
    elseif (tw(i)<tg(i))
        hew(i)=16.273*10^(-3)*hcw(i)*((pw(i)-pg(i))/((tg(i)+(k3tg(i)))-(tw(i)+(k3tw(i))));
    elseif (tw(i)==tg(i))
        hew(i)=16.273*10^(-3)*hcw(i)*((pw(i)-pg(i))/((tw(i)+(k3tw(i))+0.0025)-
(tg(i)+(k3tg(i))));
    end;
% hew(i)=16.273*10^(-3)*hcw(i)*((pw-pg)/(tw(i)-tg(i)));
hlw(i)=hcw(i)+hrw(i)+hew(i);
hcg(i)=2.8+3.*v;
if (tg(i)>ta(i))
    hrg(i)=ephilong*5.67*10^(-8)*(((tg(i)+(k3tg(i))+273.15)^4)-
(tsky(i)+273.15)^4)/((tg(i)+(k3tg(i)))-ta(i));
    elseif (tg(i)<ta(i))
        hrg(i)=ephilong*5.67*10^(-8)*(((tg(i)+(k3tg(i))+273.15)^4)-
(tsky(i)+273.15)^4)/((ta(i)+(k3tg(i)))-tg(i));
    elseif (tg(i)==ta(i))
        hrg(i)=ephilong*5.67*10^(-8)*(((tg(i)+(k3tg(i))+273.15)^4)-
(tsky(i)+273.15)^4)/((tg(i)+(k3tg(i))+0.0025)-ta(i));
    end;
% hrg(i)=ephilong*5.67*10^(-8)*(((tg(i)+273.15)^4)-(tsky+273.15)^4)/(tg(i)-ta);

```

```

hlg(i)=hcg(i)+hrg(i);
h(i)=(hw(i)/(hw(i)+hb));
hdash(i)=(hlw(i)/(hlg(i)+hlw(i).*cos(betas)));
ulb(i)=(hb.*h(i));
ulg(i)=(hlg(i).*hdash(i));
udashl(i)=((ac.*fr.*ul)+(ulb(i).*ab)+(ulg(i).*ab));
a3(i)=(udashl(i)/(mw.*cw));
f3(i)=((ac.*fr.*alphatc.*idash)/(mw.*cw))+(((ac.*fr.*ul+ulb(i).*ab+ulg(i).*ab).*ta(i))/((mw.*cw))+(((alphag.*hdash(i)+alphaw.*taog+alphab.*taog.*taow.*h(i)).*as.*j(i))/(mw.*cw)));
k4tw(i)=f3(i)-a3(i).*(tw(i)+(k3tw(i)));
k4tg(i)=(alphag.*ag.*j(i)+hlw(i).*aw.*((tw(i)+(k3tw(i)))-(tg(i)+(k3tg(i))))+hlg(i).*ag.*(ta(i)-(tg(i)+(k3tg(i)))))/(mg.*cg);
k4tb(i)=(alphab.*(1-alphag).*(1-alphaw).*ab.*j(i)-hw(i).*ab.*((tb(i)+(k3tb(i)))-(tw(i)+(k3tw(i))))+hb.*ab.*((tb(i)+(k3tb(i)))-ta(i)))/(mb.*cb);
tw(i+1)=tw(i)+(1./6).*(k1tw(i)+(2.*k2tw(i)+(2.*k3tw(i))+k4tw(i)).*t;
tg(i+1)=tg(i)+(1./6).*(k1tg(i)+(2.*k2tg(i)+(2.*k3tg(i))+k4tg(i)).*t;
tb(i+1)=tb(i)+(1./6).*(k1tb(i)+(2.*k2tb(i)+(2.*k3tb(i))+k4tb(i)).*t;
if (tw(i+1)<=70)
    lh(i)=(2.4935.*10.^6).*(1-(9.4779.*10.^(-4)).*tw(i)+(1.3132.*10.^(-7)).*tw(i).^2)-(4.7974.*10.^(-9)).*tw(i).^3);
elseif (tw(i+1)>70)
    lh(i)=3.1615.*10.^6*((1-7.616.*10.^(-4)).*tw(i));
end;
lh(i);
mew(i)=((hew(i).*(tw(i)-tg(i)).*t)/lh(i));
tsun=6000;
exoutput(i)=hew(i).*ab.*(tw(i)-tg(i)).*(1-((ta(i)+273)/(tw(i)+273)));
exstill(i)=ab.*j(i).*(1-(4/3).*((ta(i)+273)/tsun)+(1/3).*((ta(i)+273)/tsun).^4);
excollector(i)=ac.*j(i).*(1-(4/3).*((ta(i)+273)/tsun)+(1/3).*((ta(i)+273)/tsun).^4);
exinput(i)=exstill(i)+excollector(i);
end

```

## A2.2. MATLAB code for modified solar still having nanofluid

Main function

```
clc
clear all
load ta.dat;
load j.dat
%passive solar still with 0.1m water depth and nanofluid and of 1m2 area
tw(1)=input('Enter the value of basin water temperature in deg centigrade:');
tg(1)=input('Enter the value of inner glass cover temperature in deg centigrade:');
tb(1)=input('Enter the value of basin liner temperature in deg centigrade:');
for i=1:1440
    ta(i)=ta(i,1);
    j(i)=j(i,1);
    %ta(i)=input('Enter the value of ambient temperature in deg centigrade:');
    %j(i)=input('Enter the value of incident radiation:');
    tsky=ta(i)-6; idash=0; fr=0; betas=pi/6; %glass angle
    aw=1; as=1; ab=1; ac=0; ag=ab/cos(betas); lc=(ab./(2.*(1+1))); g=9.81;
    waterdepth=0.01; mw=ab.*waterdepth.*1000; cw=4190; rohg=1500;
    thickness=0.003; mg=rohg.*ag.*thickness; cg=753; mb=6; cb=460;
    li=0.009; ki=0.035; v=1;
    hb=((li/ki)+(1/(5.7+3.8*v)))^(-1); %losses through basin liner
    alphab=0.95; alphag=0.05; alphatc=0.7; rw=0.05; rg=0.05; taog=0.85;
    taow=(0.36-0.08*log(waterdepth));
    t=60; alphaw=1-rw-taow; alphataoc=0.7; ul=8;
    % nanofluid thermophysical properties
    dp=10; cpnp=773; fi=0.001; %volume fraction
    rohnp=3880; %roh of nano particle
    rohbf(i)=(1-(((tw(i)-4).^2))./(119000+1365.*tw(i)-4.*tw(i).*tw(i)))).*1000;
    rohnf(i)=(fi.*rohnp)+(1-fi).*rohbf(i); %roh of nanofluid
    mnf(i)=(rohnf(i).*ab.*waterdepth); %mass of nanofluid
    %cp of nanoparticle
    cpbf(i)=4217.629-3.20888.*tw(i)+0.09503.*tw(i).*tw(i)-0.00132.*tw(i).^3+9.415.*10.^(-
6).*tw(i).^4-2.5479.*10.^(-8).*tw(i).^5); %cp of base fluid
```

```

cpnf(i)=0.8429.*((1+(tw(i)./50)).^(-
0.3037)).*(1+(dp./50).^0.4167)).*((1+(fi./100)).^(2.272));           %cp of nanofluid
betabf=21*10.^(-5);
betanp=29*10.^(-5);
betanf=((1-fi).*betabf)+(fi.*betanp);
mubf(i)=0.0015-3.16325.*tw(i).*10.^(-5)+3.04789.*tw(i).^2.*10.^(-7)-
1.1104.*tw(i).^3.*10.^(-9);
munf(i)=(2.414.*10.^(-5)).*10.^(247.8/((tw(i)+273.15)-140));
kbf(i)=(0.55994+0.00216.*tw(i)-1.02749.*10.^(-5).*tw(i).^2)+6.7279.*10.^(-9).*tw(i).^3);
knf(i)=kbf(i).*((0.9843+0.398.*(fi).^0.467)).*((munf(i)/mubf(i)).^0.0235)).*((1./dp).^0.22
46))-
(3.951.*(fi./tw(i)))+(34.034.*((fi.*fi)./(tw(i).*tw(i).*tw(i))))+(32.51.*((fi)./(tw(i).*tw(i)))));
% knf(i)=33;
ephsilonw=0.95;
ephsilong=0.94;
ephsiloneff=((1/ephsilong)+(1/ephsilonw)-1)^(-1);
pw(i)=exp(25.317-(5144/(tw(i)+273.15)));
pg(i)=exp(25.317-(5144/(tg(i)+273.15)));
c=0.54;
n=(1./4);
pr(i)=((munf(i).*cpnf(i))./knf(i));
if (tb(i)>tw(i))
    gr(i)=(g.*betanf.*(tb(i)-tw(i)).*rohnf(i).*rohnf(i).*lc.*lc)./(munf(i).*munf(i));
elseif (tb(i)<tw(i))
    gr(i)=(g.*betanf.*(tw(i)-tb(i)).*rohnf(i).*rohnf(i).*lc.*lc)./(munf(i).*munf(i));
elseif (tb(i)==tw(i))
    gr(i)=(g.*betanf.*((tw(i)+0.001)-tb(i)).*rohnf(i).*rohnf(i).*lc.*lc)./(munf(i).*munf(i));
end;
% gr(i)=(g.*betanf.*(tb(i)-tw(i)).*rohnf(i).*rohnf(i).*lc.*lc)./(munf(i).*munf(i));
ra(i)=gr(i).*pr(i);
nu(i)=c.*(ra(i)).^(n);
hw(i)=(nu(i).*knf(i))./lc;
%
if (tw(i)>tg(i))

```

```

    hcw(i)=0.884.*(tw(i)-tg(i)+(((pw(i)-pg(i)).*(tw(i)+273.15))./(268.9.*1000-
pw(i))))).^0.33333);
    elseif (tw(i)<tg(i))
        hcw(i)=0.884.*(tg(i)-tw(i)+(((pg(i)-pw(i)).*(tw(i)+273.15))./(268.9.*1000-
pw(i))))).^0.33333);
    elseif (tw(i)== tg(i))
        hcw(i)=0.884.*((tw(i)+0.0012)-tg(i)+(((pw(i)+0.00001)-
pg(i)).*(tw(i)+273.15))./(268.9.*1000-pw(i))))).^0.33333);
    end;
% hcw(i)=0.884.*(tw(i)-tg(i)+(((pw(i)-pg(i)).*(tw(i)+273.15))./(268.9.*1000-
pw(i))))).^0.33333);
if (tw(i)>tg(i))
    hrw(i)=0.884*ephiloneff*(5.67)*10^(-8)*(((tw(i)+273.15)^4)-
(tg(i)+273.15)^4)/(tw(i)-tg(i));
    elseif (tw(i)<tg(i))
        hrw(i)=0.884*ephiloneff*(5.67)*10^(-8)*(((tg(i)+273.15)^4)-(tw(i)+273.15)^4)/(tg(i)-
tw(i));
    elseif (tw(i)==tg(i))
        hrw(i)=0.884*ephiloneff*(5.67)*10^(-8)*(((tw(i)+273.15235)^4)-
(tg(i)+273.15)^4)/((tw(i)+0.00025)-tg(i));
    end;
% hrw(i)=0.884*ephiloneff*(5.67)*10^(-8)*(((tw(i)+273.15)^4)-(tg(i)+273.15)^4)/(tw(i)-
tg(i));
if (tw(i)>tg(i))
    hew(i)=16.273*10^(-3)*hcw(i)*((pw(i)-pg(i))/(tw(i)-tg(i)));
    elseif (tw(i)<tg(i))
        hew(i)=16.273*10^(-3)*hcw(i)*((pw(i)-pg(i))/(tg(i)-tw(i)));
    elseif (tw(i)==tg(i))
        hew(i)=16.273*10^(-3)*hcw(i)*(((pw(i)+0.0001)-pg(i))/((tw(i)+0.0025)-tg(i)));
    end;
% hew(i)=16.273*10^(-3)*hcw(i)*((pw-pg)/(tw(i)-tg(i)));
hlw(i)=hcw(i)+hrw(i)+hew(i);
hcg(i)=2.8+3*v;
if (tg(i)>ta(i))

```

```

    hrg(i)=ephsilong*5.67*10^(-8)*(((tg(i)+273.15)^4)-(tsky+273.15)^4)/(tg(i)-ta(i));
elseif (tg(i)<ta(i))
    hrg(i)=ephsilong*5.67*10^(-8)*(((tg(i)+273.15)^4)-(tsky+273.15)^4)/(ta(i)-tg(i));
elseif (tg(i)==ta(i))
    hrg(i)=ephsilong*5.67*10^(-8)*(((tg(i)+273.15)^4)-(tsky+273.15)^4)/((tg(i)+0.0025)-
ta(i));
end;
% hrg(i)=ephsilong*5.67*10^(-8)*(((tg(i)+273.15)^4)-(tsky+273.15)^4)/(tg(i)-ta);
hlg(i)=hcg(i)+hr(i);
h(i)=(hw(i)/(hw(i)+hb));
hdash(i)=(hlw(i)/(hlg(i)+hlw(i).*cos(betas)));
ulb(i)=(hb.*h(i));
ulg(i)=(hlg(i).*hdash(i));
udashl(i)=(ac.*fr.*ul)+(ulb(i).*ab)+(ulg(i).*ab));
a(i)=(udashl(i)/(mnf(i).*cpnf(i)));
f(i)=((ac.*fr.*alphatc.*idash)/(mnf(i).*cpnf(i)))+(((ac.*fr.*ul+ulb(i).*ab+ulg(i).*ab).*ta(i))/(
(mnf(i).*cpnf(i))))+(((alphag.*hdash(i)+alphaw.*taog+alphab.*taog.*taow.*h(i)).*as.*j(i))/(
mnf(i).*cpnf(i)));
k1tw(i)=f(i)-a(i).*tw(i);
k1tg(i)=(alphag.*ag.*j(i)+hlw(i).*aw.*(tw(i)-tg(i))+hlg(i).*ag.*(ta(i)-tg(i)))/(mg.*cg);
k1tb(i)=(alphab.*(1-alphag).(1-alphaw).*ab.*j(i)-hw(i).*ab.*(tb(i)-tw(i))+hb.*ab.*(tb(i)-
ta(i)))/(mb.*cb);
% for k2tw
rohbf(i)=(1-(((tw(i)+(k1tw(i)/2))-4).^2)/(119000+1365.*(tw(i)+(k1tw(i)/2))-
4.*(tw(i)+(k1tw(i)/2)).*(tw(i)+(k1tw(i)/2)))).*1000;    %roh of base fluid
rohnf(i)=(fi.*rohnp)+(1-fi).*rohbf(i);    %roh of nanofluid
mnf(i)=(rohnf(i).*ab.*waterdepth);    %mass of nanofluid
%cp of nanoparticle
cpbf(i)=4217.629-
3.20888.*(tw(i)+(k1tw(i)/2))+0.09503.*(tw(i)+(k1tw(i)/2)).*(tw(i)+(k1tw(i)/2))-
0.00132.*(tw(i)+(k1tw(i)/2)).^3+9.415.*10.^(-6).*tw(i)+(k1tw(i)/2)).^4-2.5479.*10.^(-
8).*tw(i)+(k1tw(i)/2)).^5;    %cp of base fluid
cpnf(i)=0.8429.*((1+((tw(i)+(k1tw(i)/2))/50)).^(-
0.3037)).*(1+(dp/50).^0.4167)).*(1+(fi/100)).^(2.272));    %cp of nanofluid

```

```

betabf=21*10.^(-5);
betanp=29*10.^(-5);
betanf=((1-fi).*betabf)+(fi.*betanp);
mubf(i)=0.0015-3.16325.*(tw(i)+(k1tw(i)./2)).*10.^(-
5)+3.04789.*(tw(i)+(k1tw(i)./2)).^2.*10.^(-7)-1.1104.*(tw(i)+(k1tw(i)./2)).^3.*10.^(-9);
munf(i)=(2.414.*10.^(-5)).*10.^(247.8./(((tw(i)+(k1tw(i)./2))+273.15)-140));
kbf(i)=(0.55994+0.00216.*(tw(i)+(k1tw(i)./2))-1.02749.*10.^(-
5)).*(tw(i)+(k1tw(i)./2)).^2+6.7279.*10.^(-9).*(tw(i)+(k1tw(i)./2)).^3);
%
knf(i)=kbf(i).*((0.9843+0.398.*(fi).^0.467)).*((munf(i)/mubf(i)).^0.0235).*((1./dp).^0.22
46))-
(3.951.*(fi./(tw(i)+(k1tw(i)./2))))+(34.034.*((fi.*fi)./(tw(i)+(k1tw(i)./2)).*(tw(i)+(k1tw(i)./2)
).*(tw(i)+(k1tw(i)./2))))+(32.51.*((fi)./(tw(i)+(k1tw(i)./2)).*(tw(i)+(k1tw(i)./2)))));
% knf(i)=33;
ephilonw=0.95;
ephilong=0.94;
ephiloneff=((1/ephilong)+(1/ephilonw)-1)^(-1);
pw(i)=exp(25.317-(5144/((tw(i)+(k1tw(i)./2))+273.15)));
pg(i)=exp(25.317-(5144/((tg(i)+(k1tg(i)./2))+273.15)));
%
c=0.54;
n=(1./4);
pr(i)=((munf(i).*cpnf(i))./knf(i));
if (tb(i)>tw(i))
    gr(i)=(g.*betanf.*((tb(i)+(k1tb(i)./2))-
(tw(i)+(k1tw(i)./2))).*rohnf(i).*rohnf(i).*lc.*lc)./(munf(i).*munf(i));
elseif (tb(i)<tw(i))
    gr(i)=(g.*betanf.*((tw(i)+(k1tw(i)./2))-
(tb(i)+(k1tb(i)./2))).*rohnf(i).*rohnf(i).*lc.*lc)./(munf(i).*munf(i));
elseif (tb(i)==tw(i))
    gr(i)=(g.*betanf.*(((tw(i)+(k1tw(i)./2))+0.001)-
(tb(i)+(k1tb(i)./2))).*rohnf(i).*rohnf(i).*lc.*lc)./(munf(i).*munf(i));
end;
% gr(i)=(g.*betanf.*(tb(i)-tw(i)).*rohnf(i).*rohnf(i).*lc.*lc)./(munf(i).*munf(i));

```

```

ra(i)=gr(i).*pr(i);
nu(i)=c.*(ra(i)).^(n);
hw(i)=(nu(i).*knf(i))./lc;
if (tw(i)>tg(i))
    hcw(i)=0.884.*((tw(i)+(k1tw(i)./2))-(tg(i)+(k1tg(i)./2))+(((pw(i)-
pg(i)).*(tw(i)+(k1tw(i)./2)+273.15))./(268.9.*1000-pw(i))))).^0.33333);
elseif (tw(i)<tg(i))
    hcw(i)=0.884.*((tg(i)+(k1tg(i)./2))-(tw(i)+(k1tw(i)./2))+(((pg(i)-
pw(i)).*(tw(i)+(k1tw(i)./2)+273.15))./(268.9.*1000-pw(i))))).^0.33333);
elseif (tw(i)==tg(i))
    hcw(i)=0.884.*((tw(i)+(k1tw(i)./2)+0.0012)-(tg(i)+(k1tg(i)./2))+(((pw(i)+0.00001)-
pg(i)).*(tw(i)+(k1tw(i)./2)+273.15))./(268.9.*1000-pw(i))))).^0.33333);
end;
% hcw(i)=0.884.*(tw(i)-tg(i)+(((pw(i)-pg(i)).*(tw(i)+273.15))./(268.9.*1000-
pw(i))))).^0.33333);
if (tw(i)>tg(i))
    hrw(i)=0.884*ephiloneff*(5.67)*10^(-8)*(((tw(i)+(k1tw(i)./2))+273.15)^4)-
((tg(i)+(k1tg(i)./2))+273.15)^4)/((tw(i)+(k1tw(i)./2))-(tg(i)+(k1tg(i)./2)));
elseif (tw(i)<tg(i))
    hrw(i)=0.884*ephiloneff*(5.67)*10^(-8)*(((tg(i)+(k1tg(i)./2))+273.15)^4)-
((tw(i)+(k1tw(i)./2))+273.15)^4)/((tg(i)+(k1tg(i)./2))-(tw(i)+(k1tw(i)./2)));
elseif (tw(i)==tg(i))
    hrw(i)=0.884*ephiloneff*(5.67)*10^(-8)*(((tw(i)+(k1tw(i)./2))+273.15235)^4)-
((tg(i)+(k1tg(i)./2))+273.15)^4)/(((tw(i)+(k1tw(i)./2))+0.00025)-(tg(i)+(k1tg(i)./2)));
end;
% hrw(i)=0.884*ephiloneff*(5.67)*10^(-8)*(((tw(i)+273.15)^4)-(tg(i)+273.15)^4)/(tw(i)-
tg(i));
if (tw(i)>tg(i))
    hew(i)=16.273*10^(-3)*hcw(i)*((pw(i)-pg(i))/((tw(i)+(k1tw(i)./2))-(tg(i)+(k1tg(i)./2))));
elseif (tw(i)<tg(i))
    hew(i)=16.273*10^(-3)*hcw(i)*((pw(i)-pg(i))/((tg(i)+(k1tg(i)./2))-(tw(i)+(k1tw(i)./2))));
elseif (tw(i)==tg(i))
    hew(i)=16.273*10^(-3)*hcw(i)*(((pw(i)+0.0001)-pg(i))/(((tw(i)+(k1tw(i)./2))+0.0025)-
(tg(i)+(k1tg(i)./2))));

```

```

end;
% hew(i)=16.273*10^(-3)*hcw(i)*((pw-pg)/(tw(i)-tg(i)));
hlw(i)=hcw(i)+hrw(i)+hew(i);
hcg(i)=2.8+3*v;
if (tg(i)>ta(i))
    hrg(i)=ephsilong*5.67*10^(-8)*(((tg(i)+(k1tg(i)/2))+273.15)^4)-
(tsky+273.15)^4)/((tg(i)+(k1tg(i)/2))-ta(i));
elseif (tg(i)<ta(i))
    hrg(i)=ephsilong*5.67*10^(-8)*(((tg(i)+(k1tg(i)/2))+273.15)^4)-
(tsky+273.15)^4)/(ta(i)-(tg(i)+(k1tg(i)/2)));
elseif (tg(i)==ta(i))
    hrg(i)=ephsilong*5.67*10^(-8)*(((tg(i)+(k1tg(i)/2))+273.15)^4)-
(tsky+273.15)^4)/(((tg(i)+(k1tg(i)/2))+0.0025)-ta(i));
end;
% hrg(i)=ephsilong*5.67*10^(-8)*(((tg(i)+273.15)^4)-(tsky+273.15)^4)/(tg(i)-ta));
hlg(i)=hcg(i)+hrg(i);
h(i)=(hw(i)/(hw(i)+hb));
hdash(i)=(hlw(i)/(hlg(i)+hlw(i).*cos(betas)));
ulb(i)=(hb.*h(i));
ulg(i)=(hlg(i).*hdash(i));
udashl(i)=((ac.*fr.*ul)+(ulb(i).*ab)+(ulg(i).*ab));
a(i)=(udashl(i)/(mnf(i).*cpnf(i)));
f(i)=((ac.*fr.*alphatc.*idash)/(mnf(i).*cpnf(i)))+(((ac.*fr.*ul+ulb(i).*ab+ulg(i).*ab).*ta(i))/(
(mnf(i).*cpnf(i)))+(((alphag.*hdash(i)+alphaw.*taog+alphab.*taog.*taow.*h(i)).*as.*j(i))/(
mnf(i).*cpnf(i)))
k2tw(i)=f(i)-a(i).*(tw(i)+(k1tw(i)/2));
k2tg(i)=(alphag.*ag.*j(i)+hlw(i).*aw.*((tw(i)+(k1tw(i)/2))-
(tg(i)+(k1tg(i)/2)))+hlg(i).*ag.*(ta(i)-(tg(i)+(k1tg(i)/2))))./(mg.*cg);
k2tb(i)=(alphab.*(1-alphag).*(1-alphaw).*ab.*j(i)-hw(i).*ab.*((tb(i)+(k1tb(i)/2))-
(tw(i)+(k1tw(i)/2)))+hb.*ab.*((tb(i)+(k1tb(i)/2))-ta(i)))./(mb.*cb);
%for k3tw
rohbf(i)=(1-(((tw(i)+(k2tw(i)/2))-4).^2))./(119000+1365.*(tw(i)+(k2tw(i)/2))-
4.*(tw(i)+(k2tw(i)/2)).*(tw(i)+(k2tw(i)/2))).*1000;    %roh of base fluid
rohnf(i)=(fi.*rohnp)+(1-fi).*rohbf(i);                %roh of nanofluid

```

```

mnf(i)=(rohnf(i).*ab.*waterdepth); %mass of nanofluid
%cp of nanoparticle
cpbf(i)=4217.629-
3.20888.*(tw(i)+(k2tw(i)./2))+0.09503.*(tw(i)+(k2tw(i)./2)).*(tw(i)+(k2tw(i)./2))-
0.00132.*(tw(i)+(k2tw(i)./2)).^3+9.415.*10.^(-6).*(tw(i)+(k2tw(i)./2)).^4-2.5479.*10.^(-
8).*(tw(i)+(k2tw(i)./2)).^5); %cp of base fluid
cpnf(i)=0.8429.*((1+((tw(i)+(k2tw(i)./2))./50)).^(-
0.3037)).*(1+(dp./50).^(0.4167)).*(1+(fi./100)).^(2.272)); %cp of nanofluid
betabf=21*10.^(-5);
betanp=29*10.^(-5);
betanf=((1-fi).*betabf)+(fi.*betanp);
mubf(i)=0.0015-3.16325.*(tw(i)+(k2tw(i)./2)).*10.^(-
5)+3.04789.*(tw(i)+(k2tw(i)./2)).^2.*10.^(-7)-1.1104.*(tw(i)+(k2tw(i)./2)).^3.*10.^(-9);
munf(i)=(2.414.*10.^(-5)).*10.^(247.8/(((tw(i)+(k2tw(i)./2))+273.15)-140));
kbf(i)=(0.55994+0.00216.*(tw(i)+(k2tw(i)./2))-1.02749.*10.^(-
5).*(tw(i)+(k2tw(i)./2)).^2)+6.7279.*10.^(-9).*(tw(i)+(k2tw(i)./2)).^3);
knf(i)=kbf(i).*((0.9843+0.398.*(fi).^(0.467)).*((munf(i)/mubf(i)).^(0.0235)).*((1./dp).^(0.22
46))-
(3.951.*(fi./((tw(i)+(k2tw(i)./2))))+(34.034.*((fi.*fi)./((tw(i)+(k2tw(i)./2)).*(tw(i)+(k2tw(i)./2)
).*(tw(i)+(k2tw(i)./2))))+(32.51.*((fi)./((tw(i)+(k2tw(i)./2)).*(tw(i)+(k2tw(i)./2))))));
% knf(i)=33;
epsilonw=0.95;
epsilonong=0.94;
epsiloneff=((1/epsilonong)+(1/epsilonw)-1)^(-1);
pw(i)=exp(25.317-(5144/((tw(i)+(k2tw(i)./2))+273.15)));
pg(i)=exp(25.317-(5144/((tg(i)+(k2tg(i)./2))+273.15)));
c=0.54;
n=(1./4);
pr(i)=((munf(i).*cpnf(i))./knf(i));
if (tb(i)>tw(i))
    gr(i)=(g.*betanf.*((tb(i)+(k2tb(i)./2))-
(tw(i)+(k2tw(i)./2))).*rohnf(i).*rohnf(i).*lc.*lc)./(munf(i).*munf(i));
elseif (tb(i)<tw(i))

```

```

    gr(i)=(g.*betanf.*((tw(i)+(k2tw(i)./2))-
(tb(i)+(k2tb(i)./2))).*rohnf(i).*rohnf(i).*lc.*lc)./(munf(i).*munf(i));
    elseif (tb(i)==tw(i))
        gr(i)=(g.*betanf.*(((tw(i)+(k2tw(i)./2))+0.001)-
(tb(i)+(k2tb(i)./2))).*rohnf(i).*rohnf(i).*lc.*lc)./(munf(i).*munf(i));
    end;
% gr(i)=(g.*betanf.*(tb(i)-tw(i)).*rohnf(i).*rohnf(i).*lc.*lc)./(munf(i).*munf(i));
ra(i)=gr(i).*pr(i);
nu(i)=c.*(ra(i)).^(n);
hw(i)=(nu(i).*knf(i))./lc;
if (tw(i)>tg(i))
    hcw(i)=0.884.*((tw(i)+(k2tw(i)./2))-(tg(i)+(k2tg(i)./2))+(((pw(i)-
pg(i)).*(tw(i)+(k2tw(i)./2)+273.15))./(268.9.*1000-pw(i))))).^0.33333);
    elseif (tw(i)<tg(i))
        hcw(i)=0.884.*((tg(i)+(k2tg(i)./2))-(tw(i)+(k2tw(i)./2))+(((pg(i)-
pw(i)).*(tw(i)+(k2tw(i)./2)+273.15))./(268.9.*1000-pw(i))))).^0.33333);
    elseif (tw(i)==tg(i))
        hcw(i)=0.884.*((tw(i)+(k2tw(i)./2)+0.0012)-(tg(i)+(k2tg(i)./2))+(((pw(i)+0.00001)-
pg(i)).*(tw(i)+(k2tw(i)./2)+273.15))./(268.9.*1000-pw(i))))).^0.33333);
    end;
% hcw(i)=0.884.*(tw(i)-tg(i)+(((pw(i)-pg(i)).*(tw(i)+273.15))./(268.9.*1000-
pw(i))))).^0.33333);
if (tw(i)>tg(i))
    hrw(i)=0.884*ephiloneff*(5.67)*10^(-8)*(((tw(i)+(k2tw(i)./2))+273.15)^4)-
((tg(i)+(k2tg(i)./2))+273.15)^4)/((tw(i)+(k2tw(i)./2))-(tg(i)+(k2tg(i)./2)));
    elseif (tw(i)<tg(i))
        hrw(i)=0.884*ephiloneff*(5.67)*10^(-8)*(((tg(i)+(k2tg(i)./2))+273.15)^4)-
((tw(i)+(k2tw(i)./2))+273.15)^4)/((tg(i)+(k2tg(i)./2))-(tw(i)+(k2tw(i)./2)));
    elseif (tw(i)==tg(i))
        hrw(i)=0.884*ephiloneff*(5.67)*10^(-8)*(((tw(i)+(k2tw(i)./2))+273.15235)^4)-
((tg(i)+(k2tg(i)./2))+273.15)^4)/(((tw(i)+(k2tw(i)./2))+0.00025)-(tg(i)+(k2tg(i)./2)));
    end;
% hrw(i)=0.884*ephiloneff*(5.67)*10^(-8)*(((tw(i)+273.15)^4)-(tg(i)+273.15)^4)/(tw(i)-
tg(i));

```

```

if (tw(i)>tg(i))
    hew(i)=16.273*10-3*hcw(i)*((pw(i)-pg(i))/((tw(i)+(k2tw(i)/2))-(tg(i)+(k2tg(i)/2))));
elseif (tw(i)<tg(i))
    hew(i)=16.273*10-3*hcw(i)*((pw(i)-pg(i))/((tg(i)+(k2tg(i)/2))-(tw(i)+(k2tw(i)/2))));
elseif (tw(i)==tg(i))
    hew(i)=16.273*10-3*hcw(i)*(((pw(i)+0.0001)-pg(i))/(((tw(i)+(k2tw(i)/2))+0.0025)-
(tg(i)+(k2tg(i)/2))));
end;
% hew(i)=16.273*10-3*hcw(i)*((pw-pg)/(tw(i)-tg(i)));
hlw(i)=hcw(i)+hrw(i)+hew(i);
hcg(i)=2.8+3*v;
if (tg(i)>ta(i))
    hrg(i)=ephsilong*5.67*10-8*(((tg(i)+(k2tg(i)/2))+273.15)4-
(tsky+273.15)4)/((tg(i)+(k2tg(i)/2))-ta(i));
elseif (tg(i)<ta(i))
    hrg(i)=ephsilong*5.67*10-8*(((tg(i)+(k2tg(i)/2))+273.15)4-
(tsky+273.15)4)/(ta(i)-(tg(i)+(k2tg(i)/2)));
elseif (tg(i)==ta(i))
    hrg(i)=ephsilong*5.67*10-8*(((tg(i)+(k2tg(i)/2))+273.15)4-
(tsky+273.15)4)/(((tg(i)+(k2tg(i)/2))+0.0025)-ta(i));
end;
% hrg(i)=ephsilong*5.67*10-8*(((tg(i)+273.15)4-(tsky+273.15)4)/(tg(i)-ta));
hlg(i)=hcg(i)+hrg(i);
h(i)=(hw(i)/(hw(i)+hb));
hdash(i)=(hlw(i)/(hlg(i)+hlw(i).*cos(betas)));
ulb(i)=(hb.*h(i));
ulg(i)=(hlg(i).*hdash(i));
udashl(i)=((ac.*fr.*ul)+(ulb(i).*ab)+(ulg(i).*ab));
a(i)=(udashl(i)/(mnf(i).*cpnf(i)));
f(i)=((ac.*fr.*alphatc.*idash)/(mnf(i).*cpnf(i)))+(((ac.*fr.*ul+ulb(i).*ab+ulg(i).*ab).*ta(i))/(
(mnf(i).*cpnf(i))))+(((alphag.*hdash(i)+alphaw.*taog+alphab.*taog.*taow.*h(i)).*as.*j(i))/(
mnf(i).*cpnf(i)))
k3tw(i)=f(i)-a(i).*(tw(i)+(k2tw(i)/2));

```

$k3tg(i)=(\text{alphag}.*\text{ag}.*j(i)+hlw(i).*aw.*((tw(i)+(k2tw(i)/2))-(tg(i)+(k2tg(i)/2))))+hlg(i).*ag.*(ta(i)-(tg(i)+(k2tg(i)/2)))/(\text{mg}.*cg);$   
 $k3tb(i)=(\text{alphab}.*(1-\text{alphag})*(1-\text{alphaw})*ab.*j(i)-hw(i).*ab.*((tb(i)+(k2tb(i)/2))-(tw(i)+(k2tw(i)/2)))+hb.*ab.*((tb(i)+(k2tb(i)/2))-ta(i)))/(\text{mb}.*cb);$   
 % for k4tw  
 $\text{rohbf}(i)=(1-(((tw(i)+(k3tw(i))-4).^2))/((119000+1365.*(tw(i)+(k3tw(i))-4.*(tw(i)+(k3tw(i))).*(tw(i)+(k3tw(i)))))).*1000);$  %roh of base fluid  
 $\text{rohnf}(i)=(fi.*\text{rohnp})+(1-fi).*\text{rohbf}(i);$  %roh of nanofluid  
 $\text{mnf}(i)=(\text{rohnf}(i).*ab.*\text{waterdepth});$  %mass of nanofluid  
 %cp of nanoparticle  
 $\text{cpbf}(i)=4217.629-3.20888.*(tw(i)+(k3tw(i)))+0.09503.*(tw(i)+(k3tw(i))).*(tw(i)+(k3tw(i)))-0.00132.*(tw(i)+(k3tw(i))).^3+9.415.*10.^{-6}.*(tw(i)+(k3tw(i))).^4-2.5479.*10.^{-8}.*(tw(i)+(k3tw(i))).^5);$  %cp of base fluid  
 $\text{cpnf}(i)=0.8429.*((1+((tw(i)+(k3tw(i))/50)).^(-0.3037)).*(1+(dp/50).^0.4167)).*(1+(fi/100)).^2.272);$  %cp of nanofluid  
 $\text{betabf}=21*10.^{-5};$   
 $\text{betanp}=29*10.^{-5};$   
 $\text{betanf}=(1-fi).*\text{betabf}+(fi).*\text{betanp};$   
 $\text{mubf}(i)=0.0015-3.16325.*(tw(i)+(k3tw(i))).*10.^{-5}+3.04789.*(tw(i)+(k3tw(i))).^2.*10.^{-7}-1.1104.*(tw(i)+(k3tw(i))).^3.*10.^{-9};$   
 $\text{munf}(i)=(2.414.*10.^{-5}).*10.^{247.8/(((tw(i)+(k2tw(i)/2))+273.15)-140)};)$   
 $\text{kbf}(i)=(0.55994+0.00216.*(tw(i)+(k3tw(i)))-1.02749.*10.^{-5}.*(tw(i)+(k3tw(i))).^2+6.7279.*10.^{-9}.*(tw(i)+(k3tw(i))).^3);$   
 %  
 $\text{knf}(i)=\text{kbf}(i).*((0.9843+0.398.*(fi).^0.467)).*((\text{munf}(i)/\text{mubf}(i)).^0.0235)).*((1/dp).^0.2246)-$   
 $(3.951.*(fi)/(tw(i)+(k3tw(i))))+(34.034.*((fi.*fi)/(tw(i)+(k3tw(i))).*(tw(i)+(k3tw(i))).*(tw(i)+(k3tw(i))))+(32.51.*((fi)/(tw(i)+(k3tw(i))).*(tw(i)+(k3tw(i))))));$   
 % knf(i)=33;  
 $\text{ephsilonw}=0.95;$   
 $\text{ephsilong}=0.94;$   
 $\text{ephsiloneff}=(1/\text{ephsilong})+(1/\text{ephsilonw}-1)^{-1};$   
 $\text{pw}(i)=\exp(25.317-(5144/((tw(i)+(k3tw(i))+273.15)));$   
 $\text{pg}(i)=\exp(25.317-(5144/((tg(i)+(k3tg(i))+273.15)));$

```

c=0.54;
n=(1/4);
pr(i)=((munf(i).*cpnf(i))./knf(i));
%
if (tb(i)>tw(i))
    gr(i)=(g.*betanf.*((tb(i)+(k3tb(i)))-
(tw(i)+(k3tw(i))))).*rohnf(i).*rohnf(i).*lc.*lc)./(munf(i).*munf(i));
    elseif (tb(i)<tw(i))
        gr(i)=(g.*betanf.*((tw(i)+(k3tw(i)))-
(tb(i)+(k3tb(i))))).*rohnf(i).*rohnf(i).*lc.*lc)./(munf(i).*munf(i));
    elseif (tb(i)==tw(i))
        gr(i)=(g.*betanf.*(((tw(i)+(k3tw(i)))+0.001)-
(tb(i)+(k3tb(i))))).*rohnf(i).*rohnf(i).*lc.*lc)./(munf(i).*munf(i));
    end;
% gr(i)=(g.*betanf.*(tb(i)-tw(i)).*rohnf(i).*rohnf(i).*lc.*lc)./(munf(i).*munf(i));
ra(i)=gr(i).*pr(i);
nu(i)=c.*(ra(i)).^(n);
hw(i)=(nu(i).*knf(i))./lc;
if (tw(i)>tg(i))
    hcw(i)=0.884.*((tw(i)+(k3tw(i)))-(tg(i)+(k3tg(i)))+(((pw(i)-
pg(i)).*(tw(i)+(k3tw(i))+273.15))./(268.9.*1000-pw(i))))).^0.33333;
    elseif (tw(i)<tg(i))
        hcw(i)=0.884.*((tg(i)+(k3tg(i)))-(tw(i)+(k3tw(i)))+(((pg(i)-
pw(i)).*(tw(i)+(k3tw(i))+273.15))./(268.9.*1000-pw(i))))).^0.33333;
    elseif (tw(i)== tg(i))
        hcw(i)=0.884.*((tw(i)+(k3tw(i))+0.0012)-(tg(i)+(k3tg(i)))+(((pw(i)+0.0001)-
pg(i)).*(tw(i)+(k3tw(i))+273.15))./(268.9.*1000-pw(i))))).^0.33333;
    end;
% hcw(i)=0.884.*(tw(i)-tg(i)+(((pw(i)-pg(i)).*(tw(i)+273.15))./(268.9.*1000-
pw(i))))).^0.33333;
if (tw(i)>tg(i))
    hrw(i)=0.884*ephiloneff*(5.67)*10^(-8)*(((tw(i)+(k3tw(i)))+273.15)^4)-
(((tg(i)+(k3tg(i)))+273.15)^4)/(((tw(i)+(k3tw(i)))-(tg(i)+(k3tg(i)))));
    elseif (tw(i)<tg(i))

```

```

hrw(i)=0.884*ephiloneff*(5.67)*10^(-8)*(((tg(i)+(k3tg(i)))+273.15)^4)-
((tw(i)+(k3tw(i)))+273.15)^4)/((tg(i)+(k3tg(i)))-(tw(i)+(k3tw(i))));
elseif (tw(i)==tg(i))
hrw(i)=0.884*ephiloneff*(5.67)*10^(-8)*(((tw(i)+(k3tw(i)))+273.15235)^4)-
((tg(i)+(k3tg(i)))+273.15)^4)/(((tw(i)+(k3tw(i)))+0.00025)-(tg(i)+(k3tg(i))));
end;
% hrw(i)=0.884*ephiloneff*(5.67)*10^(-8)*(((tw(i)+273.15)^4)-(tg(i)+273.15)^4)/(tw(i)-
tg(i));
if (tw(i)>tg(i))
hew(i)=16.273*10^(-3)*hcw(i)*((pw(i)-pg(i))/((tw(i)+(k3tw(i)))-(tg(i)+(k3tg(i))));
elseif (tw(i)<tg(i))
hew(i)=16.273*10^(-3)*hcw(i)*((pw(i)-pg(i))/((tg(i)+(k3tg(i)))-(tw(i)+(k3tw(i))));
elseif (tw(i)==tg(i))
hew(i)=16.273*10^(-3)*hcw(i)*(((pw(i)+0.00001)-pg(i))/(((tw(i)+(k3tw(i)))+0.0025)-
(tg(i)+(k3tg(i))));
end;
% hew(i)=16.273*10^(-3)*hcw(i)*((pw-pg)/(tw(i)-tg(i)));
hlw(i)=hcw(i)+hrw(i)+hew(i);
hcg(i)=2.8+3*v;
if (tg(i)>ta(i))
hrg(i)=ephilong*5.67*10^(-8)*(((tg(i)+(k3tg(i)))+273.15)^4)-
(tsky+273.15)^4)/((tg(i)+(k3tg(i)))-ta(i));
elseif (tg(i)<ta(i))
hrg(i)=ephilong*5.67*10^(-8)*(((tg(i)+(k3tg(i)))+273.15)^4)-
(tsky+273.15)^4)/(ta(i)-(tg(i)+(k3tg(i))));
elseif (tg(i)==ta(i))
hrg(i)=ephilong*5.67*10^(-8)*(((tg(i)+(k3tg(i)))+273.15)^4)-
(tsky+273.15)^4)/(((tg(i)+(k3tg(i)))+0.0025)-ta(i));
end;
hlg(i)=hcg(i)+hrg(i);
h(i)=(hw(i)/(hw(i)+hb));
hdash(i)=(hlw(i)/(hlg(i)+hlw(i).*cos(betas)));
ulb(i)=(hb.*h(i));
ulg(i)=(hlg(i).*hdash(i));

```

```

udashl(i)=((ac.*fr.*ul)+(ulb(i).*ab)+(ulg(i).*ab));
a(i)=(udashl(i)./(mnf(i).*cpnf(i)));
f(i)=((ac.*fr.*alphatc.*idash)./(mnf(i).*cpnf(i)))+(((ac.*fr.*ul+ulb(i).*ab+ulg(i).*ab).*ta(i))./(
(mnf(i).*cpnf(i))))+(((alphag.*hdash(i)+alphaw.*taog+alphab.*taog.*taow.*h(i)).*as.*j(i))./(
mnf(i).*cpnf(i)))
k4tw(i)=f(i)-a(i).*(tw(i)+(k3tw(i)));
k4tg(i)=(alphag.*ag.*j(i)+hlw(i).*aw.*((tw(i)+(k3tw(i)))-(tg(i)+(k3tg(i))))+hlg(i).*ag.*(ta(i)-
(tg(i)+(k3tg(i)))))./(mg.*cg);
k4tb(i)=(alphab.*(1-alphag).*(1-alphaw).*ab.*j(i)-hw(i).*ab.*((tb(i)+(k3tb(i)))-
(tw(i)+(k3tw(i))))+hb.*ab.*((tb(i)+(k3tb(i)))-ta(i)))./(mb.*cb);
tw(i+1)=tw(i)+(1./6).*(k1tw(i)+(2.*k2tw(i))+(2.*k3tw(i))+k4tw(i)).*t;
tg(i+1)=tg(i)+(1./6).*(k1tg(i)+(2.*k2tg(i))+(2.*k3tg(i))+k4tg(i)).*t;
tb(i+1)=tb(i)+(1./6).*(k1tb(i)+(2.*k2tb(i))+(2.*k3tb(i))+k4tb(i)).*t;
if (tw(i+1)<=70)
    lh(i)=(2.4935*10^6)*(1-(9.4779*10^(-4))*tw(i)+(1.3132*10^(-7))*tw(i)^(2)-
(4.7974*10^(-9))*tw(i)^3);
    elseif (tw(i+1)>70)
        lh(i)=3.1615*10^6*((1-7.616*10^(-4))*tw(i));
    end;
mew(i)=((hew(i)*(tw(i)-tg(i))*t)/lh(i));
tsun=6000;
exoutput(i)=hew(i).*ab.*(tw(i)-tg(i)).*(1-((ta(i)+273)./(tw(i)+273)));
exstill(i)=ab.*j(i).*(1-(4/3).*((ta(i)+273)./tsun)+(1/3).*((ta(i)+273)./tsun).^4);
excollector(i)=ac.*j(i).*(1-(4/3).*((ta(i)+273)./tsun)+(1/3).*((ta(i)+273)./tsun).^4);
exinput(i)=exstill(i)+excollector(i);

end

```

## ORIGINALITY REPORT

13%

SIMILARITY INDEX

5%

INTERNET SOURCES

12%

PUBLICATIONS

0%

STUDENT PAPERS

## PRIMARY SOURCES

- 1** Nagarajan, P. K., S. A. El-Agouz, T. Arunkumar, and Ravishankar Sathyamurthy. "Effect of forced cover cooling technique on a triangular pyramid solar still", International Journal of Ambient Energy, 2016. **1%**

Publication
- 2** O.M. Haddad, M.A. Al-Nimr, A. Maqableh. "Enhanced solar still performance using a radiative cooling system", Renewable Energy, 2000 **1%**

Publication
- 3** Hardik K. Jani, Kalpesh V. Modi. "A review on numerous means of enhancing heat transfer rate in solar-thermal based desalination devices", Renewable and Sustainable Energy Reviews, 2018 **<1%**

Publication
- 4** Mahdi, Jassim Talib(Smith, BE). "An experimental and theoretical investigation of a wick-type solar still for water desalination", Brunel University School of Engineering and **<1%**

5

"Solar Desalination Technology", Springer Science and Business Media LLC, 2019

Publication

<1%

6

C. Elango, N. Gunasekaran, K. Sampathkumar. "Thermal models of solar still—A comprehensive review", Renewable and Sustainable Energy Reviews, 2015

Publication

<1%

7

Abhay Agrawal, R.S. Rana, Pankaj K. Srivastava. "Heat transfer coefficients and productivity of a single slope single basin solar still in Indian climatic condition: Experimental and theoretical comparison", Resource-Efficient Technologies, 2017

Publication

<1%

8

Sahota, L., and G.N. Tiwari. "Effect of nanofluids on the performance of passive double slope solar still: A comparative study using characteristic curve", Desalination, 2016.

Publication

<1%

9

[www.tandfonline.com](http://www.tandfonline.com)

Internet Source

<1%

10

Lovedeep Sahota, Shyam, G.N. Tiwari. "Analytical characteristic equation of nanofluid loaded active double slope solar still coupled

<1%

with helically coiled heat exchanger", Energy Conversion and Management, 2017

Publication

11

linknovate.com

Internet Source

<1%

12

Dwivedi, V.K.. "Experimental validation of thermal model of a double slope active solar still under natural circulation mode", Desalination, 20100101

Publication

<1%

13

T. Arunkumar, A.E. Kabeel, Kaiwalya Raj, David Denkenberger, Ravishankar Sathyamurthy, P. Ragupathy, R. Velraj. "Productivity enhancement of solar still by using porous absorber with bubble-wrap insulation", Journal of Cleaner Production, 2018

Publication

<1%

14

T. Arunkumar, D. Murugesan, Kaiwalya Raj, David Denkenberger, C. Viswanathan, D. Dsilva Winfred Rufuss, R. Velraj. "Effect of nano-coated CuO absorbers with PVA sponges in solar water desalting system", Applied Thermal Engineering, 2019

Publication

<1%

15

Kabeel, A.E.. "Theoretical and experimental parametric study of modified stepped solar still", Desalination, 20120315

<1%